

https://dspace.org/

Properties of nanometal-polyaniline composites

Kabomo, Tlhabologo Moses

2011-07-21
http://hdl.handle.net/10539/10307

Downloaded from a DSpace repository. https://dspace.org/

PROPERTIES OF NANOMETAL-POLYANILINE COMPOSITES

TLHABOLOGO MOSES KABOMO

A thesis submitted to the Faculty of Science, University of the Witwatersrand, Johannesburg, in fulfilment of the requirements for the Degree of Doctor of Philosophy.

Johannesburg, 2011

DECLARATION

I declare that this thesis is my own, unaided work. It is being submitted for the Degree of Doctor of Philosophy in the University of the Witwatersrand, Johannesburg. It has not been submitted before for any degree or examination in any other University.

Signature of candidate

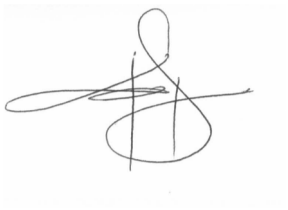

25th day of May 2011

ABSTRACT

Polymeric nanocomposites are intimate combinations of a polymer with inorganic nanoparticles. Such nanomaterials have attracted significant attention over the years because of their potential uses as chemical sensors, electronic and optical devices, and as catalysts. For catalytic applications, in particular, small and well dispersed nanoparticles are desired. We report here the synthesis of gold-polyaniline (AuPANI) nanocomposites and their catalytic performance. The simple synthetic route involved pre-organizing the gold ions in polyaniline (PANI) through complexation followed by the addition of a reducing agent. Control over the degree of reduction of tetrachloroaurate ions ($AuCl_4^-$) depends on the electrochemical potential of the system which in turn depends on the molar ratio of the nitrogen atoms on PANI to $AuCl_4^-$. Gold nanoparticles formed when the AuPANI complexes were reduced with sodium borohydride and the size of the nanoparticles could be varied with adjustment of the amount of sodium borohydride used. Low amounts of sodium borohydride induced slow nucleation rate and were associated with relatively large metallic particles. The smallest gold nanoparticles with a narrow size distribution were obtained when a ratio of sodium borohydride:gold of about 6:1 was used. Simple electrolytes like NaCl and NaOH did not induce the aggregation of Au nanoparticles as predicted by the DLVO theory. However, chain-like aggregates formed when aggregation was induced by the reduction of PANI while close-packed aggregates formed when PANI was oxidized or protonated. The Au nanoparticles were found to be more stable when dispersed on ring-substibuted PANI than on unsubstituted PANI. The catalytic performance of AuPANI was evaluated using the reduction of 4-nitrophenol by sodium borohydride. The reaction was observed to follow the Langmuir-Hinshelwood kinetics.

ACKNOWLEDGEMENTS

I would like to thank my Supervisor Prof. Mike Scurrell for the guidance and assistance he afforded me during my study. I would also like to thank Prof. Neil Coville for painstakingly going through my thesis and his comments. I am grateful to Prof. Michael Witcomb, Ms Caroline Lalkan, and Mr. Abe Seama of the Electron Microscopy Unit for the patience and assistance. Special thanks to the CATOMMAT Research Group for the camaraderie. I thank the University of Botswana for the financial support. Last but not least, I would like to thank my fiancée and my family for their love and support.

PUBLICATIONS AND PRESENTATIONS

Publications

1. Kabomo, T. M.; Scurrell, M. S.; "Synthesis of gold-polyaniline nanocomposites by complexation" *Chemitry of Materials* **submitted**.

2. Kabomo, T. M.; Scurrell, M. S.; "The stability of nanogold particles dispersed on polyaniline" *Macromolecules* **submitted**.

3. Kabomo, T. M.; Scurrell, M. S.; "Effect of substituents on the reactivity of polyaniline with hydrogen tetrachloroaurate and the stability of the resultant gold nanoparticles" *The Journal of Physical Chemistry C* **submitted**.

Oral Presentations

1. 2009 Catalysis Society of South Africa Conference, Rawsonville, South Africa

2. 2nd Post-Graduate Symposium, University of the Witwatersrand, Johannesburg, South Africa

TABLE OF CONTENTS

DECLARATION ii
ABSTRACT iii
ACKNOWLEDGEMENTS iv
PUBLICATIONS AND PRESENTATIONS v
TABLE OF CONTENTS vi
LIST OF FIGURES viii
LIST OF SCHEMES xii
LIST OF TABLES xiii

1 INTRODUCTION AND LITERATURE REVIEW 1
1.1 INTRODUCTION 1
1.2 LITERATURE REVIEW 4
1.2.1 Polyaniline Nanofibers 4
1.2.1.1 Determination of the Oxidation State of PANI 6
1.2.1.2 Controlling the Shape of PANI Structures 7
1.2.2 Composites of Polyaniline Nanofibers and Metal Nanoparticles 9
1.2.2.1 Formation of Au Nanoparticles on Preformed PANI 10
1.2.2.2 "One-Pot" Synthesis 11
1.2.3 The Interaction of Au Nanoparticles with PANI 14
1.3 REFERENCES 16

2 SYNTHESIS OF GOLD-POLYANILINE NANOCOMPOSITES BY COMPLEXATION 20
2.1 INTRODUCTION 20
2.2 EXPERIMENTAL 21
2.3 RESULTS AND DISCUSSION 24
2.3.1 The Formation of Gold-Polyaniline Complex 24
2.3.2 The Effect of Molar Ratio of Reducing Agent to Au Precursor on the Size and Shape of Au Nanoparticles 41
2.4 CONCLUSIONS 45
2.5 REFERENCES 45

3 THE STABILITY OF GOLD NANOPARTICLES DISPERSED ON POLYANILINE 49
3.1 INTRODUCTION 49
3.2 EXPERIMENTAL 50
3.3 RESULTS AND DISCUSSION 51
3.3.1 Effect of $NaBH_4$ on the Size and the Stability of Gold Nanoparticles 51
3.3.2 The Effect of the Degree of Protonation of PANI on the Stability of Gold Nanoparticles 58
3.3.3 Effect of $(NH_4)_2S_2O_8$ on the Size and the Stability of Gold Nanoparticles 62
3.3.4 Mechanism of Aggregation of AuNPs 64
3.4 CONCLUSIONS 66
3.5 REFERENCES 67

4 THE EFFECT OF SUBSTITUENTS ON THE REACTIVITY OF PANI WITH $HAuCl_4$ AND THE STABILITY OF GOLD NANOPARTICLES 70

4.1 INTRODUCTION 70
4.2 EXPERIMENTAL 72
4.3 RESULTS AND DISCUSSION 74
4.3.1 Synthesis of PANI and its derivatives 74
4.3.2 The Reactions of PANI, PANIMe, and PANICl with $HAuCl_4$ 81
4.3.3 Stability of the Nanocomposites in Acidic Media 84
4.4 CONCLUSIONS 87
4.5 REFERENCES 87

5 THE CATALYTIC ACTIVITY OF GOLD NANOPARTICLES DISPERSED ON PANI AND ITS DERIVATIVES 90
5.1 INTRODUCTION 90
5.2 EXPERIMENTAL 91
5.3 RESULTS AND DISCUSSIONS 92
5.3.1 Influence of the Concentration of 4-NP and Borohydride 95
5.3.2 Influence of Catalyst Dose 98
5.3.3 Influence of Substituents on the Polymer 100
5.4 CONCLUSIONS 103
5.5 REFERENCES 103

LIST OF FIGURES

Figure 1.1. Uv-vis spectra of 11 PANI (emeraldine base) solutions in *N*-methyl-2-pyrrolidinone, which four were reduced and six were oxidized. Solutions were prepared in ambient atmosphere and temperature.[32] 6

Figure 1.2. Transmission electron microscopy images of polyaniline nanofibers made by using (a) HCl (scale bar = 100 nm), (b) camphorsulphonic acid (scale bar = 100 nm), and (c) $HClO_4$ (scale bar = 1 μm).[41] 8

Figure 1.3. Schematic illustrations and images showing how the nucleation mode of polyaniline is related to the shape and aggregation of the resulting particles during the synthetic process.[44] 9

Figure 1.4. (a) TEM image of PANI nanofibers. (b) Enlarged TEM image of a branched network of PANI nanofibers. (c) SEM image of PANI nanofibers. (d) Cross-sectional view of a PANI nanofibers film.[62] 12

Figure 1.5. SEM images of gold particles at low magnification (a), showing the size distribution of the particles, and at high magnification (b), revealing that an individual gold microparticle is the aggregation of many nanoparticles. TEM images of gold particles at low magnification (c), showing their size distribution, and at high magnification (d), revealing that they are coated by a thin layer of polymer.[62] 13

Figure 1.6. Transmission electron microscopy images of AuPANI composite with several Au nanoparticles encapsulated in the PANI tetrahedron. The arrows show the motion of the small Au nanoparticles toward the larger one.[68] 14

Figure 1.7. Binding energy shift of the $Au4f_{7/2}$ peak for each particle size and (inset) the same values plotted vs. the particle size. [14] 15

Figure 2.1. Consumption of $AuCl_4^-$ followed by uv-vis spectroscopy measurements. The peaks at 225 nm and 310 nm due to LMCT decreased in intensity and disappeared within 2 minutes after addition of $HAuCl_4$ to an aqueous suspension of deprotonated PANI. Samples were filter through a 0.45 mm membrane filtered before recording the spectrum. 25

Figure 2.2. In-situ uv-vis spectra of the complexation of PANI and $AuCl_4^-$ in ethanol. Insert shows the peaks at 205 nm and 275 nm. 26

Figure 2.3. Uv-vis spectra of (a) deprotonated PANI and AuPANI complexes prepared using N/Au ratios of (b) 21, (c) 11, (d) 5.4, and (e) 2.7. A new peak around 1000 nm which tails down to the IR regime is observed in the spectra of AuPANI complexes. 27

Figure 2.4. TEM imgaes of (a) AuPANI-C and (b) AuPANI-R for a N/Au ratio of 21 and $NaBH_4$/Au = 3.2. Gold nanoparticles in AuPANI-R, with an average particle diameter of 2.6 nm, were identified by EDX. 28

Figure 2.5. PXRD pattern of gold nanoparticles dispered on polyaniline. 29

Figure 2.6. Electrochemical potential profiles of PANI complexation at different N/Au ratios: (a) 2.7, (b) 5.4, (c) 11, (d) 21. Time = 0 seconds is the time when the highest E was reached. 30

Figure 2.7. TEM images of AuPANI complexes for N/Au ratios of (a) 5.4 and (b) 2.7 indicating that $AuCl_4^-$ is only reduced to Au(0) by PANI at a ratio of 2.7..... 31

Figure 2.8. FTIR spectra of (a) deprotonated PANI, (b) AuPANI-C, and (c) AuPANI-R. Ratio of N/Au = 21 and $NaBH_4$/Au = 3.2..... 33

Figure 2.9. FTIR spectra of AuPANI complexes in the mid-IR range showing structural changes in the polymer backbone with an increase in the amount of HAuCl4. Spectrum (a) is for deprotonated PANI and spectra (b) - (e) are for AuPANI complexes at N\Au ratio of 21, 11, 5.4 and 2.7. 34

Figure 2.10. FTIR spectra of (a) depronated PANI and AuPANI complexes at N/Au ratio of (b) 21, (b) 11, (c) 5.4 and (e) 2.7 in the IR region of 2800 – 3500 cm^{-1}. .. 36

Figure 2.11. Variation of Au nanoparticles diameter with amount of $NaBH_4$. Averages were calculated by measuring at least 300 particles from TEM images using ImageJ. All error bars are 1 standard deviation of the distributions. 42

Figure 2.12. TEM images of AuPANI-R showing the variation of Au particle size and shape with variation in the amount of $NaBH_4$ used. The images correspond to $NaBH_4$/Au ratio of (a) 1.0, (b) 1.6, (c) 3.2, (d) 6.4, (e) 10, and (f) 12..... 44

Figure 3.1. TEM images of AuPANI-R after reduction using $NaBH_4$/Au ratio of (a) 12 and (b) 20. Both the length of the Au nanowires and the degree of branching of the nanowires increase with an increase in the amount of $NaBH_4$. 54

Figure 3.2. FTIR specatra of (a) AuPANI-C (N/Au = 21) and AuPANI-R reduced using the varying ratios of $NaBH_4$/Au (b) 3.2, (c) 12, (d) 26. The spectra show changes in the extent and type of H-bonding. 55

Figure 3.3. An illustration of the formation of Au NPs in which $AuCl_4^-$ ions form Au_nCl_{n+x} complex clusters during the initial stages of nucleation. Taken from Ref 20. 57

Figure 3.4. The effect of pH and the degree of protonation of PANI on the stability of Au nanoparticles. The degree of protonation was calculated on the basis that protonation occurs only at the imine N and that 50% of the nitrogen atoms are imine N. 59

Figure 3.5. TEM images and particles size distribution of AuPANI-R (a) before and (b) after soaking in 1.0 M NaCl for 24 hours. 60

Figure 3.6. FTIR spectra of (a) AuPANI-R after treatment with $(NH_4)_2S_2O_8$ and (b) AuPANI-R without treatment with oxidizing agent. 63

Figure 3.7. TEM image and particle size distribution for AuPANI-R after oxidizing with 0.1 M $(NH_4)_2S_2O_8$. The size of the gold nanoparticles increased from about 2.6 ±. 0.6 nm to 8.2 ±. 2.0 nm 64

Figure 4.1. Potential-time profiles of the polymerization of aniline, methylaniline, and chloroaniline with ammonium peroxydisulphate in 1 M HCl**.** 75

Figure 4.2. Uv-vis spectra of (a) PANI, (b) PANIMe, and (c) PANICl in 1-methyl-2-pyrrolidinone. 77

Figure 4.3. FTIR spectra of (a) PANIMe, (b) PANICl, and (c) PANI. 79

Figure 4.4. FTIR spectra of (a) PANIMe, (b) PANICl, and (c) PANI in the IR region of 2800 cm^{-1} to 3500 cm^{-1}. 80

Figure 4.5. The reactivity of polyaniline and its derivatives towards $HAuCl_4$.]..... 81

Figure 4.6. TEM images and particle size distributions of gold nanoparticles on (a) PANI, (b) PANICl, and (c) PANIMe 83

Figure 4.7. FTIR spectra indicating the protonation of (a) AuPANICl, (b) AuPANIMe, and (c)AuPANI. Spectra (a) to (c) are the unprotonated composites and spectra (d) to (f) are the spectra of the corresponding composites after HCl treatment at pH 1. 86

Figure 5.1. Time dependent absorption spectra for the reduction of 4-NP in the presence of Au-PANI. Conditions: [4-AP] = 1 mM; $[NaBH_4]$ = 0.67 M; [Catalyst] = 0.7 g/L. 93

Figure 5.2. First order decay of the absorbance at 400 nm and the linearized data for the reduction of 4-NP. 94

Figure.5.3. Schematic representation of the catalytic reduction of 4-NP in the presence of Au nanoparticles (Langmuir-Hinshelwood mechanism). Adapted from Ref 18. 95

Figure 5.4. Variation of apparent rate constant k_{app} on the concentration of 4-AP. The concentration of the catalyst was 0.7 g/L. 96

Figure 5.5. Variation of apparent rate constant k_{app} with the concentration of borohydride. The concentration of the catalyst was 0.7 g/L. 97

Figure 5.6. Variation of apparent rate constant k_{app} with the concentration of the catalyst. The concentration of the catalyst was 0.7 g/L. 99

Figure 5.7. Rate constant k_{app} as a function of mass of catalyst for AuPANI, AuPANIMe, AuPANICl. The concentrations of the reactants were: [4-AP] = 1×10^{-4} M, [$NaBH_4$] = 0.68 M. 100

Figure 5.8. Rate constant k_{app} as a function of surface area Au nanoparticles normalized to the unit volume of the system for AuPANI, AuPANIMe, AuPANICl. The concentrations of the reactants were: [4-AP] = 1×10^{-4} M, [$NaBH_4$] = 0.68 M. 102

LIST OF SCHEMES

Scheme 1.1. Schematic diagram show the chemical structure, synthesis, reversible acid/base doping/dedoping, and the redox chemistry of polyaniline. 5

Scheme 2.1. Proposed mechanism for the formation of AuPANI complex. 40

Scheme 2.2. Possible interactions of Au and PANI through electron transfer from N to Au and H-bonding. 40

Scheme 3.1. Protonation of PANI and the subsequent formation of a polysemiquinone cation radical. 58

Scheme 3.2. Hydrolysis of PANI through (a) chain breakage and (b) elimination of terminal N and replacement with O..... 62

Scheme 3.3. The distribution of electric field around (a) monomeric Au NPs and (b) linearly aggregated AuNPs. The scheme shows the preferential attachment of AuNPs at the end of a chain. Adapted from Yang and co-workers.[32] 66

LIST OF TABLES

Table 2.1. A summary of FTIR and electrochemical results showing an increase in the degree of oxidation of PANI with increasing amount of $HAuCl_4$..... 35

Table 2.2. Variation of solution pH and degree of oxidation with ratio of $NaBH_4$/Au. 43

Table 3.1. Variation of solution pH and degree of oxidation with ratio of $NaBH_4$/Au. 54

Table 4.1. An indication of the electronic and steric effects of the various substituent groups studied. 76

Table 4.2. Absorptions and *Q*/*B* ratios in the UV-vis spectra of PANI and its derivatives in NMP. 77

Table 4.3. The variation of the size of gold nanoparticles on PANI, PANIMe, and PANICl with pH 85

Table 5.1. Comparison of the catalytic activity of Au nanoparticles on PANI, PANIMe, and PANICl. 101

1 INTRODUCTION AND LITERATURE REVIEW

1.1 INTRODUCTION

Polymeric nanocomposites are intimate combinations of a polymer with one or more inorganic nanoparticles. Such nanomaterials have attracted significant attention over the years because of their potential uses as chemical sensors[1, 2], electronic devices[3], and as catalysts. For catalytic applications, in particular, small and well dispersed nanoparticles are desired. There has been an interest lately on the use of metal nanoparticles dispersed on polymers for use as catalysts in liquid-phase reactions.[4-7] For instance Pt supported on polyaniline (PANI) has been used in the catalytic oxidation of methanol[8, 9] and hydrazine.[10] Nanoparticles of Au supported on polymers have been used for the catalytic decomposition of hydrogen peroxide[7], the oxidation of glucose[7], and the reduction of 4-nitrophenol.[4, 11]

Polymers are known to stabilize metal nanoparticles mainly by charge transfer interactions between the metal particles and functional groups or heteroatoms on the polymer.[5, 12-14] Metals dispersed on polyaniline are believed to interact with the polymer through charge transfer between the imine N on PANI and the metal.[13, 15] The chemistry of PANI is well known. PANI can exist in three different oxidation states viz., the fully reduced (leocuemeraldine) form, the fully oxidized (pernigraniline) form and partially reduced/oxidized (emeraldine) form. The major difference between these forms of PANI is the proportion of amine groups to imine groups. In addition, PANI can be easily protonated at the imine nitrogen using protonic acids such as hydrochloric acid or sulphuric acid. The protonation of PANI in the emeraldine form using HCl, for example, converts it to a hydrochloride salt which is believed to exist as stable delocalized polysemiquinone radical cations.[16, 17]

Ponzio and co-workers[18] have shown that the formation of the polysemiquinone radical cation in which the amine N acquires a positive charge leads to a decrease in the polymer's ability to form H-bonds. It is important to understand how these structural changes on PANI would affect the stability and catalytic activity of metal nanoparticles dispersed on PANI. For instance, the catalytic activity of Au nanoparticles often tested using the reduction of 4-nitrophenol as a model reaction.[19] This reaction is usually carried out in excess sodium borohydride which can reduce PANI by converting the metal stabilizing imine groups to amine groups.

This thesis reports on the properties of gold-polyaniline composites. Chapter 2 shows that gold nanoparticles composited with polyaniline nanofibres can be synthesized by the complexation technique in water at room temperature. Using what is a molecular mixing approach, an intimate contact between the nanometal and polymer can be achieved. Control over the degree of reduction of hydrogen tetrachloroaurate ($AuCl_4^-$) depends on the electrochemical potential of the system which in turn depends on the molar ratio of the polymer repeat unit to Au expressed as N/Au. Gold nanoparticles formed when the AuPANI complexes were reduced with $NaBH_4$ and the size of the nanoparticles could be varied with adjustment of the amount of sodium borohydride used. Low amounts of sodium borohydride induced a slow nucleation rate and were associated with the formation of relatively large metallic particles. The smallest gold nanoparticles with a narrow size distribution were obtained when a ratio of sodium borohydride: gold of about 6:1 was used.

Chapter 3 focuses on the stability of Au nanoparticles dispersed on PANI. The stability of the Au nanoparticles was tested by soaking the nanocomposites in various

aqueous solutions to vary the oxidation state of PANI and its "degree" of protonation. It will be shown in Chapter 3 that simple electrolytes like NaCl and NaOH did not induce the aggregation of Au nanoparticles dispersed on PANI as predicted by the Derjaguin-Landau-Verwey-Overbeek (DLVO) theory for electrostatically stabilized colloidal systems. However, chain-like aggregates (nanowires) of Au formed when aggregation was induced by the reduction of PANI, while close-packed aggregates formed when PANI was oxidized or protonated.

The effect of substituents on the reactivity of polyaniline with hydrogen tetrachloroaurate and the stability of the resultant gold nanoparticles are explored in Chapter 4. Theoretical[20, 21] and experimental[22, 23] studies have shown marked differences between ring-substituted polyanilines and unsubstituted PANI. The results of Chapter 4 show that the rate of polymerization was determined largely by electronic effects of the substituent groups while the reactivity of the resultant polymers was determined by the steric effects. The order of the rate of reaction of the polymers with $AuCl_4^-$ will be shown to be PANIMe < PANICl << PANI. Gold nanoparticles dispersed on PANICl and PANIMe were more stable in acidic media than those on PANI.

Finally, Chapter 5 deals with the evaluation of the catalytic activity of the AuPANI nanocomposites using the reduction of 4-NP by $NaBH_4$ as a model reaction. The reaction was observed to follow the Langmuir-Hinshelwood mechanism.

1.2 LITERATURE REVIEW

1.2.1 Polyaniline Nanofibers

Polyaniline (PANI) is the simple 1,4-coupling product of monomeric aniline molecules.[24] The coupling reaction is usually initiated through the use of strong oxidizing agents such as ammonium peroxydisulphate, in an acidic solution. MacDiarmid and coworkers[25] illustrated that the structure of the polymer can be represented by the following formulas shown in Scheme 1.1. The terms "leucoemeraldine", "emeraldine", and "pernigraniline" refer to the different oxidation states of the polymer when it is completely reduced, half reduced/half oxidized, completely oxidized, respectively. The emeraldine oxidation state consists of alternating reduced and oxidized groups.[26] A lot of research has been conducted to study the mechanism of the polymerization. The generally accepted mechanism is one that starts with the protonation of aniline to form an anilinium cation. In aqueous acidic medium, the polymerization is known to be initiated by the formation of aniline cation radicals through the redox process of $S_2O_8^{2-}$ (when ammonium peroxydisulphate is used as an oxidizing agent) and anilinium ions.[27, 28] These cation radicals then proceed to simultaneously form polyaniline in the pernigraniline oxidation state (blue). The process continues until all the oxidizing agent is consumed, after which, the polymer chains grow through a redox process between pernigraniline (as an oxidizing agent) and aniline (as a reducing agent) to form the emeraldine salt.[29] During this process the reaction mixture turns from blue to green.[30] Side reactions include the formation of benzidine or N-phenyl-p-phenylenediamine.

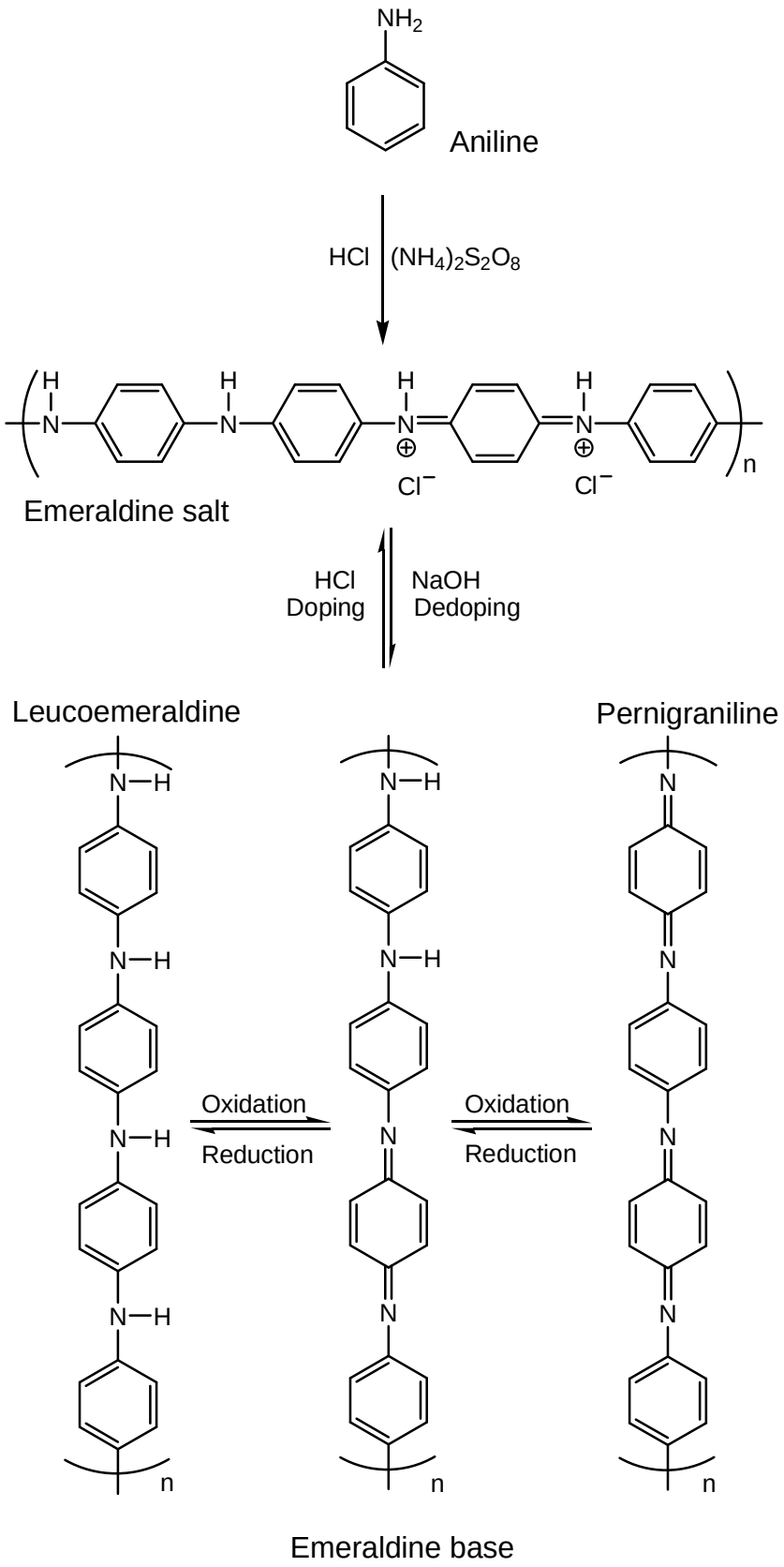

Scheme 1.1. Schematic diagram show the chemical structure, synthesis, reversible acid/base doping/dedoping, and the redox chemistry of polyaniline.

1.2.1.1 Determination of the Oxidation State of PANI

PANI can easily interconvert between its various oxidation states by the use of common oxidizing and reducing agents such as ammonium peroxydisulphate, sodium borohydride, or ascorbic acid.[31] The oxidation state of PANI can be easily estimated from the relative intensities of the FTIR absorption peaks of the quinoind group and the benzenoid groups. In a series of publications MacDiarmid and coworkers showed that the oxidation state of PANI varies continuously from leucoemeraldine to pernigranilie and vice-versa with the addition of an oxidizing agent and reducing agent, respectivlely.[25, 31, 32] Figure 1.1 shows the uv-vis spectra of PANI transitioning through the various oxidation states.[31] A method based on uv-vis to determine the oxidation state of PANI was developed.[32]

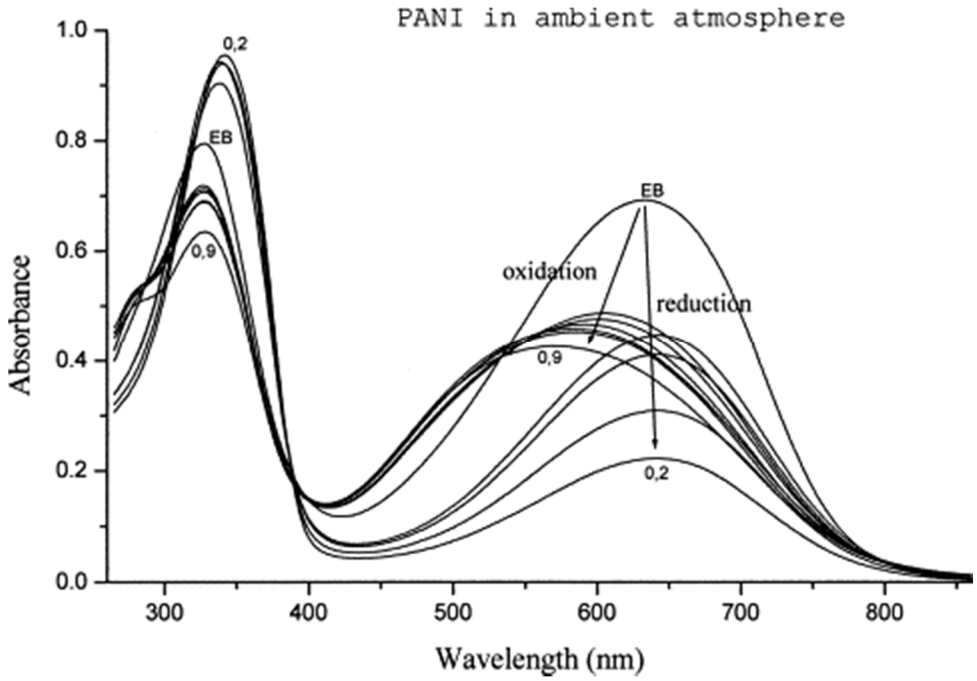

Figure 1.1. Uv-vis spectra of 11 PANI (emeraldine base) solutions in *N*-methyl-2-pyrrolidinone, which four were reduced and six were oxidized. Solutions were prepared in ambient atmosphere and temperature.[32]

This method relies on the accurate determination of the oxidation states of a series of PANI samples to obtain a calibration curve. The calibration curves were based on the variation of the ratio of the absorbance of the $\pi - \pi^*$ transition around 320 nm (*Q* band) to the absorbance due to an excitation of an electron from the HOMO of the benzeniod to the LUMO of quinoid moiety around 634 nm (*B* band).

A similar but slightly easier method based on uv-vis spectroscopy for the estimation of the oxidation state of PANI has been proposed by other authors. Yang and Mattes[33] simply used the ratio A_Q/A_B as an indication of the oxidation state, where A_Q is the uv-vis absorbance of the *Q* band and A_B is the absorbance of the *B* band. Others have used X-ray photoelectron spectroscopy (XPS) for the determination of the oxidation of PANI.[34, 35] Although this method is usually considered more accurate, XPS is an expensive technique and the results depend on carefully fitting the N1s core-level spectra.[36] A simpler and commonly used technique for estimating the oxidation state of PANI is Fourier Transform Infra-red (FTIR) spectroscopy. Similar to the uv-vis method, this method uses the relative intensities of the characteristic peaks around 1600 cm^{-1} for the quinoid ring (stretching of N=Q=N) and around 1500 cm^{-1} for the benzoniod rings (stretching of N–B–N).[37]

1.2.1.2 Controlling the Shape of PANI Structures

There are several methods described in literature for making PANI nanostructures. Some of these methods employed "hard" templates such as zeolites[38] while others used "soft" templates such as micelles[39] and surfactants.[40] The disadvantage with the template method is that a postsynthesis process to remove the template is required. Recently Huang and Kaner[41] synthesized PANI nanofibers using interfacial

polymerization without the need for templates. Although the authors had initially assumed that the nanofibrillar morphology was the result of confining the polymerization to the water/toluene interface, they later demonstrated that the nanofibrillar morphology of PANI appears to be intrinsic to the polymer. High quality PANI nanofibers were obtained by rapidly adding ammonium peroxydisulphalte to an acid solution of aniline with minimal stirring.[42] The average diameter of the PANI nanofibers could be tuned from 30 nm using hydrochloric acid to 120 nm using perchloric acid.

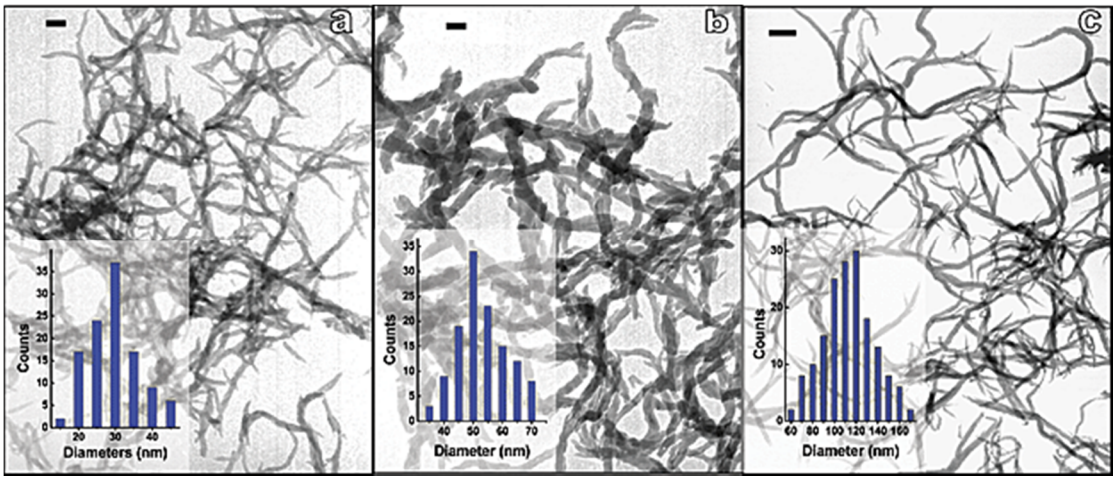

Figure 1.2. Transmission electron microscopy images of polyaniline nanofibers made by using (a) HCl (scale bar = 100 nm), (b) camphorsulphonic acid (scale bar = 100 nm), and (c) $HClO_4$ (scale bar = 1 μm).[41]

In a series of publications, Kaner and coworkers correlated the shape of polyaniline particles with the nucleation mode.[43, 44] They demonstrated that homogenous nucleation (which occurs spontaneously) led to the formation of nanofibers. Heterogeneous nucleation, which predominates during the later stages of the polymerization, leads results in granular PANI. Thus the shape of the PANI can be controlled by controlling the mode of nucleation. A rapid reaction with no stirring suppresses heterogeneous nucleation and favors the formation of nanofibers.[45] This is

summarized in Figure 1.3 in which the green bars represent PANI fibers formed form homogenous nucleation while the pink dots are particulates from heterogeneous nucleation.

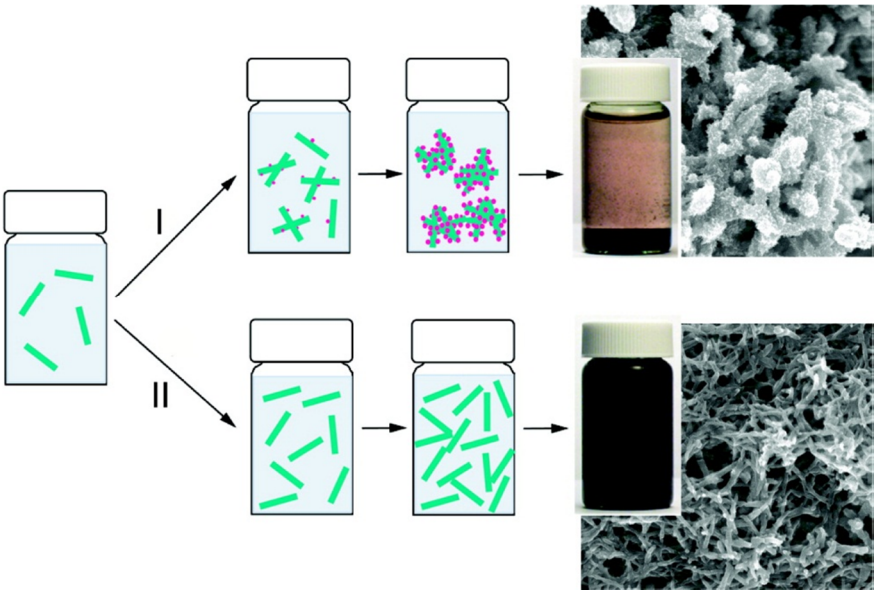

Figure 1.3. Schematic illustrations and images showing how the nucleation mode of polyaniline is related to the shape and aggregation of the resulting particles during the synthetic process.[44]

1.2.2 Composites of Polyaniline Nanofibers and Metal Nanoparticles

It has been reported that the electrical properties of an organic thin film can be drastically modified when metallic nanoparticles are embedded within the organic film.[33] PANI-metal nanoparticle composites have been reported to show enhanced response to hydrogen sulfide[46], as well as interesting electrical[3] and biosensing[47] properties. These composites are often prepared by (1) polymerization of aniline around preformed metal nanoparticles[48, 49], (2) reduction of metal ions in the presence of preformed PANI[50, 51] and, (3) "one-pot" polymerization of aniline using a gold salt as an oxidizing agent.[12, 52-56]

1.2.2.1 Formation of Au Nanoparticles on Preformed PANI

One of the earliest reports to demonstrate the formation of Au nanoparticles of preformed PANI was publish by Neoh and coworkers[50] in 1993. Metallic gold particles were observed to form from the reaction of acidic $AuCl_3$ and emeraldine PANI. The proposed mechanism involved the protonation of PANI at the imine N, the reduction of Au^{3+} ions (and the oxidation of PANI accompanied by deprotonation), and as a final step the reprotonation of PANI. The mechanism was supported by XPS results which showed the presence of Au^0, imine N, amine N, and protonated N. In a later publication, Neoh and coworkers showed that the size of the Au nanoparticles varied with the initial molar ratio of $AuCl_3$ to the nitrogen groups in PANI, Au/N.[51] The size of the gold particles varied from about 4 nm to 14 nm. The major setback with this method of preparing composites of Au and PANI is the high concentration of the gold salt required to oxidize PANI. The oxidation of PANI from emeraldine to pernigraniline requires an electrochemical potential of 0.5 V (vs. SCE) or above. However if high electrochemical potentials are sustained for a long time, PANI undergoes degradation by the hydrolysis of the imine group.[57] Indeed Neoh and coworkers reported that PANI did degrade during the synthesis of nanosized gold in PANI and observed an increase in the amount of carbonyl groups at longer reaction times.[58] Another problem with this method is that it is a slow reaction. In their work, Neoh and coworkers detected Au nanoparticles after about 10 minutes of reaction time for the highest Au/N of 1:1. Gold nanoparticles were detected after about 30 minutes for the lowest Au/N ratio of 1:20.[51] In a different study Drelinkiewicz and coworkers[59] observed that the amount of palladium incorporated into PANI reached 100% of the initial amount after 25 hours of reaction time. Such long reaction times make it difficult to control the size of the nanoparticles. The classical nucleation-

growth model requires a fast nucleation rate in order to form small metal particles with a narrow particle size distribution.[60, 61]

1.2.2.2 "One-Pot" Synthesis

There has been a surge in the number of reports over the last years for "one-pot" synthesis of gold-polyaniline (AuPANI) composites.[12, 52, 56, 62-65] Metals such as Pt and Pd have also been used. In this method $AuCl_4^-$ is used an oxidizing agent for the polymerization of aniline. This results in the simultaneous formation of PANI and metallic gold. That is, aniline acts a reducing agent and provides a support or stabilizing agent once it is polymerized to PANI. One of the commonly cited advantages of this method is that the metal particles synthesized this way are more evenly distributed in the polymer matrix compared to when they are formed on preformed PANI.[12, 56] The mechanism for the polymerization of PANI using a gold salt is thought to be similar to the conventional way of synthesizing PANI.

Wang and coworkers[62] obtained PANI nanofibers with a diameter of about 35 ± 5 nm in the one pot synthesis of AuPANI composite in which a molar ratio of aniline:$HAuCl_4$ was 1:5. The gold particles formed large aggregates of 100 nm. These were nonetheless believed to be made up of smaller particles of about 30 nm. Scanning electron microscopy and TEM images of the products are shown in Figures 1.4 and 1.5. Kinyanjui and Hatchett[12] used a molar ratio of $KAuCl_4$:aniline of 1:10 and obtained AuPANI composite with Au content of 54% by weight. These studies and a few others demonstrated the major disadvantages of this method, i.e., (1) a high concentration of $AuCl_4^-$ is required to oxidize aniline, and (2) it is difficult to control the size of the gold nanoparticles. Kinetic studies of this reaction have been conducted

by Qiu and coworkers.[66] The formation of a PANI film formed from the reaction of aniline with $HAuCl_4$ was monitored using a quartz crystal microbalance. The results obtained showed that the reaction was 0.5 order and 1.5 order with respect to $HAuCl_4$ and aniline, respectively. In-situ uv-vis studies of this reaction showed that $AuCl_4^-$ was gradually consumed during the course of the reaction.[66] This observation explains why controlling the size of the Au particles is difficult under this method. The gradual consumption of $AuCl_4^-$ implies that the rate of nucleation is slow leading to the formation of only a few Au nuclei. As a result large particles of Au are formed.

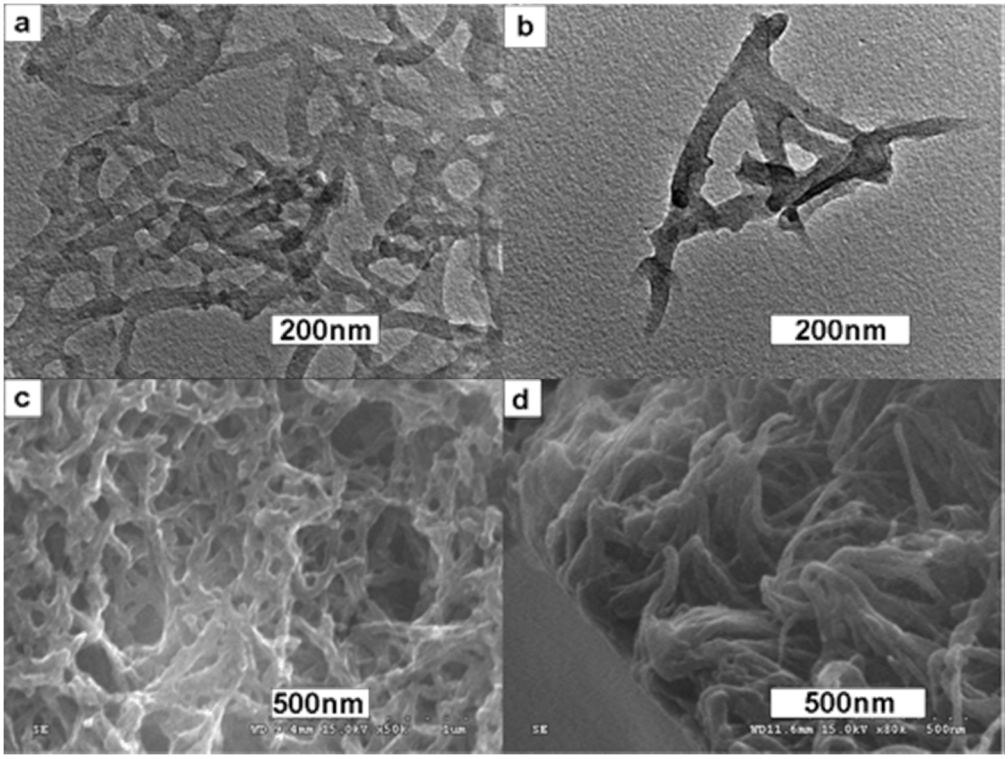

Figure 1.4. (a) TEM image of PANI nanofibers. (b) Enlarged TEM image of a branched network of PANI nanofibers. (c) SEM image of PANI nanofibers. (d) Cross-sectional view of a PANI nanofibers film.[62]

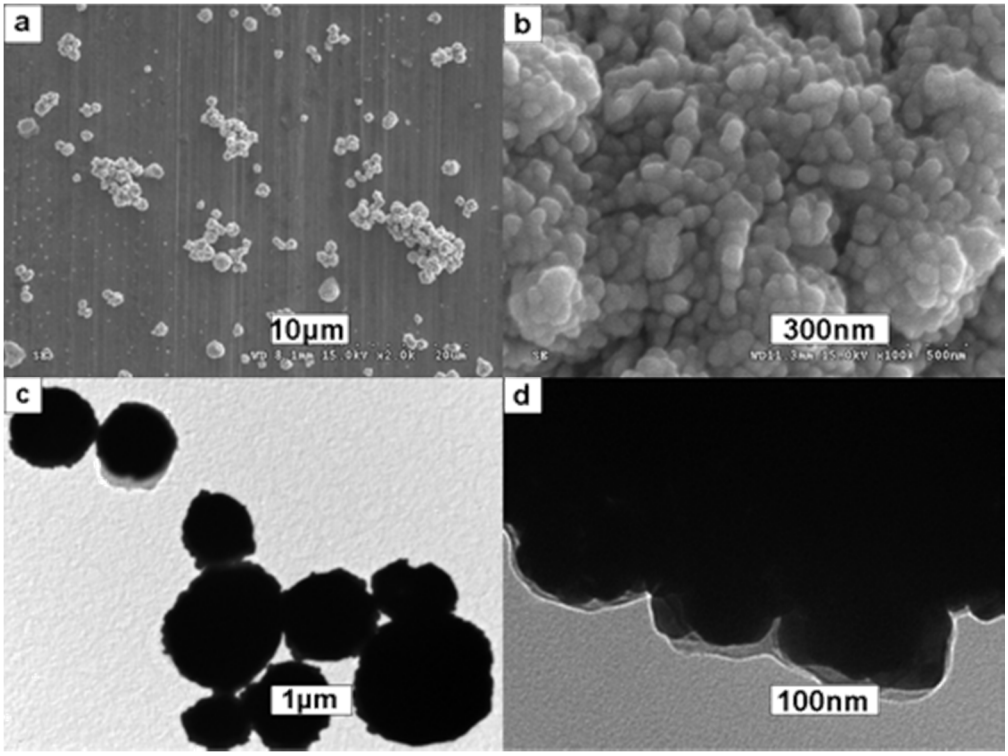

Figure 1.5. SEM images of gold particles at low magnification (a), showing the size distribution of the particles, and at high magnification (b), revealing that an individual gold microparticle is the aggregation of many nanoparticles. TEM images of gold particles at low magnification (c), showing their size distribution, and at high magnification (d), revealing that they are coated by a thin layer of polymer.[62]

Variations of this method have appeared in the literature where surface and phase transfer agents were introduced into the reaction mixture to direct the shape of PANI.[52, 53, 64, 67] For instance, Mallick and coworkers[52] obtained PANI nanoballs decorated with Au nanoparticles in their one-pot synthesis using tricaprylylmethylammonium chloride as a phase-transfer agent. Peng and coworkers[68] prepared AuPANI composites in the presence of sodium dodecyl sulphate. They obtained Au nanoparticles (~20 nm) encapsulated by tetrahedron shaped PANI as shown in Figure 1.6.

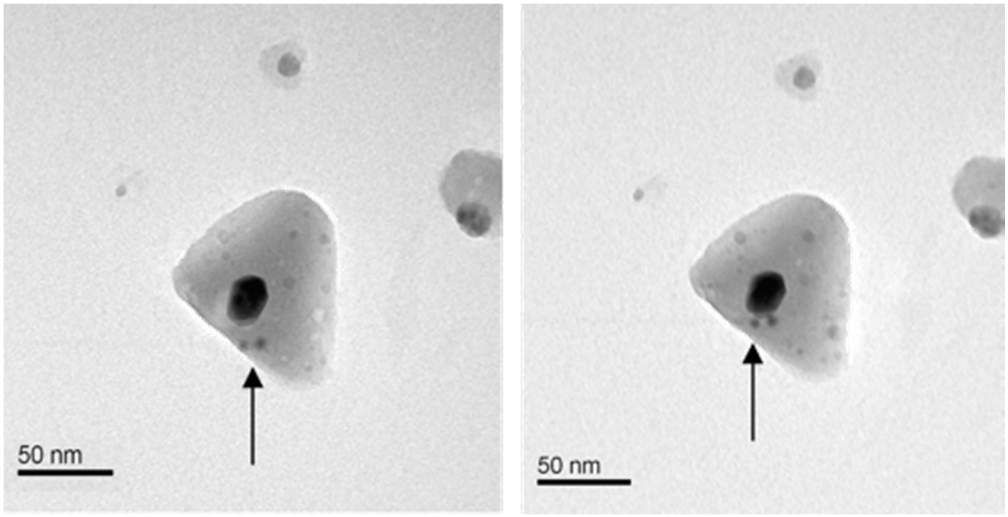

Figure 1.6. Transmission electron microscopy images of AuPANI composite with several Au nanoparticles encapsulated in the PANI tetrahedron. The arrows show the motion of the small Au nanoparticles toward the larger one.[68]

Metal particles have been incorporated into polyaniline in a somewhat indirect manner. Rossi and co-workers[69, 70] polymerized aniline using a variety of oxidizing agents, namely oxygen and hydrogen peroxide, in the presence of gold and copper catalysts. The interesting aspect of this work is that the presence of these nanometal catalysts significantly improved the yield of polymerization from about 13 – 43% to as high as 90%.

1.2.3 The Interaction of Au Nanoparticles with PANI

Despite a large number of reports on the synthesis of AuPANI composites, there are only a few reports on the nature of the interaction of Au nanoparticles with PANI. Polymers are known to stabilize metal nanoparticles mainly by charge transfer interactions between the metal particles and functional groups or heteroatoms on the polymer.[5, 12-14] The direction of this transfer is however in dispute. A detailed XPS

study of the interaction of Au and PANI by Janata and coworkers concluded that PANI (oxidized) has a higher electron affinity than Au nanoparticles.[14] Electrons, therefore, flow from gold to PANI. This was observed by the positive shifts in the binding energies of the gold, the $4_{f7/2}$ peak. The binding energy of the Au electrons was found to be dependent on the size of the nanoparticles, especially when the size of the particles was less than ~5 nm. These results are summarized in Figure 1.7. These results were somewhat corroborated by FTIR results in which the position of the C–N stretch shifted to lower energy for AuPANI relative to PANI. This shift was said to indicate that Au donated electron density to the imino nitrogen in PANI.

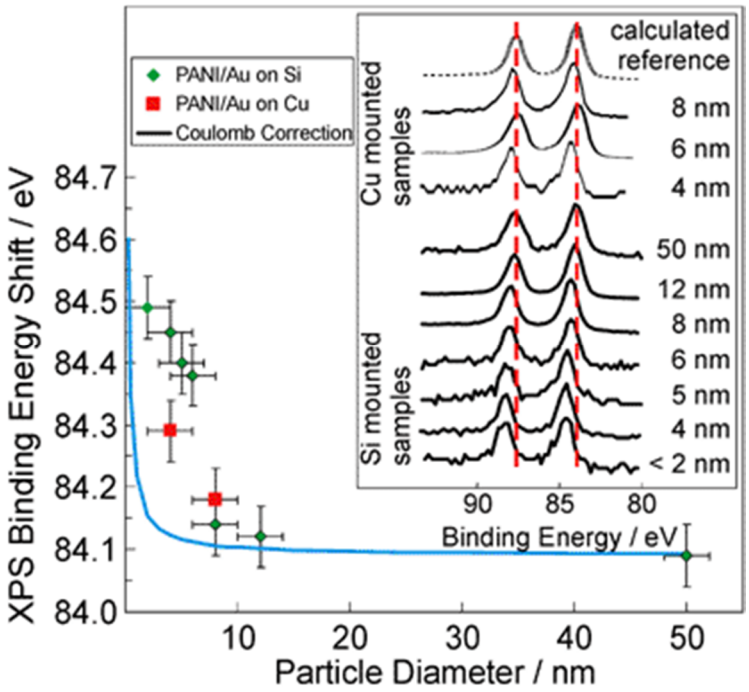

Figure 1.7. Binding energy shift of the Au4f$_{7/2}$ peak for each particle size and (inset) the same values plotted vs. the particle size. [14]

In a study to probe the charge transfer effect in the AuPANI memory system, Tseng and coworkers observed a shift in the binding energy of Au_{4f} from 87.7 eV to 87.5 eV for Au-PANI compared with pure Au film.[13] In addition, the Raman bands of C=N

and $C=N^+$ shifted to high wavenumbers in Au-PANI. All these observations led to the conclusion that charge was being transferred from PANI to Au, contrary to the observations by Janata and coworkers.[14]

1.3 REFERENCES

(1) Virji, S.; Fowler, J. D.; Baker, O.; Huang, J.; Kaner, R. B.; Wieller, B. H. *Small* **2005**, *1*, 624-627.

(2) Sadek, A. Z.; Wlodarski, W.; Kalantar-Zadeh, K.; Baker, C.; Kaner, R. B. *Sens. Actuators, A* **2007**, *139*, 53-57.

(3) Tseng, R. J.; Huang, J.; Ouyang, J.; Kaner, R. B.; Yang, Y. *Nano Lett.* **2005**, *5*, 1077-1080.

(4) Hayakawa, K.; Yoshimura, T.; Esumi, K. *Langmuir* **2003**, *19*, 5517-5521.

(5) Liu, W.; Yang, X.; Xie, L. *J. Colloid Interface Sci.* **2007**, *313*, 494-502.

(6) Imawoto, M.; Kuroda, K.; Zaporojtchenko, V.; Hayashi, S.; Faupel, F. *Eur. Phys. J. D* **2003**, *24*, 365-367.

(7) Ishida, T.; Kuroda, K.; Kinoshita, N.; Minagawa, W.; Haruta, M. *J. Colloid Interface Sci.* **2008**, *323*, 105-111.

(8) Hable, C. T.; Wrighton, M. S. *Langmuir* **1991**, *7*, 1305-1309.

(9) Hable, C. T.; Wrighton, M. S. *Langmuir* **1993**, *9*, 3284-3290.

(10) O'Mullane, A. P.; Dale, S. E.; Macpherson, J. V.; Unwin, P. R. *Chem. Commun.* **2004**, 1606-1607.

(11) Kuroda, K.; Ishida, T.; Haruta, M. *J. Mol. Catal. A: Chem.* **2009**, *298*, 7-11.

(12) Kinyanjui, J. M.; Hatchett, D. W.; Smith, J. A.; Josowicz, M. *Chem. Mater.* **2004**, *16*, 3390-3398.

(13) Tseng, R. J.; Baker, C. O.; Shedd, B.; Huang, J.; Kaner, R. B.; Ouyang, J.; Yang, Y. *Appl. Phys. Lett.* **2007**, *90*, 053101-3.

(14) Smith, J. A.; Josowicz, M.; Engelhard, M.; Baer, D. R.; Janata, J. *Phys. Chem. Chem. Phys.* **2005**, *7*, 3619-3625.

(15) Bialek, B. *Surf. Sci.* **2006**, *600*, 1679-1683.

(16) Huang, W.; MacDiarmid, A. G.; Epstein, A. J. *J. Chem. Soc. , Chem. Commun.* **1987**, 1784-1786.

(17) MacDiarmid, A. G.; Epstein, A. J. *Synth. Met.* **1995**, *69*, 85-92.

(18) Ponzio, E. A.; Echevarria, R.; Morales, G. M.; Barbero, C. *Polym. Int.* **2001**, *50*, 1180-1185.

(19) Wunder, S.; Polzer, F.; Lu, Y.; Mei, Y.; Ballauff, M. *J. Phys. Chem. C* **2010**, *114*, 8814-8820.

(20) Vaschetto, M. E.; Retamal, B. A. *J. Phys. Chem. A* **1997**, *101*, 6945-6950.

(21) Vaschetto, M. E.; Retamal, B. A.; Monkman, A. P. *J. Mol. Struct. THEOCHEM* **1999**, *468*, 209-221.

(22) Focke, W. W.; Wnek, G. E.; Wei, Y. *J. Phys. Chem.* **1987**, *91*, 5813-5818.

(23) Wei, Y.; Focke, W. W.; Wnek, G. E.; Ray, A.; MacDiarmid, A. G. *J. Phys. Chem.* **1989**, *93*, 495-499.

(24) Lux, F. *Polymer*, **1994**, *35*, 2915-2936.

(25) Masters, J. G.; Sun, Y.; MacDiarmid, A. G.; Epstein, A. J. *Synth. Met.* **1991**, *41*, 715-718.

(26) MacDiarmid, A. G.; Epstein, A. J. *Faraday. Discuss. Chem. Soc.* **1989**, *88*, 317-322.

(27) Gospodinova, N.; Terlemezyan, L. *Prog. Polym. Sci.* **1998**, *23*, 1443-1484.

(28) Stejskal, J.; Kratochvíl, P.; Jenkins, A. D. *Polymer*, **1996**, *37*, 367-369.

(29) Manohar, S. K.; Macdiarmid, A. G.; Epstein, A. J. *Synth. Met.* **1991**, *41*, 711-714.

(30) Stejskal, J.; Kratochvil, P.; Spírková, M. *Polymer*, **1995**, *36*, 4135-4140.

(31) de Albuquerque, J. E.; Mattoso, L. H. C.; Faria, R. M.; Masters, J. G.; MacDiarmid, A. G. *Synthetic Metals*, **2004**, *146*, 1-10.

(32) Albuquerque, J. E.; Mattoso, L. H. C.; Balogh, D. T.; Faria, R. M.; Masters, J. G.; MacDiarmid, A. G. *Synth. Met.* **2000**, *113*, 19-22.

(33) Yang, D.; Mattes, B. R. *Synth. Met.* **2002**, *129*, 249-260.

(34) Kang, E. T.; Neoh, K. G.; Khor, S. H.; Tan, K. L.; Tan, B. T. G. *J. Chem. Soc., Chem. Commun.* **1989**, 695-697.

(35) Snauwaert, P.; Lazzaroni, R.; Riga, J.; Verbist, J. J.; Gonbeau, D. *J. Chem. Phys.* **1990**, *92*, 2187-2193.

(36) Kang, E. T.; Neoh, K. G.; Tan, K. L. *Prog. Polym. Sci.* **1998**, *23*, 277-324.

(37) Tang, J.; Jing, X.; Wang, B.; Wang, F. *Synth. Met.* **1988**, *24*, 231-238.

(38) Wu, C.; Bein, T. *Science* **1994**, *264 IS 5166*, 1757-1759.

(39) Qiu, H.; Wan, M. *J. Polym. Sci., Part A: Polym. Chem.* **2001**, *39*, 3485-3497.

(40) Michaelson, J. C.; McEvoy, A. J. *J. Chem. Soc., Chem. Commun.* **1994**, 79-80.

(41) Huang, J.; Kaner, R. B. *J. Am. Chem. Soc.* **2004**, *126*, 851-855.

(42) Huang, J.; Kaner, R. B. *Chem. Commun.* **2006**, 367-376.

(43) Li, D.; Kaner, R. B. *J. Am. Chem. Soc.* **2006**, *128*, 968-975.

(44) Li, D.; Kaner, R. B. *J. Mater. Chem.* **2007**, *17*, 2279-2282.

(45) Li, D.; Huang, J.; Kaner, R. B. *Acc. Chem. Res.* **2009**, *42*, 135-145.

(46) Virji, S.; Fowler, J.; Baker, C.; Huang, J.; Kaner, R.; Weiller, B. *Small* **2005**, *1*, 624-627.

(47) Xian, Y.; Hu, Y.; Liu, F.; Xian, Y.; Wang, H.; Jin, L. *Biosens. Bioelectron.* **2006**, *21*, 1996-2000.

(48) Sarma, T. K.; Chowdhury, D.; Paul, A.; Chattopadhyay, A. *Chem. Commun.* **2002**, 1048-1049.

(49) Sajanlal, P. R.; Sreeprasad, T. S.; Nair, A. S.; Pradeep, T. *Langmuir* **2008**, *24*, 4607-4614.

(50) Kang, E. T.; Ting, Y. P.; Neoh, K. G.; Tan, K. L. *Polymer*, **1993**, *34*, 4994-4996.

(51) Wang, J.; Neoh, K. G.; Kang, E. T. *J. Colloid Interface Sci.* **2001**, *239*, 78-86.

(52) Mallick, K.; Witcomb, M. J.; Dinsmore, A.; Scurrell, M. S. *Macromol. Rapid Commun.* **2005**, *26*, 232-235.

(53) Peng, Z.; Guo, L.; Zhang, Z.; Tesche, B.; Wilke, T.; Ogermann, D.; Hu, S.; Kleinermanns, K. *Langmuir* **2006**, *22*, 10915-10918.

(54) Zhang, L.; Peng, H.; Kilmartin, P. A.; Soeller, C.; Tilley, R.; Travas-Sejdic, J. *Macromol. Rapid Commun.* **2008**, *29*, 598-603.

(55) Zhang, X.; Chechik, V.; Smith, D. K.; Walton, P. H.; Duhme-Klair, A. *Macromolecules* **2008**, *41*, 3417-3421.

(56) Pillalamarri, S. K.; Blum, F. D.; Tokuhiro, A. T.; Bertino, M. F. *Chem. Mater.* **2005**, *17*, 5941-5944.

(57) Gospodinova, N.; Mokreva, P.; Terlemezyan, L. *Polym. Int.* **1996**, *41*, 79-84.

(58) Neoh, K. G.; Young, T. T.; Looi, N. T.; Kang, E. T.; Tan, K. L. *Chem. Mater.* **1997**, *9*, 2906-2912.

(59) Drelinkiewicz, A.; Hasik, M.; Choczyski, M. *Mater. Res. Bull.* **1998**, *33*, 739-762.

(60) Turkevich, J.; Stevenson, P. C.; Hillier, J. *Disc. Faraday Soc.* **1951**, *11*, 55-75.

(61) Frens, G. *Nat. Phys. Sci.* **1973**, *241*, 20-22.

(62) Wang, Y.; Liu, Z.; Han, B.; Sun, Z.; Huang, Y.; Yang, G. *Langmuir* **2005**, *21*, 833-836.

(63) Mallick, K.; Witcomb, M. J.; Scurrell, M. S. *J. Phys. D* **2009**, *42*, 095409.

(64) Guo, Z.; Zhang, Y.; Huang, L.; Wang, M.; Wang, J.; Sun, J.; Xu, L.; Gu, N. *J. Colloid Interface Sci.* **2007**, *309*, 518-523.

(65) Nirmala Grace, A.; Pandian, K. *J.Phys. Chem. Solids* **2007**, *68*, 2278-2285.

(66) Qiu, W.; Huang, H.; Zeng, S.; Xue, T.; Liu, J. *J. Polym. Res.* **2010**, 1-5.

(67) Li, W.; Jia, Q. X.; Wang, H. *Polymer* **2006**, *47*, 23-26.

(68) Peng, Z.; Guo, L.; Zhang, Z.; Tesche, B.; Wilke, T.; Ogermann, D.; Hu, S.; Kleinermanns, K. *Langmuir* **2006**, *22*, 10915-10918.

(69) Chen, Z.; Pina, C. D.; Falletta, E.; Faro, M.; Pasta, M.; Rossi, M.; Santo, N. *J. Catal.* **2008**, *258*, 1-4.

(70) Chen, Z.; Pina, C. D.; Falletta, E.; Pasta, M.; Rossi, M. *J. Catal.* **2009**, *267*, 93-96.

2 SYNTHESIS OF GOLD-POLYANILINE NANOCOMPOSITES BY COMPLEXATION

2.1 INTRODUCTION

A number of catalytic systems based on metal nanoparticles embedded in a polymer have been reported over the last years.[1-3] One of the major advantages of using polymers is that they usually act as both reducing and protecting agent for the metal nanoparticles. An example is polyaniline. A number of synthetic procedures have been used to disperse metal nanoparticles on polyaniline and they can be classified depending on whether (1) the polymer (or monomer in some cases)[4] was used as both a reducing and protecting agent[5, 6] or (2) a strong reducing agent was added to a mixture of metal precursor and polymer.[7, 8] In the latter case, small metal particles in the range of 1 – 4 nm are usually formed because of the formation of a large number of metal nuclei. For instance the rapid addition of $NaBH_4$ to an aqueous solution of $HAuCl_4$ and poly(*N*-vinyl-2-pyrrolidone) (PVP) led to the formation of evenly dispersed Au nanoparticles with an average diameter of 1.3 ± 0.3 nm while an average diameter of 9.5 ± 1.0 nm was obtained by the use of the weaker reducing agent, Na_2SO_3.[9]

In this Chapter we report a technique to synthesize gold-polyaniline (AuPANI) nanocomposites. The technique extends the work of Amaya and co-workers[10] in which they showed that pre-organizing Pd(II) species on polyaniline leads to the formation of well dispersed Pd nanoparticles. The technique involves two stages: (1) complexation of metal ions with polyaniline, and (2) reduction of metal ions and their aggregation to form metal nanoparticles. In their work, Amaya and co-workers[10]

performed the complexation reaction in tetrahydrofuran (THF) under argon. The resulting complex was refluxed in ethanol at 80 ºC for 1 hour to reduce Pd(II) ions to metallic Pd. We report here the synthesis of gold-polyaniline nanocomposites via the complexation technique with all reactions carried out in water at room temperature. Small gold nanoparticles of 3 nm and less were obtained. Previous studies have suggested that the complexation of PANI with metals is a two step process.[11] In the first step the amine nitrogen on PANI is first oxidized to imine by a metal cation with subsequent coordination of the reduced metal cation to an imine nitrogen. The final step of this process is a reverse oxidation of the metal cation and reduction of imine group to amine. We show in this Chapter that in our case the mechanism of complexation involves the partial oxidation of polyaniline from emeraldine to pernigraniline and there is no reversal of the redox reactions. In addition the degree of reduction of the metal ions is shown to be dependent on the molar ratio of the metals ions to the nitrogen atoms.

2.2 EXPERIMENTAL

All chemicals were of analytical grade and were used as received. A stock solution of 10^{-2} M $HAuCl_4$ was prepared by dissolving 0.394g of $HAuCl_4.3H_2O$ in enough distilled water to make a 100mL solution. All chemicals, except $HAuCl_4.3H_2O$, were obtained from Sigma-Aldrich. $HAuCl_4.3H_2O$ was sourced from SA Precious Metal (Pty) Ltd.

Synthesis of polyaniline. Polyaniline was synthesized using a scaled up "rapidly mixed reaction"[12] in which a solution of 20 g aniline in 1 M HCl (800 mL) was rapidly mixed with a solution of 32 g $(NH_4)_2S_2O_8$ in 200 mL of 1 M HCl. The mixture was stirred immediately to ensure efficient mixing before polymerization

began (about 2 minutes). The reaction vessel was then left un-stirred overnight at room temperature. The resultant green suspension was filtered and washed several times with about 2 L of distilled water and about 250 mL of methanol and dried at room temperature for 24 hours and in an oven at 50 ºC for 12 hours.

Synthesis of gold-polyaniline (AuPANI) nanocomposites. A typical protocol for the synthesis of AuPANI is as follows. PANI was first deprotonated by mixing 1 g of PANI (emeraldine form) with 50 mL of 0.1 M NaOH solution. This mixture was stirred for 30 minutes and washed with distilled water until the pH of the filtrate dropped to 7. The moist cake was then suspended in 100 mL of distilled to which 25 mL of 10^{-2} M $HAuCl_4$ solution was rapidly added while stirring. This should yield a maximum of 5% Au loading by weight. The actual loading was measured by thermogravimetric analysis using a Perkin Elmer Thermogravimetric Analyser. After 2 hours the mixture was filtered, washed with distilled water, and divided in two equal parts. One part was labelled AuPANI Complex (AuPANI-C) and dried while the other was suspended in 50 mL of water to which 15 mg of $NaBH_4$ in 10 mL of distilled water was rapidly added. After stirring for 1 hour the final product was filtered, washed with distilled water, and dried. This product was labelled Au-PANI Reduced (AuPANI-R). The synthesis can easily be scaled up to produce up to 5 g of Au-PANI-R. Various ratios, from ~21 to 3, of N/Au were used. In addition, the ratio of $NaBH_4$/Au was varied from 1 to 15 to study of effect of amount of reducing agent on the size and shape of Au nanoparticles. A mild reducing agent was used to study the effect of the strength of the reducing agent on the size of the gold nanoparticles. Ascorbic acid produced very large gold particles and this reducing agent was abondened as the goal was to synthesize small gold particles with a narrow particle size distribution.

Uv-vis spectroscopy. Absorbance UV-VIS spectra were recorded on a Varian Cary 50 spectrometer. All measurements were performed in a single quartz cuvette with a 1 cm path length. For in-situ measurements, 1 mL of 10^{-3} M $HAuCl_4$ was diluted to 10 mL in ethanol. This solution was added to a 1 mg/10 mL suspension of deprotonated PANI in ethanol (10 mL). A sample of 3 mL of this mixture was rapidly transferred to a UV-vis cuvette. Measurements were taken in the range of 200 nm – 450 nm every 1 minute at room temperature (about 22 ºC). The first measurement was recorded after about 20 seconds of mixing the reactants.

Transmission electron microscopy. A small amount of powdered sample was dispersed in methanol by sonication and a drop of the suspension placed on a lacey copper grid. A Technai Spirit G2 microscope was used to record images at 200 kV. The same instrument was used for energy dispersive spectroscopy (EDS).

FTIR spectroscopy. All FTIR spectra in the mid-infrared range were collected using a Bruker Tensor 27 spectrometer equipped with a MIRacle™ ATR accessory (Pike Technologies). A total of 64 scans were recorded for each sample with a resolution of 4 cm^{-1}. Far IR measurements were recorded on a Brucker Tensor 37 spectrometer.

Open circuit potential measurements. The synthesis of AuPANI complexes was monitored as a function of time using a two electrode cell Pt|reaction solution||saturated calomel electrode (SCE).

Powder X-ray diffraction. The PXRD data were collected using a Bruker AXS D8 using Cu-K radiation (40kV, 40mA).

2.3 RESULTS AND DISCUSSION

2.3.1 The Formation of Gold-Polyaniline Complex

Uv-vis Spectroscopy. Polyaniline was synthesized via the "rapidly mixed reaction" and produced fibrous PANI in the emeraldine oxidation state. [12] Uv-vis spectroscopy was used to follow the consumption of $AuCl_4^-$ during complexation by the disappearance of the strong ligand to metal charge transfer (LMCT) peaks at 225 nm and 313 nm.[13-15] Figure 2.1 shows that the reaction of $AuCl_4^-$ with PANI was very fast under our reaction conditions. No $AuCl_4^-$ was detected by uv-vis spectroscopy after 2 minutes of addition of $HAuCl_4$ to PANI. The supernatant liquid obtained after centrifuging the reacted mixture of $HAuCl_4$ and PANI (AuPANI-C) turned milky on addition of $AgNO_3$ indicating the precipitation of AgCl. The only source of chloride ions in this system was $HAuCl_4$. This indicates that the reaction of $HAuCl_4$ with PANI involves the evolution of chloride ions from $HAuCl_4$ through either ligand substitution or reduction. When the reaction was slowed down by reducing the concentration of both the reactants and changing solvent from water to ethanol, the uv-vis spectrum recorded in-situ, showed a similar trend and two residual peaks around 205 nm and 275 nm. These peaks belong to neither PANI nor $AuCl_4^-$.

The uv-vis spectrum of PANI after treatment with NaOH shows two peaks, one around 320 nm and the other at 700 nm. These correspond to a $\pi - \pi^*$ transition associated with the electrons of the benzene ring delocalized on N atoms and to an excitation of electron from the HOMO of the benzeniod to the LUMO of quinoid moiety[16-18](Figure 2.3), respectively. After addition of $HAuCl_4$ to an aqueous dispersion of the deprotonated PANI, the uv-vis spectrum of the complex shows two peaks, albeit slightly shifted, around 320 nm and 700 nm, and a new peak around

1000 nm which tails to the IR region. The emergence of the peak at 1000 nm is consistent with the complexation of deprotonated PANI with metal ions.[10, 19] The intensity of this new peak increases with an increase in

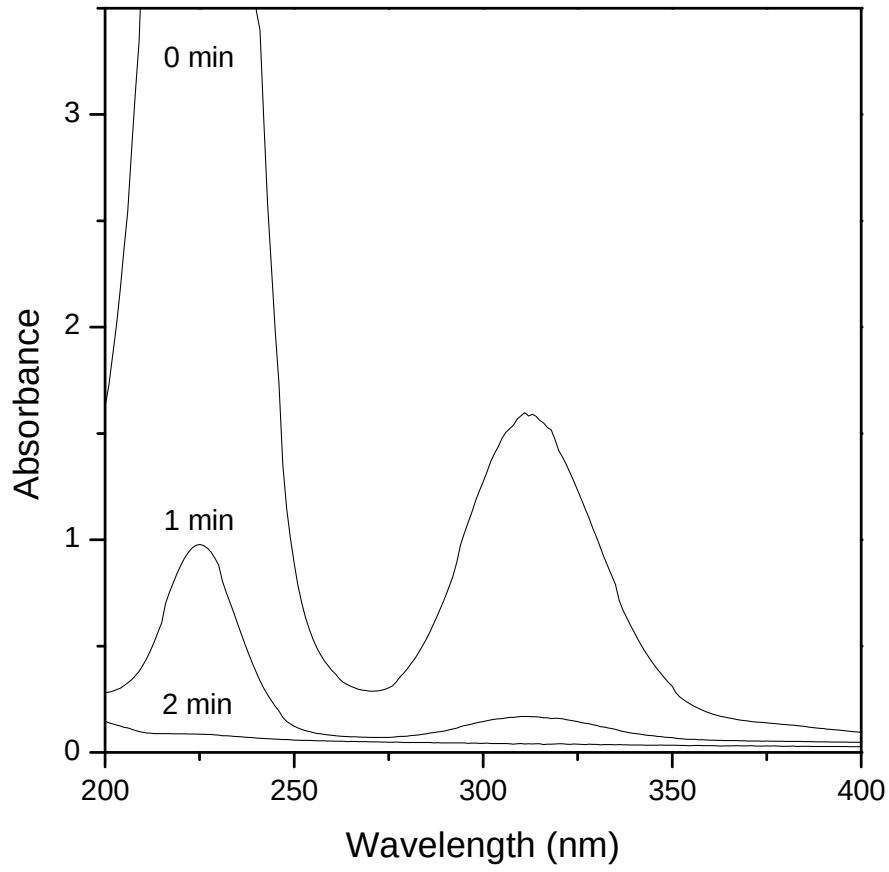

Figure 2.1. Consumption of $AuCl_4^-$ followed by uv-vis spectroscopy measurements. The peaks at 225 nm and 310 nm due to LMCT decreased in intensity and disappeared within 2 minutes after addition of $HAuCl_4$ to an aqueous suspension of deprotonated PANI. Samples were filter through a 0.45 mm membrane filtered before recording the spectrum.

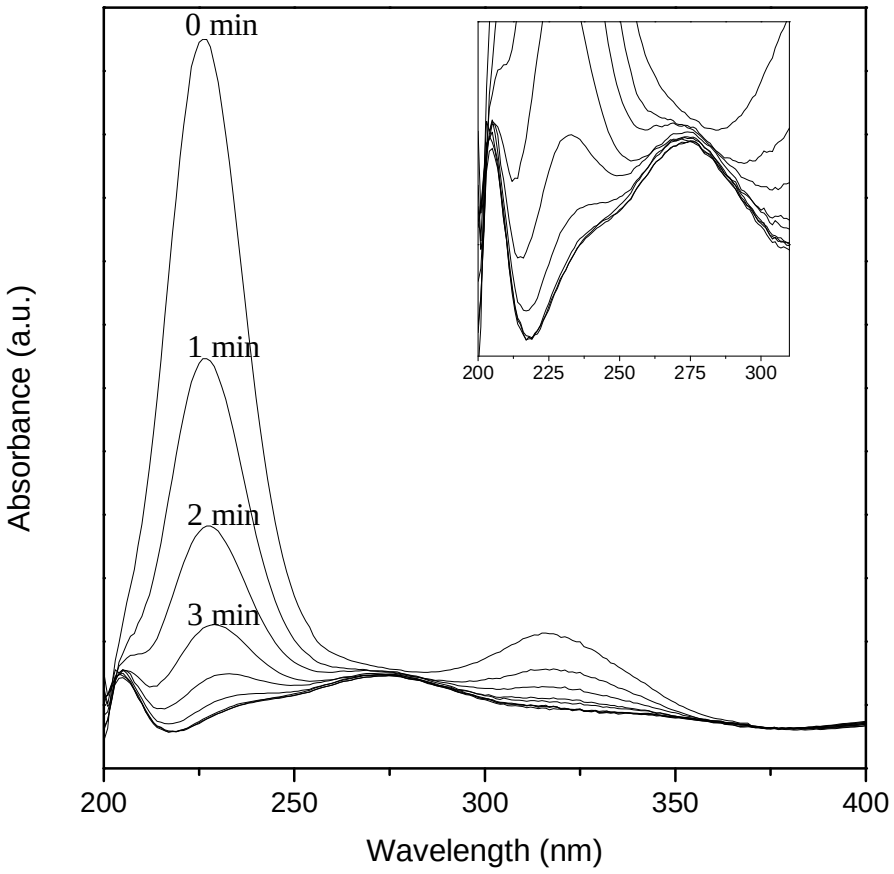

Figure 2.2. In-situ uv-vis spectra of the complexation of PANI and $AuCl_4^-$ in ethanol. Insert shows the peaks at 205 nm and 275 nm.

the amount of $HAuCl_4$ used (decrease in ratio of N\Au).This new peak (the so called free carrier tail)[20], due to delocalization of electrons in the HOMO (polaron band) of PANI, is dependent on the conformation of PANI chains. The delocalization of π electrons in the polaron band, and consequently the free carrier tail, is suppressed in "coiled" chains with π defects caused by ring twisting.[20] This delocalization of π electrons can be brought about by the formation of a polysemiquinone radical cation during both protonic and pseudo-protonic doping of PANI.[21, 22] Transition metals ions with high electrode potentials ions such as Ag(I)[23], Cu(II)[24], Au(III)[25], and Pd(II)[26] can oxidize the benzenoid group of PANI. The reduced metal ions can then form a complex with PANI. Such a complexation process has been confirmed by changes in

the uv-vis spectra of metal-PANI complexes through either the appearance of a blue-shifted peak around 540 nm[24] or the appearance of a free-carrier peak.[10] The peak at 540 nm indicates that PANI has been oxidized from the emeraldine to pernigraniline form.[27]

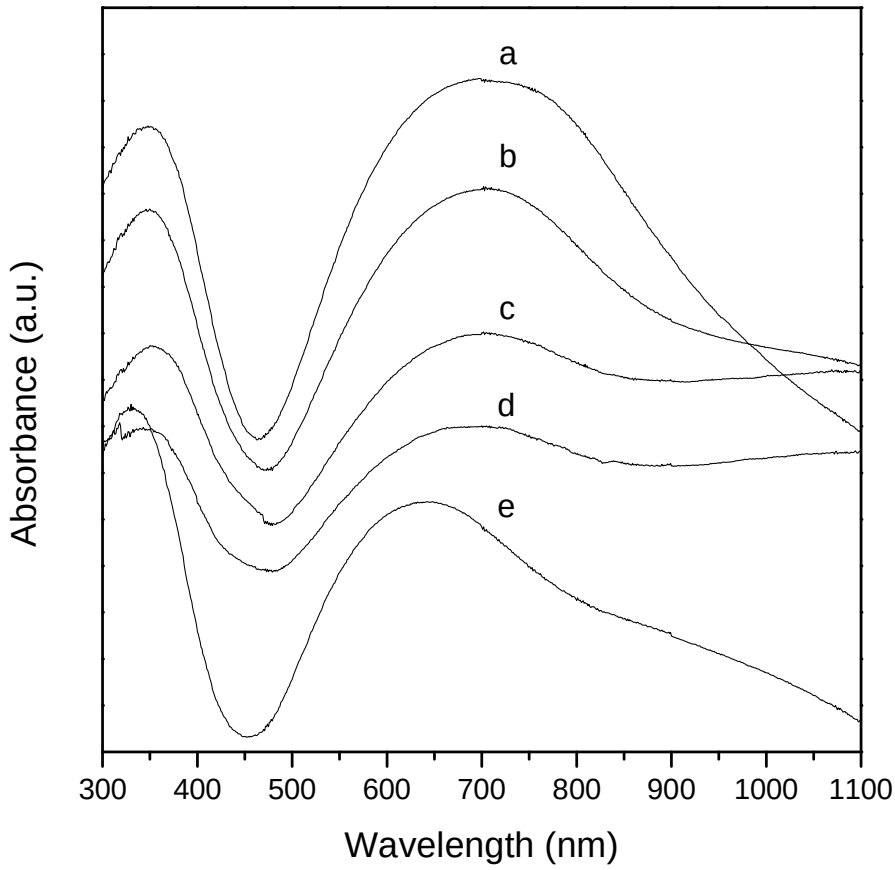

Figure 2.3. Uv-vis spectra of (a) deprotonated PANI and AuPANI complexes prepared using N/Au ratios of (b) 21, (c) 11, (d) 5.4, and (e) 2.7. A new peak around 1000 nm which tails down to the IR regime is observed in the spectra of AuPANI complexes.

In Figure 2.3, the polaronic peak at 700 nm is slightly blue-shifted after an increase in the concentration of $HAuCl_4$. This suggests that PANI has been partially oxidized

from the emeraldine state to pernigraniline state. The gold precursor that was used in this study, $HAuCl_4$, is a fairly strong acid and it is possible that the changes in the uv-vis spectrum after reacting PANI with $HAuCl_4$ are due to both protonation and complexation of Au ions with PANI. It is also possible that $AuCl_4^-$ ions could act as counter-ions to the positively charged N atom on PANI after protonation. Deprotonated PANI is known to readily reduce a number of transition metal ions including Au ions to lower oxidation states or even the metallic form.[25, 25]

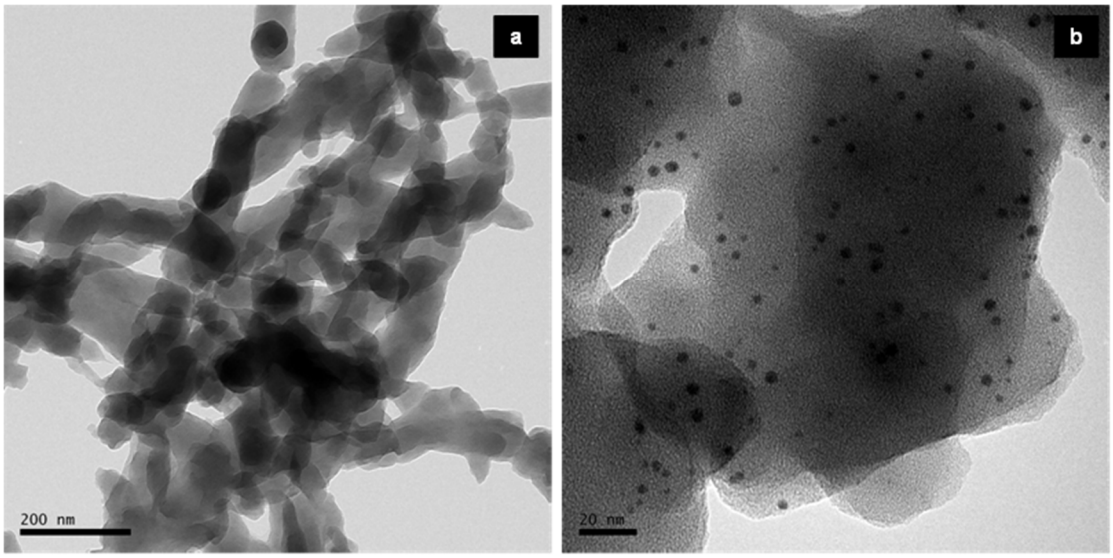

Figure 2.4. TEM imgaes of (a) AuPANI-C and (b) AuPANI-R for a N/Au ratio of 21 and $NaBH_4$/Au = 3.2. Gold nanoparticles in AuPANI-R, with an average particle diameter of 2.6 nm, were identified by EDX.

However, TEM images of AuPANI-C do not show any Au nanoparticles at N/Au ratios higher than 2.7; these are only observed after treating AuPANI-C with $NaBH_4$ (Figure 2.4). In addition the free-carrier tail in the uv-vis spectrum of AuPANI-C was still observed after treating AuPANI-C with a solution of 0.1 M NaOH. The interaction of PANI with NaOH results in the deprotonation of PANI. That this peak persisted after base treatment points towards the complexation of Au ions to PANI.

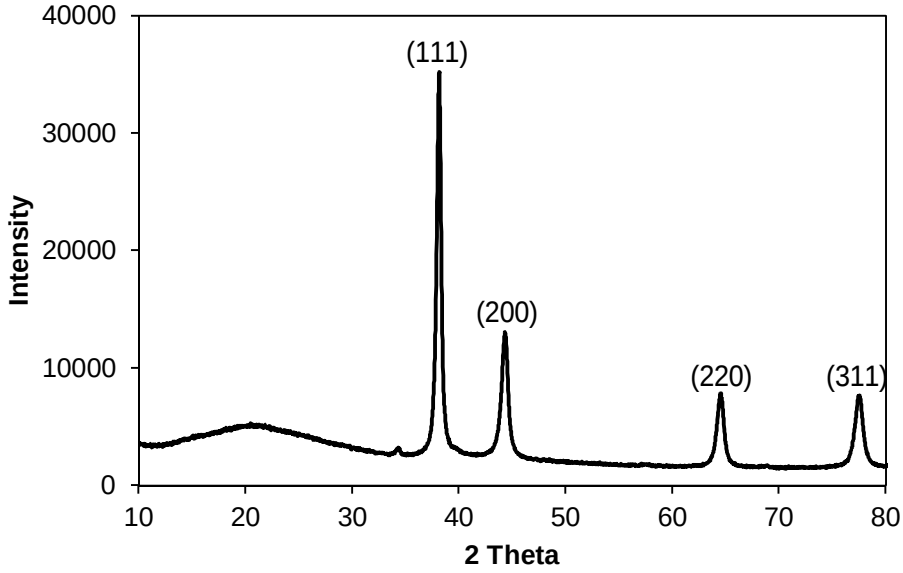

Figure 2.5. PXRD pattern of gold nanoparticles dispered on polyaniline.

The PXRD pattern for the gold nanoparticles dispersed on polyaniline is shown in Figure 2.5. Peaks at 2θ values of 38˚, 44˚, 65˚, and 78˚ corresponding to Miller indices (111), (200), (220), and (311), respectively, confirmed the fcc crystalline geometry of gold nanoparticles.

Open Circuit Potential Measurements: The oxidation of PANI from emeraldine to the pernigraniline state depends on the electrochemical potential of the system which in turn depends on (1) the oxidation potential and concentration of oxidizing agents used[21], (2) the oxidation potential of PANI chains and (3) the pH of the system.[28-30]

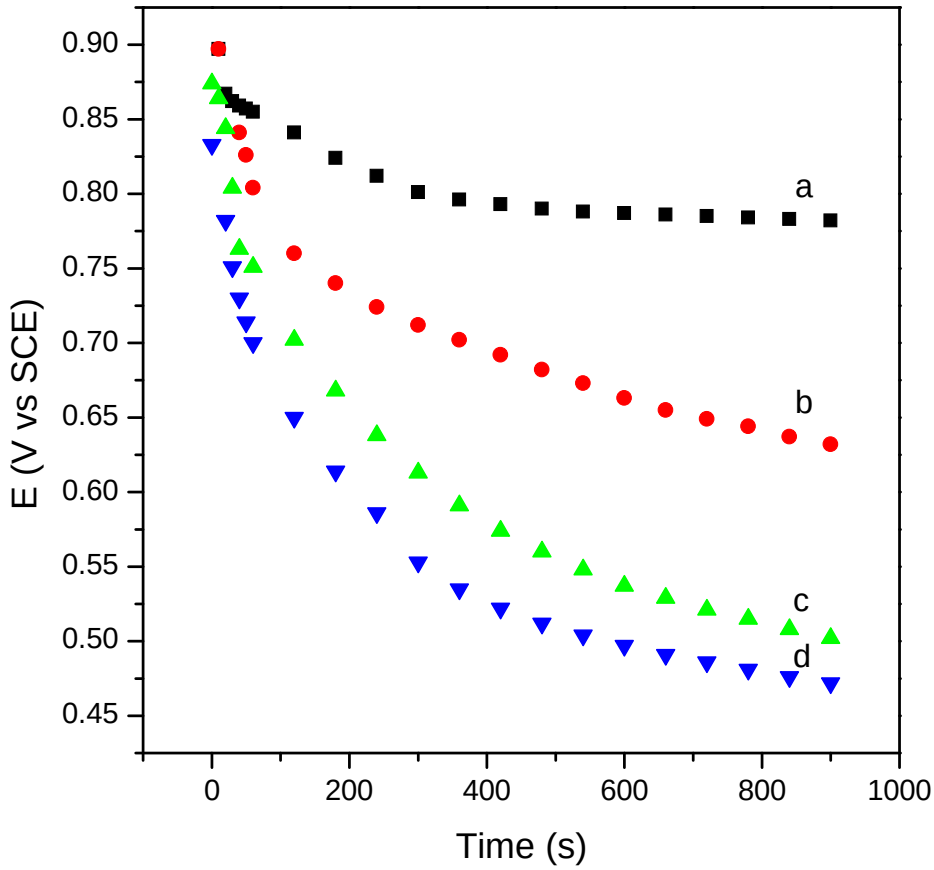

Figure 2.6. Electrochemical potential profiles of PANI complexation at different N/Au ratios: (a) 2.7, (b) 5.4, (c) 11, (d) 21. Time = 0 seconds is the time when the highest E was reached.

The difference in the electrochemical potential of pernigraniline and emeraldine decreases with an increase in the pH of reaction medium and a decrease in the degree of protonation of PANI. Cyclic voltammetric studies have shown that the oxidation of PANI from emeraldine to pernigraniline occurs at a potential of about 0.55 V vs. SCE.[31-33] Figure 2.6 shows the electrochemical potential profile of PANI complexation at different N/Au molar ratios. In all cases, when a solution of $HAuCl_4$ was added to a suspension of PANI the electrochemical potential (E) of the systems rose sharply to some maximum and immediately declined. Both the maximum E

reached and the rate at which E dropped varied with the ratio of N/Au. At the highest ratio used (21) the electrochemical potential rises to about 0.83 V vs. SCE and drops off rapidly to about 0.50 V vs. SCE, Figure 2.6 (d). For the lowest ratio of N/Au = 2.7 (the highest concentration of $HAuCl_4$) the potential rises to about 0.90 V vs. SCE and drops slightly to about 0.80 V where it remains fairly constant for the duration of the experiment.

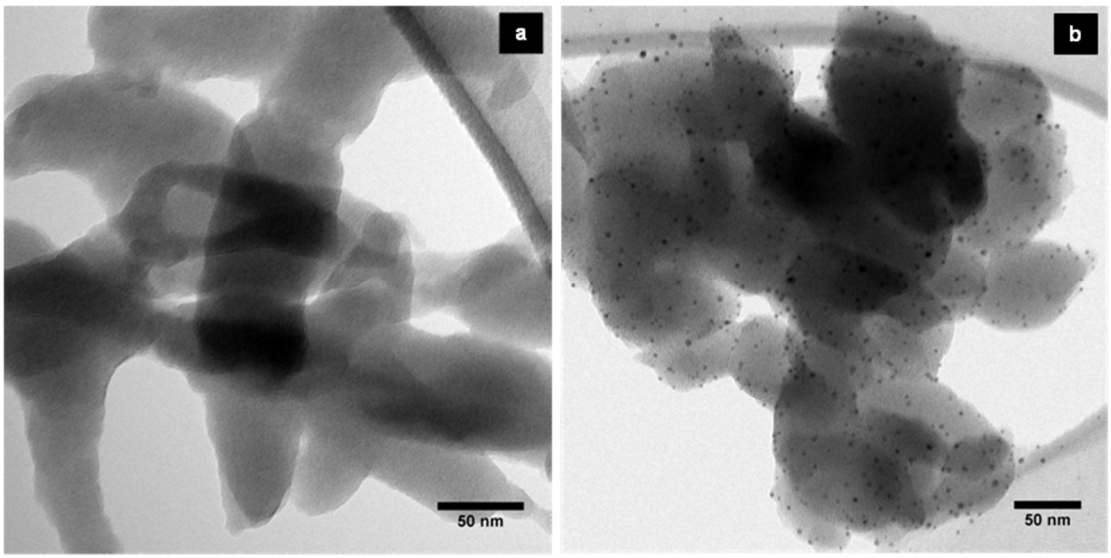

Figure 2.7. TEM images of AuPANI complexes for N/Au ratios of (a) 5.4 and (b) 2.7 indicating that $AuCl_4^-$ is only reduced to Au(0) by PANI at a ratio of 2.7.

This difference in the electrochemical potential implies that the extent of oxidation of PANI (and reduction of Au^{3+}) is different under the different reaction conditions. A high electrochemical potential implies a higher degree of oxidation of PANI and reduction of Au^{3+}. These results are in agreement with the observed variation in the electrochemical potential and extent of oxidation of PANI using $(NH_4)_2S_2O_8$ as an oxidizing agent.[21] Indeed both FTIR (discussed further below) and TEM measurements show this variation. TEM images only show gold nanoparticles for AuPANI-C prepared at a ratio of Au/N = 2.7 in which the electrochemical potential of the system was the highest (Figure 2.7).

FTIR Spectroscopy. FTIR spectra recorded in the fingerprint region has proved quite useful in studying the interaction of metals ions with PANI.[8, 34] Figure 2.8 shows the FTIR spectra of PANI, Au-PANI-C, and AuPANI-R at a ratio of N/Au = 21. Characteristic deprotonated PANI IR bands are observed at 1590 cm^{-1} (stretching of N=Q=N), 1496 cm^{-1} (stretching of N–B–N), 1304 cm^{-1} (C–N stretch in QBB or BBQ), 1165 cm^{-1} (a mode of N=Q=N), and 825 cm^{-1} (C–H out of plane bending)[35, 36], where Q denotes quinoid unit and B is the benzenoid unit. The IR spectrum of AuPANI-C shows the characteristic PANI peaks, albeit shifted to lower frequencies, and a new peak at 1134 cm^{-1}. Such shifts, the disappearance of the 1165 cm^{-1} band, and the appearance of a peak at 1135 cm^{-1} are an indication of the transition of PANI from the emeraldine base to the emeraldine salt[35] or the complexation of PANI with Lewis acids and metal ions.[34, 37]

However, after treating AuPANI-C with $NaBH_4$ the peak at 1134 cm^{-1} disappears and a peak at 1165 cm^{-1} reappears (Figure 2.8). In addition, the positions of the benzenoid stretch and the C-N stretch in QBB or BBQ do not change while the quinoid stretch shifts from 1580 cm^{-1} to 1587 cm^{-1}. The relative integral intensities of the quinoid and benzenoid peaks are often used as an indication of the degree of oxidation of PANI.[31] The ratio of the integral intensities $I_{Quinoid}/I_{Benzenoid}$ increases from about 0.68 to 0.80 for PANI and AuPANI-C. This increase indicates a slight oxidation of the amine N to imine when $AuCl_4^-$ is added to PANI and further supports the suggestion that Au ions form a complex with PANI via a redox process. Since a slight excess of $NaBH_4$ was used the value of $I_{Quinoid}/I_{Benzenoid}$ dropped to 0.67 after reducing AuPANI-C indicating that some imine N were reduced to the amine form.

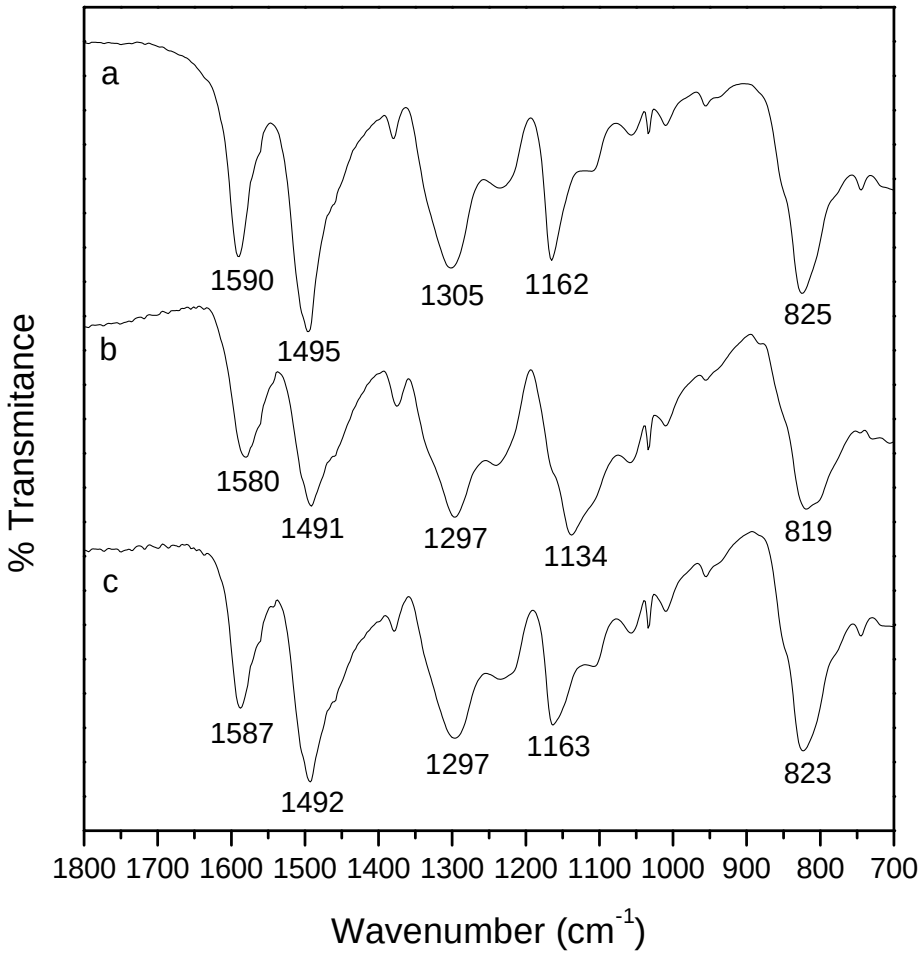

Figure 2.8. FTIR spectra of (a) deprotonated PANI, (b) AuPANI-C, and (c) AuPANI-R. Ratio of N/Au = 21 and $NaBH_4$/Au = 3.2.

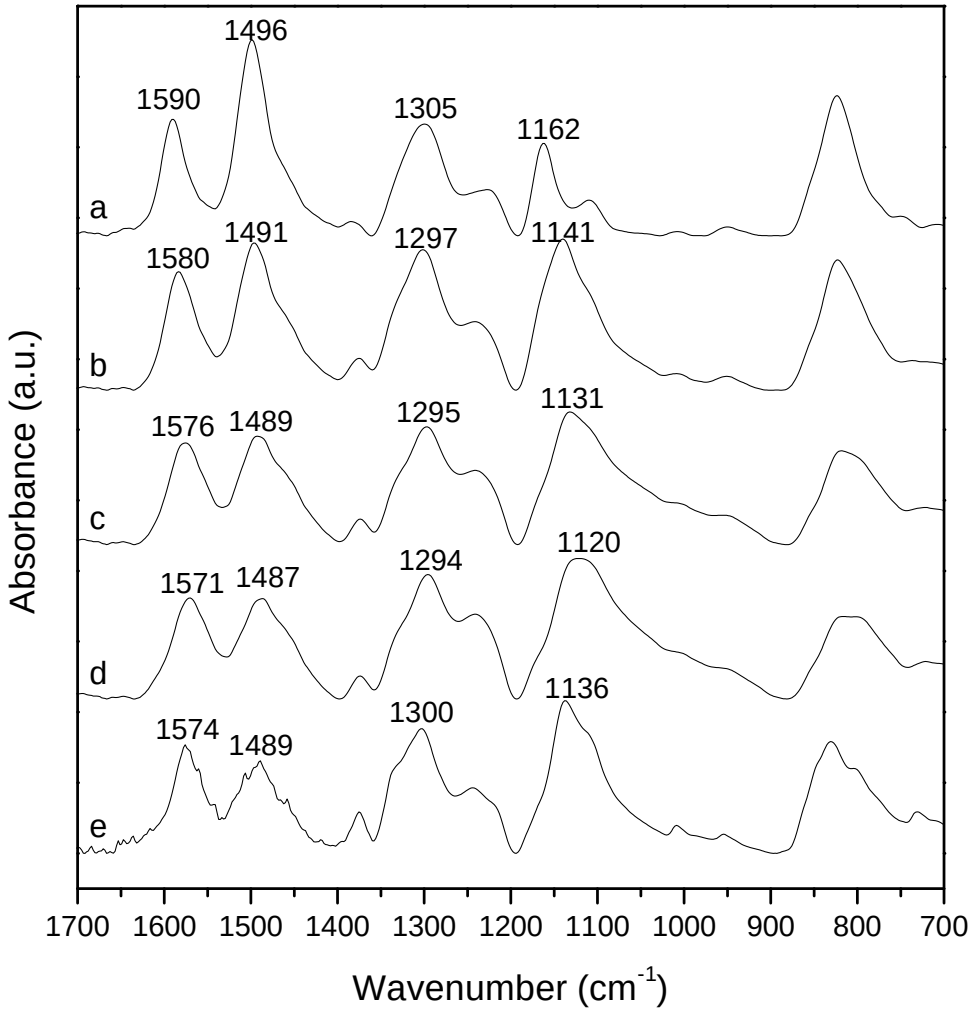

Figure 2.9. FTIR spectra of AuPANI complexes in the mid-IR range showing structural changes in the polymer backbone with an increase in the amount of HAuCl4. Spectrum (a) is for deprotonated PANI and spectra (b) - (e) are for AuPANI complexes at N\Au ratio of 21, 11, 5.4 and 2.7.

When the ratio of N/Au was decreased from 21 to ~3 by increasing the amount of $HAuCl_4$, the value of $I_{Quinoid}/I_{Benzenoid}$ increased from 0.80 to 1.2 indicating an increase in the degree of oxidation of PANI as predicted by an increase in the electrochemical potential of the system. The spectra are shown in Figure 2.9 and data summarised in

Table 2.1 alongside the electrochemical potential results. The interaction of $HAuCl_4$ with N containing compounds has been shown to occur at the N atom through ligand substitution which is often accompanied by the reduction of gold ions.[38] Density functional theory (DFT) studies of the interaction of amino acids and DNA with Au_3 clusters have shown they occur by electron transfer from N, O, and S (from amine, carboxylic, and sulphur groups) to 5d and 6s orbitals of Au via lone pairs.[39, 40] In addition a nonconventional H-bond between amine and Au, N–H···Au, in which Au acts as a proton acceptor was identified. It was further observed that the complexation resulted in the weakening of the C–N bonds in amino acids and a red shift in the stretching modes of these bonds. The observed red shift in the frequency of the stretching of N=Q=N and others in AuPANI-C complexes indicates the interaction of PANI and Au ions.

Table 2.1. A summary of FTIR and electrochemical results showing an increase in the degree of oxidation of PANI with increasing amount of $HAuCl_4$.

N/Au	$I_{Quinoid}/I_{Benzenoid}$	E after 30 min (V vs SCE)	$\Delta\nu$ (N=Q=N)[a] cm^{-1}	$\Delta\nu$ (N=Q=N)[b] cm^{-1}
21	0.80	0.47	10	21
10.7	0.94	0.50	14	31
5.4	1.00	0.63	19	52
2.7	1.20	0.78	16	36

$\Delta\nu$ is the difference between the frequency of stretching of N=Q=N between the complex and deprotonated PANI at (a) 1590 cm^{-1} and (b) 1162 cm^{-1}.

Figure 2.10 shows FTIR spectra (in the region of 2800 – 3500 cm^{-1}) of AuPANI-C samples prepared by varying the molar ratio of N/Au from 21 to 2.7. The spectrum of

deprotonated PANI (Figure 2.10), shows two absorbance peaks at 3384 cm^{-1} and 3318 cm^{-1} due to non-hydrogen bonded N–H and hydrogen bonded N–H stretching vibrations, respectively.[17, 41-43]

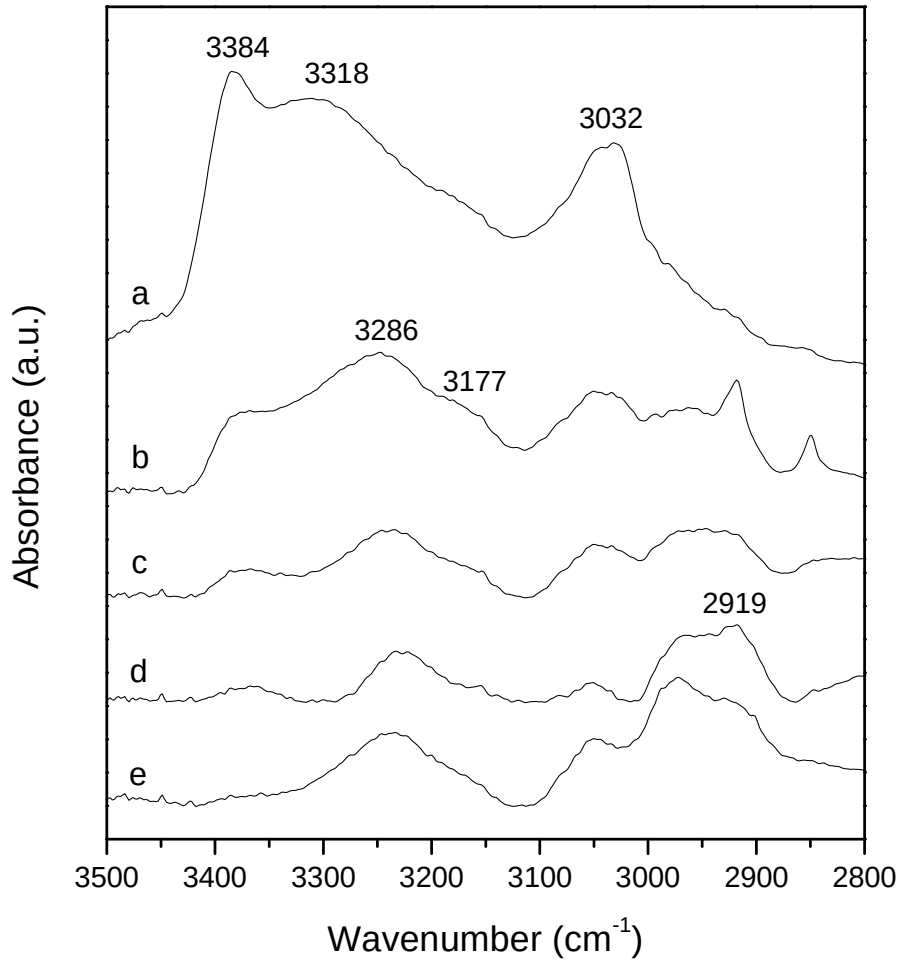

Figure 2.10. FTIR spectra of (a) depronated PANI and AuPANI complexes at N/Au ratio of (b) 21, (b) 11, (c) 5.4 and (e) 2.7 in the IR region of 2800 – 3500 cm^{-1}.

The peak at 3032 cm^{-1} which is seen in the spectra of all the other samples is assigned to the stretching vibration of the benzene ring C–H bonds.[44] Hydrogen bonding in

PANI has been shown to be stronger when it occurs between imine and amine sites than between amine-amine sites. In emeraldine base (deprotonated PANI) this is seen by a broad peak at ~3300 cm^{-1}. The stretching frequencies of N–H bonds have been correlated with the N···N distances and the strength of the hydrogen bond with low frequencies indicating that the corresponding hydrogen bond is strong and short.[41]

The FITR spectrum of AuPANI-C with N/Au = 21 shows an absorption peak due to stretching vibrations of non-hydrogen bonded N–H at 3384 cm^{-1}, a new peak at 3286 cm^{-1} which we assign to hydrogen bonded N–H stretching vibrations, and two new peaks at 3000 – 2900 cm^{-1}. The relative intensity of the 3384 cm^{-1} peak to the 3286 cm^{-1} peak decreases with a decrease in the ratio of N atoms in PANI to Au atoms (N/Au). This decrease indicates that the degree of hydrogen bonding increases with an increase in the amount of $HAuCl_4$. It is tempting to assign the cause of this increased hydrogen bonding to protonation of PANI. However, the lack of a very broad and intense absorption centred around 1100 cm^{-1} rule out this possibility. In addition, no significant protonation of PANI is expected from the addition of a 10^{-2} M solution $HAuCl_4$ to PANI. An estimate of the extent of protonation calculated using Equations 1 and 2 below shows that less than 10% of imine nitrogens would be protonated at pH = 2.

$$\left[\text{PANI}-\text{H}^+\right]=\frac{\left[\text{H}^+\right]}{K_a+\left[\text{H}^+\right]} \qquad (2.1)$$

$$pK_a = 0.48\,pH - 0.043 \qquad (2.2)$$

In Equation 2.1 $\left[\text{PANI}-\text{H}^+\right]$ is the fraction of protonated PANI and K_a is the acid dissociation constant of PANI.[45] The peak at 3286 cm^{-1} is therefore assigned to N–

H···Cl hydrogen bonds between N–H and a gold chloride complex. The disappearance of the absorbance peak at 3384 cm^{-1} and the appearance of the peak at 3286 cm^{-1} indicate that the incorporation of gold chloride in the PANI matrix breaks the N–H···N hydrogen bonds and introduces N–H···Cl hydrogen bonds. A similar observation was made in thin films of deprotonated PANI in *N*-methyl-2-pyrrolidinone (NMP) in which N–H···N bonds were broken by N–C=O···H–N bonds.[43] When NMP was extracted with methanol the peak due to free N–H stretching vibrations reappeared. This observation is consistent with uv-vis results which show a free-carrier tail in the spectra of AuPANI complexes. There are two possible explanations which are not necessarily mutually exclusive that show the link between the uv-vis and FTIR results. Firstly, the incorporation of $AuCl_4^-$ into the PANI matrix breaks the N–H···N bonds, some of which could be intra-chain. The breakage of these H-bonds and the formation of a gold-polyaniline complex would results in the polymer chains assuming a more expanded configuration. Secondly, the doping of PANI results in the formation of a polysemiquinone radical. Both situations would lead to the appearance of a free-carrier tail in the uv-vis spectrum of AuPANI complexes.

Complexation Mechanism. The complexation of $AuCl_4^-$ as a step in its reduction was first postulated by Turkevich and co-workers[46] in their "organizer" mechanism for nucleation. In this mechanism $AuCl_4^-$ forms a complex with a multidentate reducing agent in some sort of a macromolecule which at some point undergoes molecular rearrangement to redox products. Several recent reports have shown that indeed the reduction of $AuCl_4^-$ proceeds via a complexation step.[47-51] In most cases the complexation of $AuCl_4^-$ occurs by substitution of a chloride ion to form a short-

lived complex which maintains the square planar geometry. A two-electron transfer from the coordinated reducing agent to Au(III) takes place by an intermolecular process which often leads to decomposition of the reducing agent. For example, the reduction of Au(III) by glycine proceeds by formation of a complex (*O*-coordination) which decomposes to formaldehyde, carbon dioxide and an ammonium ion.[49]

Based on experimental observations and existing literature it is possible to postulate a mechanism for the complexation and reduction of Au(III) by deprotonated PANI.[24, 52] First, PANI coordinates to Au(III) **1** via an amine N **2** by substituting a chloride ion (Scheme 2.1) to give a complex **3**. This is then followed by a two-electron transfer from PANI to Au(III) transforming the benzenoid group to quinoid **5**. The resultant $[AuCl_2]^-$ then coordinates to an imine N of the quinoid group through electron transfer from N to Au and N–H···Cl hydrogen bonds (Scheme 2.2). The actual structure of the complex is not known. However, a necessary requirement for the formation of nuclei in the classical LaMer theory is a large local concentration of atoms which coalesce only when a stable particle can be formed.[53] Turkevich and coworkers postulated this requirement being met by the formation of complex between gold ions and reducing agent in the production of gold sols.[46] Kumar and co-workers envisioned this complex between gold(I) ions and dicarboxy acetone being a chain-like structure with three Au^+ ions joined by at least two dicarboxy acetone molecules. A recent *in-situ* X-ray absorbance fine structure (XAFS) spectroscopy study has also revealed the formation of di- and trimetric gold chloride complexes during prior to full reduction of $AuCl_4^-$ in the presence of poly(vinylpyrrolidone).[54] The polymeric gold species comprised Au^+ ions.

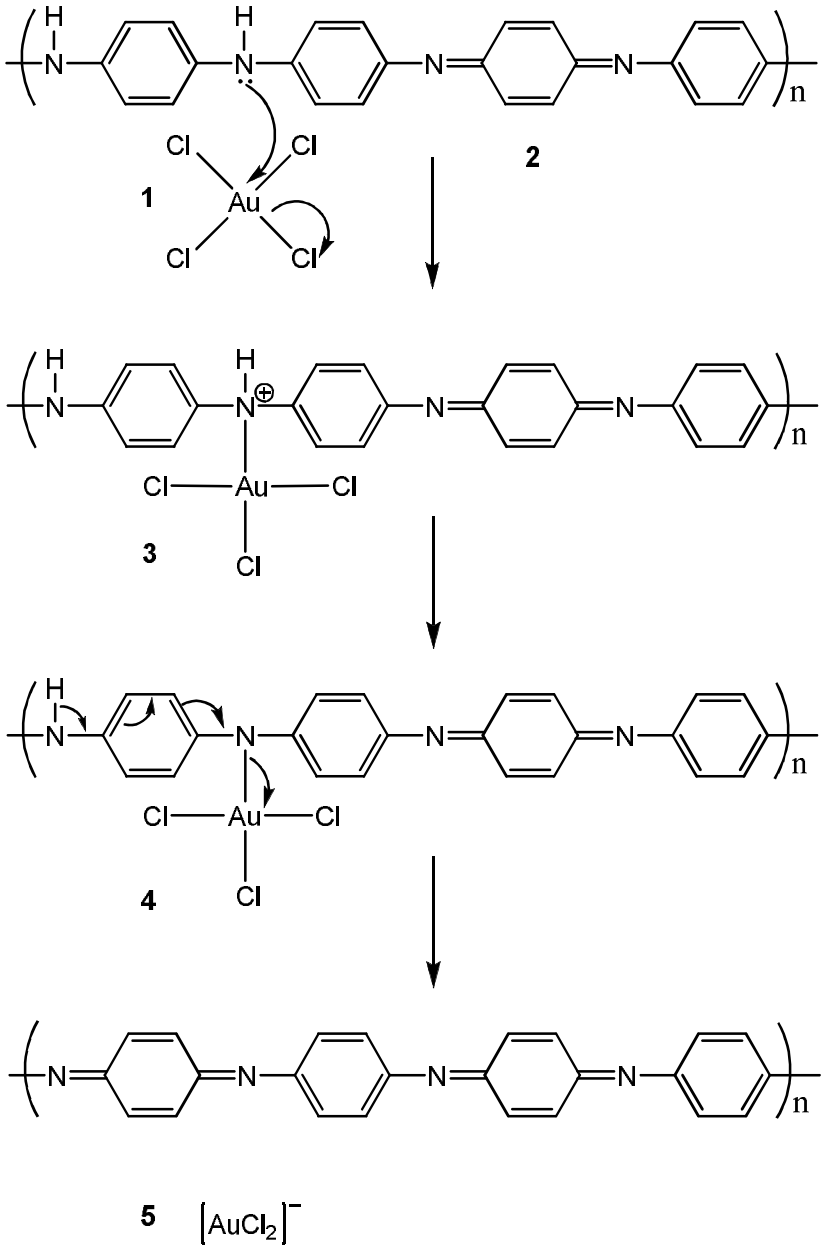

Scheme 2.1. Proposed mechanism for the formation of AuPANI complex.

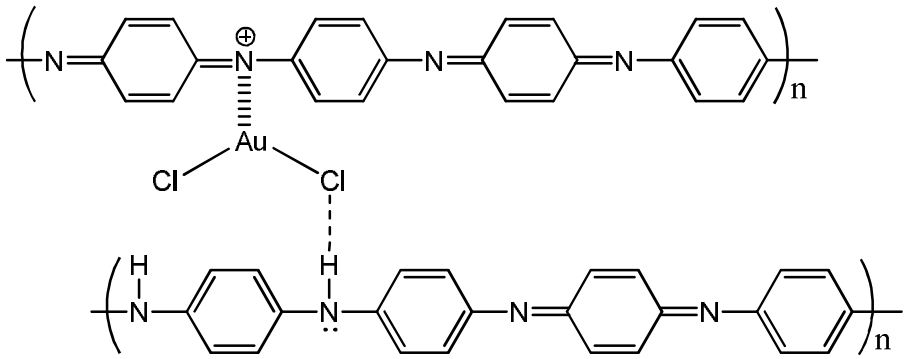

Scheme 2.2. Possible interactions of Au and PANI through electron transfer from N to Au and H-bonding.

2.3.2 The Effect of Molar Ratio of Reducing Agent to Au Precursor on the Size and Shape of Au Nanoparticles

The formation of gold nanoparticles (Au NPs) was achieved by reducing the Au ions in AuPANI-C (N/Au = 21) with $NaBH_4$. As shown in Figures 2.11 and 2.12 the size of the Au NPs decreased with an increase in the ratio of $NaBH_4$ to $HAuCl_4$. A steep decrease in particle size, from 9.5 ± 2.1 nm to 2.6 ± 0.6 nm, is observed when the ratio changes from 1:1 to 3:1. A decrease in particle size with an increase in the ratio $NaBH_4$:$HAuCl_4$ is in accordance with the nucleation-growth model of nanoparticles formation which predicts a monotonic decrease in particle size with increasing reductant:metal-precusor ratio.[55] A fast nucleation, achieved at higher concentrations of reductant, followed by a diffusion controlled growth leads to the formation of small particles with a narrow size distribution.[46, 55] When the $NaBH_4$:$AuCl_4^-$ ratio was increased further from 3:1 to 6:1 the size of the particles dropped slightly from 2.6 ± 0.6 nm to 2.2 ± 0.5 nm. Data from Turkevich et. al.[46] and Frens[55], among others, also showed a disproportionate decrease in the gold particle size when the ratio of citrate to gold increased from 0.4 to 2 but almost no change in particle size when the ratio changed from 2 to 7.[48] At low ratios of reductant to gold precursor the number of Au nuclei formed is limited by the concentration of the reducing agent. This then causes a sharp increase in the number of Au nuclei and the observed steep decrease in the size of Au particles when the concentration of reducing agent is increased.[48]

However, a slight increase in the particle size was observed when the ratio $NaBH_4$:$AuCl_4^-$ was greater than 6. In addition a number of networked Au structures appeared. The observed increase in the size of Au particles could be a demonstration of a weakening of the attractive interactions of Au NP's and PANI when higher

concentrations of $NaBH_4$ are used and/or a slower nucleation rate. The interaction of metal nanoparticles with PANI is believed to occur via charge transfer between PANI

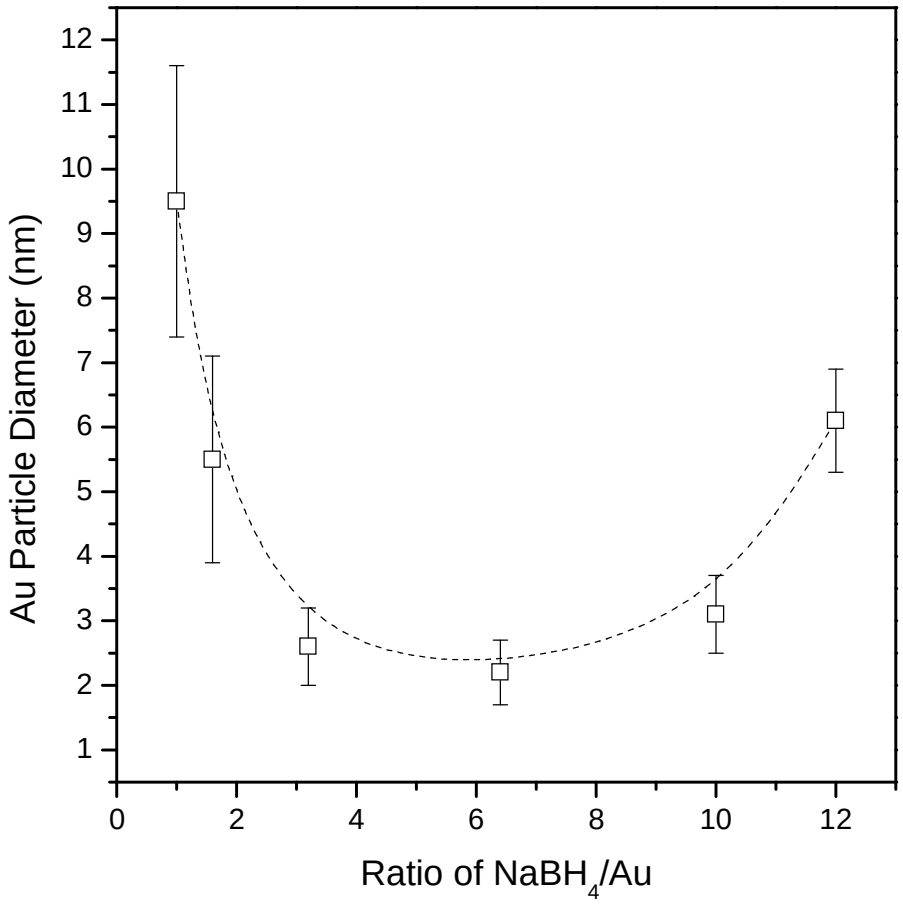

Figure 2.11. Variation of Au nanoparticles diameter with amount of $NaBH_4$. Averages were calculated by measuring at least 300 particles from TEM images using ImageJ. All error bars are 1 standard deviation of the distributions.

and metal in which electron clouds at conjugate C=N partially transfer to metal NP's.[56, 57] Such charge transfer was not observed when PANI was reduced from emeraldine to leucoemeraldine using N_2H_4.[56] As shown in Table 2.2 the ratio of the integral intensities $I_{Quinoid}/I_{Benzenoid}$ decreased from 0.93 to 0.62 when the ratio of

$NaBH_4$ to Au was increased from 1:1 to 10:1 indicating a decrease in the degree of oxidation of PANI. A decrease in the degree of oxidation implies a decrease in the number of C=N to interact with Au NP's and a consequent increase in particle size. $[AuCl_4]^-$ is known to gradually transform to $[AuCl_x(OH)_{4-x}]^-$ (where x ranges from 0 to 4) with increasing pH.[13, 58] Table 2.2 shows that the pH of the reaction solution increased with an increase in the amount of $NaBH_4$ used for reducing Au ions. Ji and coworkers[59] observed a substantial decrease in the reactivity of Au(III) towards reduction by citrate at pH = 6.2. This decrease in reactivity coincided with the structural change of Au(III) complexes from the more reactive $[AuCl_3(OH)]^-$ to the less reactive $[AuCl_2(OH)_2]^-$. It is likely that the gold-chloride/PANI complexes formed before reduction in our experiments are transformed to hydroxyl containing gold complexes at high ratios of $NaBH_4$:$HAuCl_4$. This transformation would similarly cause a decrease in the reactivity of Au ions towards reduction resulting in a slower nucleation rate and large Au particles.

Table 2.2. Variation of solution pH and degree of oxidation with ratio of $NaBH_4$/Au.

$NaBH_4$:$HAuCl_4$	$I_{Quinoid}/I_{Benzenoid}$	%Oxidized	pH of Solution
1.0:1	0.93	48	3.5
1.6:1	0.85	46	3.6
3.2:1	0.77	44	4.9
6.3:1	0.70	41	5.8
10:1	0.62	38	7.4
12:1	0.58	37	7.9

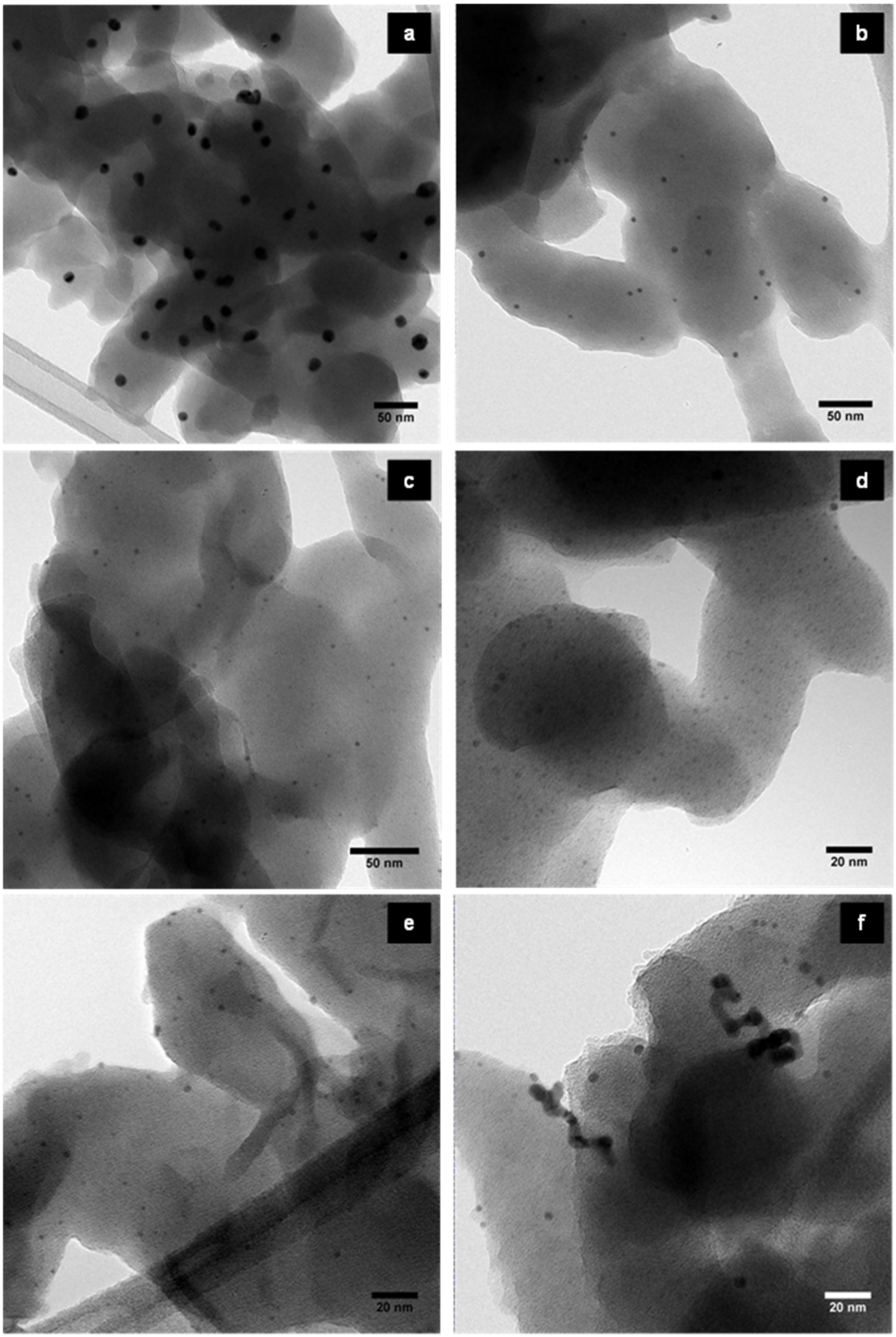

Figure 2.12. TEM images of AuPANI-R showing the variation of Au particle size and shape with variation in the amount of $NaBH_4$ used. The images correspond to $NaBH_4$/Au ratio of (a) 1.0, (b) 1.6, (c) 3.2, (d) 6.4, (e) 10, and (f) 12.

2.4 CONCLUSIONS

In conclusion, we have demonstrated that composites of gold nanoparticles and polyaniline nanofibres can be synthesized by the complexation technique in water at room temperature. The degree of reduction of $AuCl_4^-$ depends on the electrochemical potential of the system which in turn depends on the ratio N/Au. At N/Au ratios greater than 2.7 $AuCl_4^-$ was complexed with PANI via partial reduction of the gold ions and oxidation of PANI. Complete reduction of $AuCl_4^-$ was observed when the ratio of N/Au was about 2.7. Gold nanoparticles formed when the AuPANI complexes were reduced with $NaBH_4$. The size of the nanoparticles varied with the amount of $NaBH_4$ used. Low amounts of $NaBH_4$ induced slow nucleation rates and large particles formed as a result. The smallest Au nanoparticles with a narrow size distribution were obtained when a ratio of $NaBH_4$ to Au of about 6 was used.

2.5 REFERENCES

(1) Drelinkiewicz, A.; Hasik, M.; Kloc, M. *Synth. Met.* **1999**, *102*, 1307-1308.

(2) Houdayer, A.; Schneider, R.; Billaud, D.; Ghanbaja, J.; Lambert, J. *Appl. Organomet. Chem.* **2005**, *19*, 1239-1248.

(3) Ishida, T.; Kuroda, K.; Kinoshita, N.; Minagawa, W.; Haruta, M. *J. Colloid Interface Sci.* **2008**, *323*, 105-111.

(4) Kinyanjui, J. M.; Hatchett, D. W.; Smith, J. A.; Josowicz, M. *Chem. Mater.* **2004**, *16*, 3390-3398.

(5) Imawoto, M.; Kuroda, K.; Zaporojtchenko, V.; Hayashi, S.; Faupel, F. *Eur. Phys. J. D* **2003**, *24*, 365-367.

(6) Sakai, T.; Alexandridis, P. *J. Phys. Chem. B* **2005**, *109*, 7766-7777.

(7) Drelinkiewicz, A.; Zięba, A.; Sobczak, J. W.; Bonarowska, M.; Karpiński, Z.; Waksmundzka-Góra, A.; Stejskal, J. *React Funct Polym* **2009**, *69*, 630-642.

(8) Nyczyk, A.; Sniechota, A.; Adamczyk, A.; Bernasik, A.; Turek, W.; Hasik, M. *Eur. Polym. J.* **2008**, *44*, 1594-1602.

(9) Tsunoyama, H.; Sakurai, H.; Ichikuni, N.; Negishi, Y.; Tsukuda, T. *Langmuir* **2004**, *20*, 11293-11296.

(10) Amaya, T.; Saio, D.; Hirao, T. *Tetrahedron Lett.* **2007**, *48*, 2729-2732.

(11) Dimitriev, O. P. *Polym. Bull.* **2003**, *50*, 83-90.

(12) Huang, J.; Kaner, R. B. *Angew. Chem. Int. Ed.* **2004**, *43*, 5817.

(13) Peck, J. A.; Tait, C. D.; Swanson, B. I.; Brown Jr., G. E. *Geochim. Cosmochim. Acta* **1991**, *55*, 671-676.

(14) Usher, A.; McPhail, D. C.; Brugger, J. *Geochim. Cosmochim. Acta* **2009**, *73*, 3359-3380.

(15) Gangopadhayay, A. K.; Chakravorty, A. *J. Chem. Phys.* **1961**, *35*, 2206-2209.

(16) de Albuquerque, J. E.; Mattoso, L. H. C.; Faria, R. M.; Masters, J. G.; MacDiarmid, A. G. *Synth. Met.*, **2004**, *146*, 1-10.

(17) Yang, D.; Mattes, B. R. *Synth. Met.* **2002**, *129*, 249-260.

(18) Huang, W. S.; MacDiarmid, A. G. *Polymer* **1993**, *34*, 1833-1845.

(19) Izumi, C. M. S.; Constantino, V. R. L.; Ferreira, A. M. C.; Temperini, M. L. A. *Synth. Met.* **2006**, *156*, 654-663.

(20) MacDiarmid, A. G.; Epstein, A. J. *Synth. Met.* **1995**, *69*, 85-92.

(21) Gospodinova, N.; Mokreva, P.; Terlemezyan, L. *Polym. Int.* **1996**, *41*, 79-84.

(22) Ponzio, E. A.; Echevarria, R.; Morales, G. M.; Barbero, C. *Polym. Int.* **2001**, *50*, 1180-1185.

(23) Li, W.; Jia, Q. X.; Wang, H. *Polymer* **2006**, *47*, 23-26.

(24) Izumi, C. M. S.; Ferreira, D. C.; Costa Ferreira, A. M. D.; Temperini, M. L. A. *Synth. Met.* **2009**, *159*, 1165-1173.

(25) Wang, J.; Neoh, K. G.; Kang, E. T. *J. Colloid Interface Sci.* **2001**, *239*, 78-86.

(26) Gao, Y.; Chen, C.; Gau, H.; Bailey, J. A.; Akhadov, E.; Williams, D.; Wang, H. *Chem. Mater.* **2008**, *20*, 2839-2844.

(27) Albuquerque, J. E.; Mattoso, L. H. C.; Balogh, D. T.; Faria, R. M.; Masters, J. G.; MacDiarmid, A. G. *Synth. Met.* **2000**, *113*, 19-22.

(28) Gospodinova, N.; Mokreva, P.; Terlemezyan, L. *Polymer* **1993**, *34*, 1330-1332.

(29) Gospodinova, N.; Mokreva, P.; Terlemezyan, L. *Polymer* **1995**, *36*, 3585-3587.

(30) Cushman, R. J.; McManus, P. M.; Cheng Yang, S. *J. Electroanal. Chem.* **1987**, *219*, 335-346.

(31) Hatchett, D. W.; Josowicz, M.; Janata, J.; Baer, D. R. *Chem. Mater.* **1999**, *11*, 2989-2994.

(32) Genies, E. M.; Lapkowski, M. *J. Electroanal. Chem.* **1987**, *220*, 67-82.

(33) Saheb, A.; Smith, J. A.; Josowicz, M.; Janata, J.; Baer, D. R.; Engelhard, M. H. *J. Electroanal. Chem.* **2008**, *621*, 238-244.

(34) Hasik, M.; Drelinkiewicz, A.; Wenda, E.; Paluszkiewicz, C.; Quillard, S. *J. Mol. Struct.* **2001**, *596*, 89-99.

(35) Tang, J.; Jing, X.; Wang, B.; Wang, F. *Synth. Met.* **1988**, *24*, 231-238.

(36) Ohira, M.; Sakai, T.; Takeuchi, M.; Kobayashi, Y.; Tsuji, M. *Synth. Met.* **1987**, *18*, 347-352.

(37) Yang, C.; Chen, C.; Zeng, Y. *Spectrochim. Acta, Part A* **2007**, *66*, 37-41.

(38) Nagel, Y.; Beck, W. *Z. Anorg. Allg. Chem.* **1985**, *529*, 57-60.

(39) Pakiari, A. H.; Jamshidi, Z. *J. Phys. Chem. A* **2007**, *111*, 4391-4396.

(40) Kryachko, E. S.; Remacle, F. *Nano Lett.* **2005**, *5*, 735-739.

(41) Colomban, P.; Gruger, A.; Novak, A.; Régis, A. *J. Mol. Struct.* **1994**, *317*, 261-271.

(42) Gruger, A.; Novak, A.; Régis, A.; Colomban, P. *J. Mol. Struct.* **1994**, *328*, 153-167.

(43) Zheng, W.; Angelopoulos, M.; Epstein, A. J.; MacDiarmid, A. G. *Macromolecules* **1997**, *30*, 2953-2955.

(44) Socrates, G. In *Infrared and Raman Characteristic Group Frequencies;* John Wiley & Sons: Chichester, 2001; pp 157-167.

(45) Chiang, J.; MacDiarmid, A. G. *Synth. Met.* **1986**, *13*, 193-205.

(46) Turkevich, J.; Stevenson, P. C.; Hillier, J. *Disc. Faraday Soc.* **1951**, *11*, 55-75.

(47) Zou, J.; Guo, Z.; Parkinson, J. A.; Chen, Y.; Sadler, P. S. *Chem. Commun.* **1999**, 1359-1360.

(48) Kumar, S.; Gandhi, K. S.; Kumar, R. *Ind Eng Chem Res* **2007**, *46*, 3128-3136.

(49) Sen, P.; Gani, N.; Midya, J.; Pal, B. *Transition Met. Chem.* **2008**, *33*, 229-236.

(50) Vujačić, A. V.; Savić, J. Z.; Sovilj, S. P.; Mészáros Szécsényi, K.; Todorović, N.; Petković, M. Ž.; Vasić, V. M. *Polyhedron* **2009**, *28*, 593-599.

(51) Ojea-Jiménez, I.; Romero, F. M.; Bastús, N. G.; Puntes, V. *J. Phys. Chem. C* **2010**, *114*, 1800-1804.

(52) Dimitriev, O. P.; Kislyuk, V. V. *Synth. Met.* **2002**, *132*, 87-92.

(53) LaMer, V. K.; Dinegar, R. H. *J. Am. Chem. Soc.* **1950**, *72*, 4847-4854.

(54) Yao, T.; Sun, Z.; Li, Y.; Pan, Z.; Wei, H.; Xie, Y.; Nomura, M.; Niwa, Y.; Yan, W.; Wu, Z.; Jiang, Y.; Liu, Q.; Wei, S. *J. Am. Chem. Soc.* **2010**, *132*, 7696-7701.

(55) Frens, G. *Nat. Phys. Sci.* **1973**, *241*, 20-22.

(56) Tseng, R. J.; Baker, C. O.; Shedd, B.; Huang, J.; Kaner, R. B.; Ouyang, J.; Yang, Y. *Appl. Phys. Lett.* **2007**, *90*, 053101-3.

(57) Turek, W.; Nyczyk, A.; Stochmal, E.; Bernasik, A.; Sniechota, A.; Hasik, M.; *Catal. Lett.* **2009**, *127*, 304-311.

(58) Cotton, F. A.; Wilkinson, G. In *Advanced Inorganic Chemistry: A Comprehensive Text;* John Wiley & Sons: New York, 1966.

(59) Ji, X.; Song, X.; Li, J.; Bai, Y.; Yang, W.; Peng, X. *J. Am. Chem. Soc.* **2007**, *129*, 13939-13948.

3 THE DISPERSION OF GOLD NANOPARTICLES ON POLYANILINE

3.1 INTRODUCTION

Among the conjugated polymers, polyaniline (PANI) has been extensively studied because of its tunable electrical properties (the polymer can be easily converted to different oxidation states)[1], and its ability to stabilize dispersed metal nanoparticles.[2] The interaction of PANI (emeraldine base) with metal ions is well documented. These interactions fall into two categories; *pseudo-protonation* and oxidative doping. The former, similar to protonation of PANI by acids such as hydrochloric acid, involves the interaction of a metal cation with imine nitrogens of PANI without a change in the number of electrons associated with PANI.[3, 4] The latter is believed to occur in a two-step redox process in which the amine nitrogen is first oxidized to imine by a metal cation with subsequent coordination of the reduced metal cation to an imine nitrogen. The final step of this process is a reversal of the first.[5] While there seems to be a consensus on the interaction of PANI with metal cations, the literature is scant of reports on the interaction of PANI and metal nanoparticles. Although Pillalamarri and co-workers[6] reported that metal nanoparticles were fairly strongly attached to polymer fibers in their PANI-silver (and gold) nanocomposites, they were however unable to probe the polymer-metal interaction in depth as the polyaniline signal dominated both the uv-vis and FT-IR spectra. A recent report by Tseng and co-workers also suggested a strong bond between gold nanoparticles and PANI with charge transfer between PANI and the metal.[7] A shift in the binding energy of Au_{4f} from 87.7 eV to 87.5 eV for Au-PANI compared with pure Au film, as well as a shift in the Raman bands of C=N and $C=N^+$ to high wavenumbers in Au-PANI was said to suggest charge transfer

from the positively charged nitrogen on PANI to the slightly negatively charged Au nanoparticles.[8]

The interaction of metal particles with polymer is proposed to affect the activity of the metal particle. For instance, Ishida and co-workers[9] showed that even though Au particles on poly(melamine formaldehyde) (MF) were smaller to those on poly(methyl methacrylate), the later catalyst exhibited a higher catalytic activity in the decomposition of hydrogen peroxide. This was said to be caused by the stronger interactions between Au particles and MF. In this Chapter we probe the interactions between Au particles and PANI. In particular we look at how the various oxidation states of PANI would affect the stability of the Au particles. We show that the Au nanoparticles are stable in emeraldine polyaniline. Addition of a reducing agent to a suspension of the Au-PANI, which reduces polyaniline, also induces the formation of irregular chainlike Au aggregates. When the polymer is oxidized using ammonium peroxydisulphate the size of gold nanoparticles increased. We also studied the effect protonation of PANI on the stability of Au particles. Regular close-packed Au aggregates formed when polyaniline was protonated by addition of hydrochloric acid at pH values lower than 2. PANI can easily interconvert between its various oxidation states but there are no reports in the literature on how the various oxidation states affect metal particles dispersed on PANI.

3.2 EXPERIMENTAL

All chemicals, except $HAuCl_4.3H_2O$, were obtained from Sigma-Aldrich. $HAuCl_4.3H_2O$ was sourced from SA Precious Metal (Pty) Ltd.

Synthesis of gold-polyaniline (AuPANI) nanocomposites. These nanocomposites were prepared as detailed in Chapter 2.

Stability tests. The stability of AuPANI-R nanocomposite was tested by soaking the nanocomposite in aqueous solutions to vary the oxidation state of PANI and its "degree" of protonation. For example, 500 mg of AuPANI-R powder was soaked in 25 mL of an aqueous solution of hydrochloric acid (concentrations ranging from 10^{-4} M to 1 M) and then adjusted to a particular pH for 24 hours. The solid was then collected by centrifugation, washed with water and dried. The dried samples were labelled AuPANI-R-pH*x* where *x* (0 to 6) indicates the pH of the solution.

To vary the oxidation state of PANI, $NaBH_4$ and $(NH_4)_2S_2O_8$ were used to reduce and oxidise PANI to leucoemeraldine and pernigraniline, respectively. In a typical experiment 50 mL of 0.1 M aqueous solution of reducing/oxidizing agent was added to 500 mg of AuPANI-R in a volumetric flask with constant stirring for 30 minutes. The solid was then collected by centrifugation, washed with distilled water and dried.

3.3 RESULTS AND DISCUSSION

3.3.1 Effect of $NaBH_4$ on the Size and the Stability of Gold Nanoparticles

It was shown in the last Chapter that the size of the gold nanoparticles is affected by the amount of reducing agent used. When the molar ratio of $NaBH_4$ to gold ($NaBH_4$:$HAuCl_4$) was increased beyond 10 a number of networked Au structures were observed. Similar structures were also observed when AuPANI-R with Au

particle diameters of 2.6 nm ($NaBH_4$:$HAuCl_4$ = 3.2:1) was treated with excess $NaBH_4$ (500 mg of AuPANI-R in 50 mL of 0.1 M $NaBH_4$). These observations suggest that some Au ions remained unreduced and probably adsorbed on the surface of metallic Au particles. Indeed AFM studies have shown that during the reduction of $AuCl_4^-$ by citrate, some gold ions ($AuCl_4^-$) adsorbs on the metallic gold in preference to citrate ions.[10, 11] The displacement of citrate ions on the surface of metallic gold by $AuCl_4^-$ was accompanied by the disappearance of repulsive forces between gold particles which implied that $AuCl_4^-$ adsorbs as a neutral species.[11]

The classical Derjaguin-Landau-Verwey-Overbeek (DLVO) theory is often used to explain and estimate the stability of nanoparticles in aqueous media.[12] This theory states that the total interaction potential between two nanoparticles (V_T) is the sum of the van der Waals attraction potential (V_a) and the electrostatic repulsion potential (V_e):[12-14]

$$V_T = V_a + V_e \tag{3.1}$$

$$V_a = -\frac{A_H}{6}\left[\frac{2}{R^2-4} + \frac{2}{R^2} + \ln\left(\frac{R^2-4}{R^2}\right)\right] \tag{3.2}$$

$$V_e = 2\pi\varepsilon_c\varepsilon_o a\psi_o^2 \ln\left[1+\exp(-a\kappa(R-2)\right] \tag{3.3}$$

In these equations A_H is the Hamaker coefficient, R = (r/a) where r is the centre to centre separation of spheres of equal radius a, ε_c is the dielectric constant of the solvent, ε_o is the dielectric constant of vacuum, ψ_o is the surface potential of the

particles, and κ is the Debye-Huckel parameter. The addition of an electrolyte to a colloidal system that is entirely stabilized by electrostatic double layer interactions diminishes the diffuse parts of the double layer.[9] The thickness of the double layer is the inverse of the Debye parameter ($1/\kappa$) and is proportional to the ionic strength:[15, 16]

$$\frac{1}{\kappa} = \left(\frac{e^2 \sum n_i z_i^2}{\varepsilon_c \varepsilon_o kT} \right)^{-\frac{1}{2}} \tag{3.4}$$

where z is the ionic valance, n is the ionic concentration, k is the Boltzmann constant, and T is the temperature. Aggregation occurs when the thickness of the double layer repulsive interaction is small enough for the van der Waals attractive forces to predominate. We suspect that in our case the reduction in the degree of oxidation of PANI at a high concentration of $NaBH_4$ weakens the attractive interactions between gold nanoparticles (Au NPs) and PANI. In addition, the introduction of $NaBH_4$ increases the ionic strength of the system. One or more Au nanoparticles then fuse and form networked structures. Indeed theoretical studies of the interactions between PANI and Pd atom have shown that PANI interacts strongly with Pd at the quinoid moiety by bonding with the imine N and the nearest C on the quinoid ring.[17] Pd was found to interact very weakly with the benzenoid moiety through weak bonds with C atoms of the benzenoid ring. Amine nitrogens were found not to donate their free electrons to bond with Pd unlike the imine nitrogens. Table 3.1 shows that increasing the amount of $NaBH_4$ leads to the reduction of PANI, that is, the number of imine nitrogens which form strong bonds with Au is reduced. This results in the weakened interaction of PANI and Au nanoparticles as the amount of $NaBH_4$ increases.

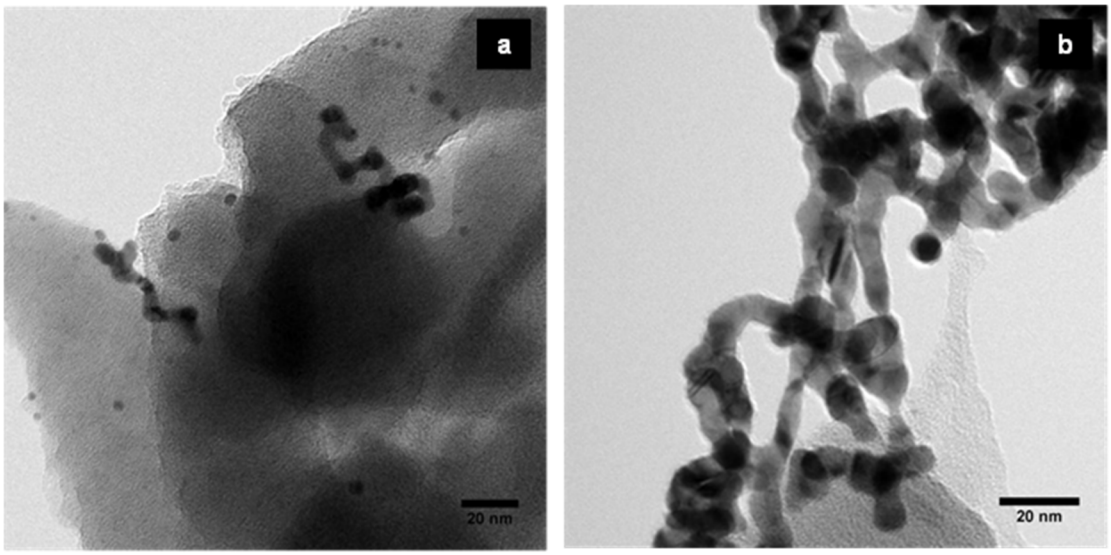

Figure 3.1. TEM images of AuPANI-R after reduction using $NaBH_4$/Au ratio of (a) 12 and (b) 20. Both the length of the Au nanowires and the degree of branching of the nanowires increase with an increase in the amount of $NaBH_4$.

Table 3.1. Variation of solution pH and degree of oxidation with ratio of $NaBH_4$/Au.

$NaBH_4$:$HAuCl_4$	$I_{Quinoid}/I_{Benzenoid}$	%Oxidized	pH of Solution
1.0:1	0.93	48	3.5
1.6:1	0.85	46	3.6
3.2:1	0.77	44	4.9
6.3:1	0.70	41	5.8
10:1	0.62	38	7.4
12:1	0.58	35	7.8

A closer look at the TEM images of these structures does indeed suggest the fusion of Au NP's with diameters of about 6 nm. A number of mechanisms for the formation of gold nanowires (or networked structures) have been proposed and the unifying theme

among them is the coalescence of small gold particles caused by either $AuCl_4^-$ ions adsorbed on the surface[18] or the reduction in the surface charge of Au particles.[19] In some cases, however, these nanowires exist only in a transitory state as they were observed to fragment into spherical-like particles.[18] In our case, the nanowires did not fragment and grew both in length and diameter with an increase in the amount of $NaBH_4$ used.

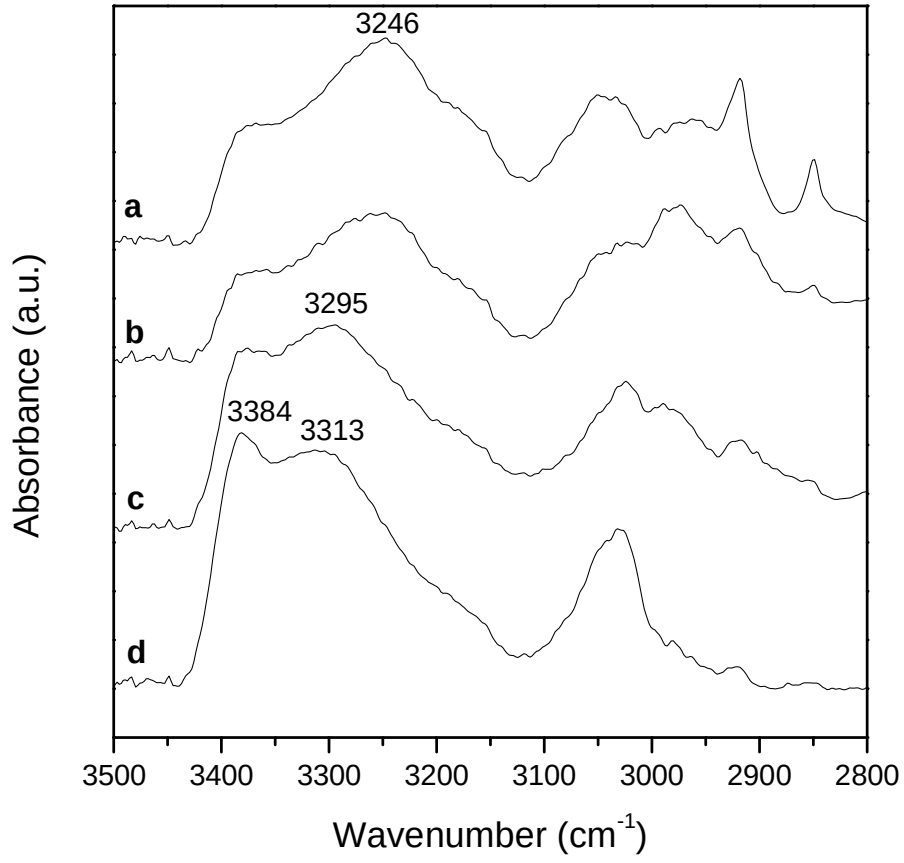

Figure 3.2. FTIR specatra of (a) AuPANI-C (N/Au = 21) and AuPANI-R reduced using the varying ratios of $NaBH_4$/Au (b) 3.2, (c) 12, (d) 26. The spectra show changes in the extent and type of H-bonding.

In addition, the degree of branching of these nanowires increased (Figure 3.1). At a ratio of $NaBH_4$:$AuCl_4$ of 12:1 the average diameter of the nanowires was 6.2 ± 0.6 nm and the radius increased slightly to about 6.7 ± 0.7 nm when the ratio was increased to 20. The end to end distance of the nanowires averaged about 26 nm for nanowires at $NaBH_4$/Au ratio of 12, that is, about 4 particles fused together. However some wires were as long as 50 nm. At a ratio of $NaBH_4$/Au = 20 the nanowires were so networked that it was impossible to tell where one started or ended. These results are somewhat consistent with those of Xie and co-workers[19] in which the extent of nanowire formation varied with solvent polarity. In pure water spherical particles with a diameter of 3.7 nm were formed while "nano-peanuts" (2 or 3 spheres joined) were formed in a mixture of water and ethanol. Extended Au nanowires formed in pure ethanol in which the repulsive forces between Au nanoparticles were weakened by a decrease in their surface charge.

The idea of incomplete reduction of gold chloride complexed to PANI is supported by FTIR measurements in the range 2800 – 3500 cm^{-1} which shows the H-bonding behaviour when the complexes are treated with $NaBH_4$. Figure 3.2 shows that after reducing 500 mg of AuPANI-C (N/Au = 21) with 15 mg of $NaBH_4$ ($NaBH_4$/Au ~ 3.2) the peak at 3246 cm^{-1} which we assigned to N–H stretch hydrogen bonded to Cl (N–H···Cl) is still present. This peak gradually shifts to 3313 cm^{-1} and is accompanied by an increase in the intensity of the non-hydrogen bonded N–H at 3384 cm^{-1} when the amount of $NaBH_4$ was increased to $NaBH_4$/Au ~ 26. The FTIR spectra (in the region 2800 – 3500 cm^{-1}) of AuPANI-R at $NaBH_4$/Au ~ 26 resembles that of deprotonated PANI. This implies that complete breakage of H-bonds of the type N–H···Cl is

achieved at high concentrations of $NaBH_4$ which coincides with the formation of networked Au structures.

The ideas presented here are consistent with a model of the formation of Au NPs recently advanced by Yao and co-workers.[20] In their report, in which $AuCl_4^-$ was reduced by citric acid in the presence of poly(vinyl pyrrolidone) (PVP), the authors showed that $AuCl_4^-$ ions are initially partially reduced to $AuCl_3^-$ ions. The reduced ions then combine through Au-Au bonds to form Au_nCl_{n+x} complex clusters attached to PVP. Structured Au NPs (fcc) formed when the number of Au atoms in a complex cluster exceeded the value of 13. This mechanism is illustrated in Figure 3.3.

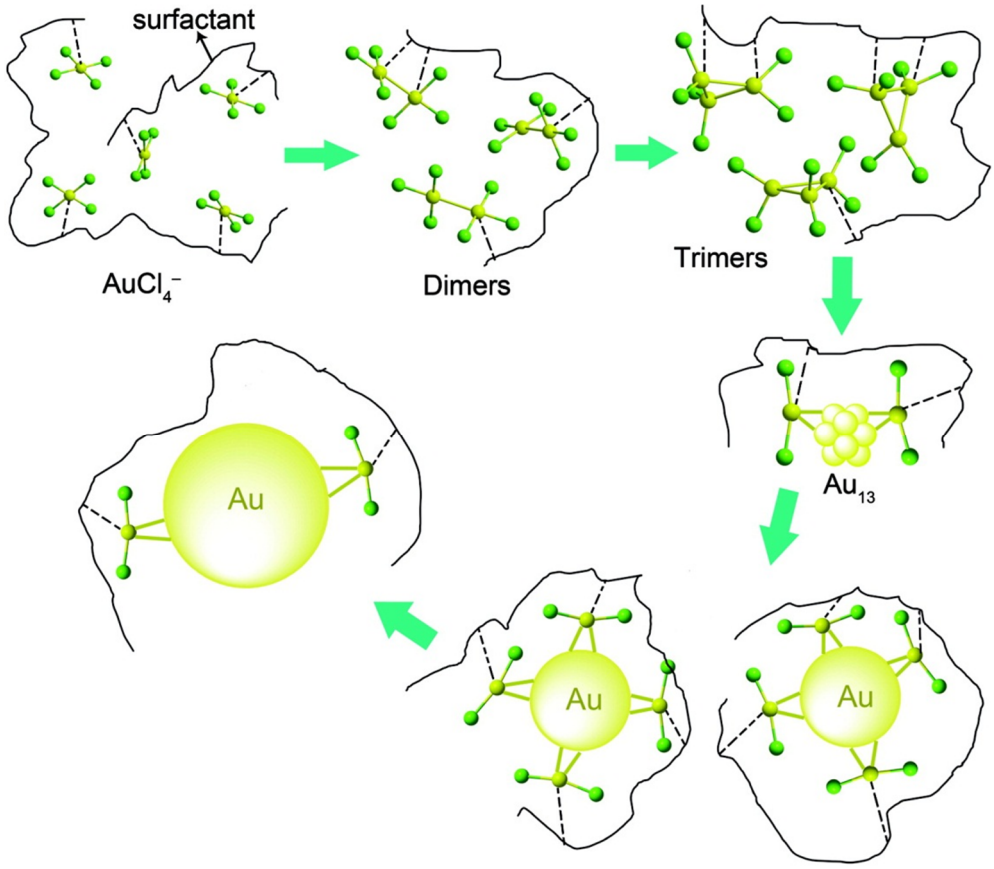

Figure 3.3. An illustration of the formation of Au NPs in which $AuCl_4^-$ ions form Au_nCl_{n+x} complex clusters during the initial stages of nucleation. Taken from Ref 20.

3.3.2 The Effect of the Degree of Protonation of PANI on the Stability of Gold Nanoparticles.

The effect of changing the electronic environment of nitrogen atoms on the interaction was also observed upon soaking AuPANI-R (d_{Au} ~ 2.6nm) in hydrochloric acid at various pH (0 – 6). Soaking deprotonated PANI in protonic acids leads to the protonation of PANI at the imine nitrogen.[21] As already indicated above, protonation of PANI (**1**) (Scheme 3.1) in the emeraldine form converts it to a hydrochloride salt (**2**) which is believed to exist as stable delocalized polysemiquinone radical cations (**3**).[22, 23] The formation of these radical cations is accompanied by an increase in the conductivity of PANi by ~10^{10} indicating an increase in the number and mobility of charge carriers. In addition, Ponzio and co-workers[24] have shown that the formation of polysemiquinone radical cation in which the amine N acquires a positive charge leads to a decrease in the polymer's ability to form H-bonds. The authors were able to remove NMP hydrogen bonded to PANI films by protonation-deprotonation cycles.

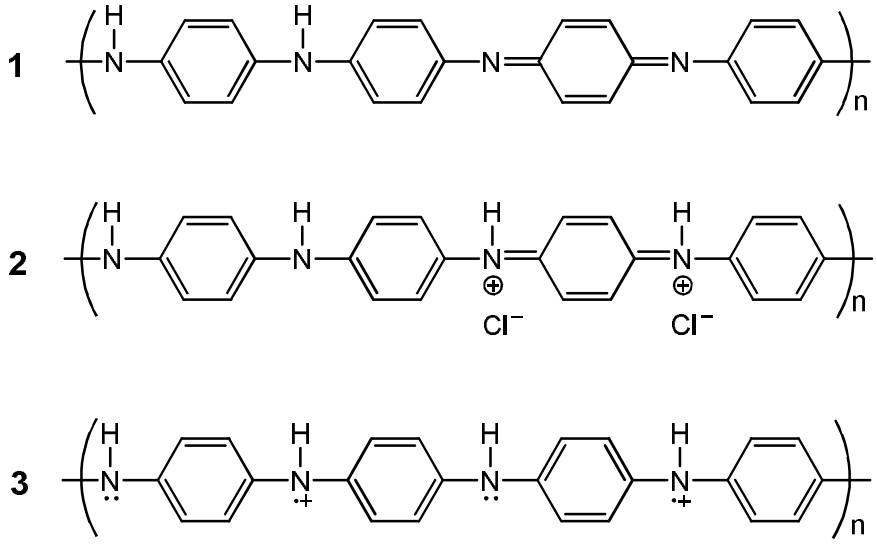

Scheme 3.1. Protonation of PANI and the subsequent formation of a polysemiquinone cation radical.

Figure 3.4 shows that the average particle size of Au nanoparticles increased slightly from about 2.6 nm to about 3.9 nm when the pH was decreased from 6 to 3. A sharp increase in particle size, from 3.9 nm to ~23 nm, was observed when the pH was decreased further from 3 to 0. A similar trend was observed for the variation of the degree of protonation with a change in pH. Figure 3.4 shows that PANI is only significantly protonated below pH 1.[25] Following our earlier submission that Au interacts strongly with PANI at imine N, the conversion of imine N to amine N after protonation should, therefore, cause a weakening in the interaction of PANI with Au NPs.

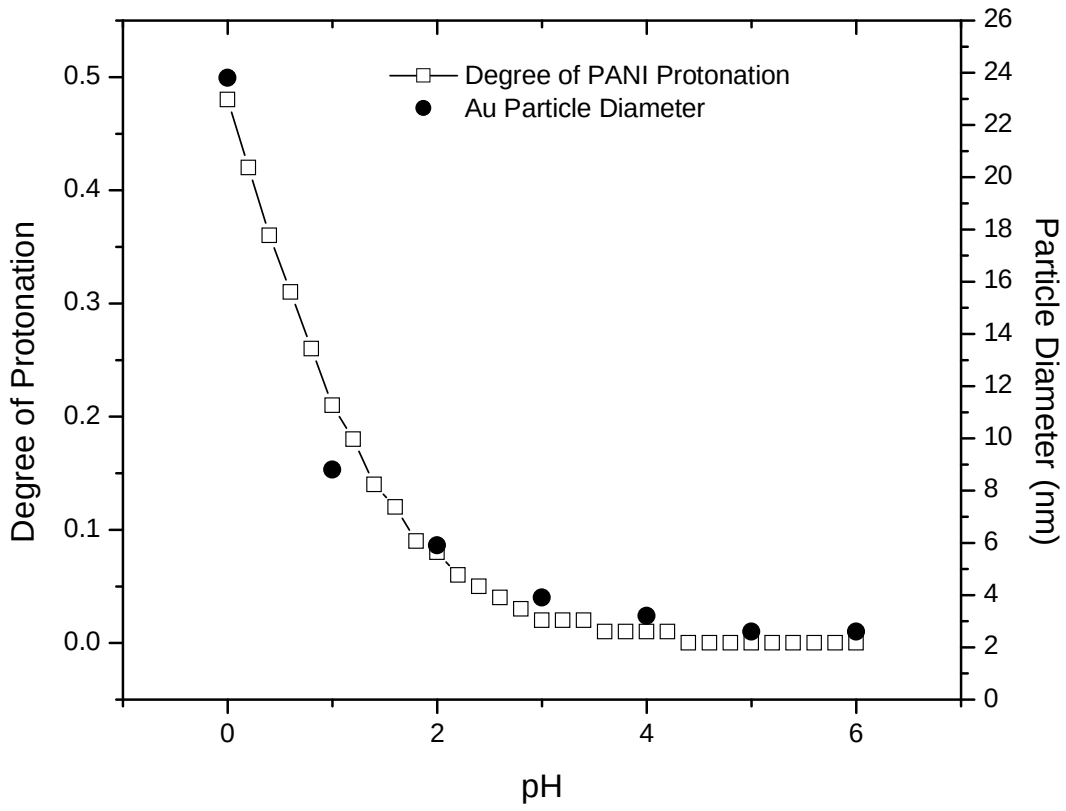

Figure 3.4. The effect of pH and the degree of protonation of PANI on the stability of Au nanoparticles. The degree of protonation was calculated on the basis that protonation occurs only at the imine N and that 50% of the nitrogen atoms are imine N.

In addition, the formation of a polysemiquinone radical cation at low values of pH causes a decrease in the ability of PANI to form H-bonds with unreduced gold chloride through N–H····Cl bonds. Since the gold nanoparticles have negative surface charge due to adsorbed $AuCl_4^-$ ions, the added H^+ ions possibly adsorb on the surface of Au nanoparticles rendering them neutral. It has been shown that citrate capped Au nanoparticles coagulated when the pH of the suspension was dropped below 5 by addition of HCl. The H^+ ions interacted with the negatively charged citrate ions on the surface of Au nanoparticles resulting in the decrease in the electrostatic repulsions between Au particles.[26]

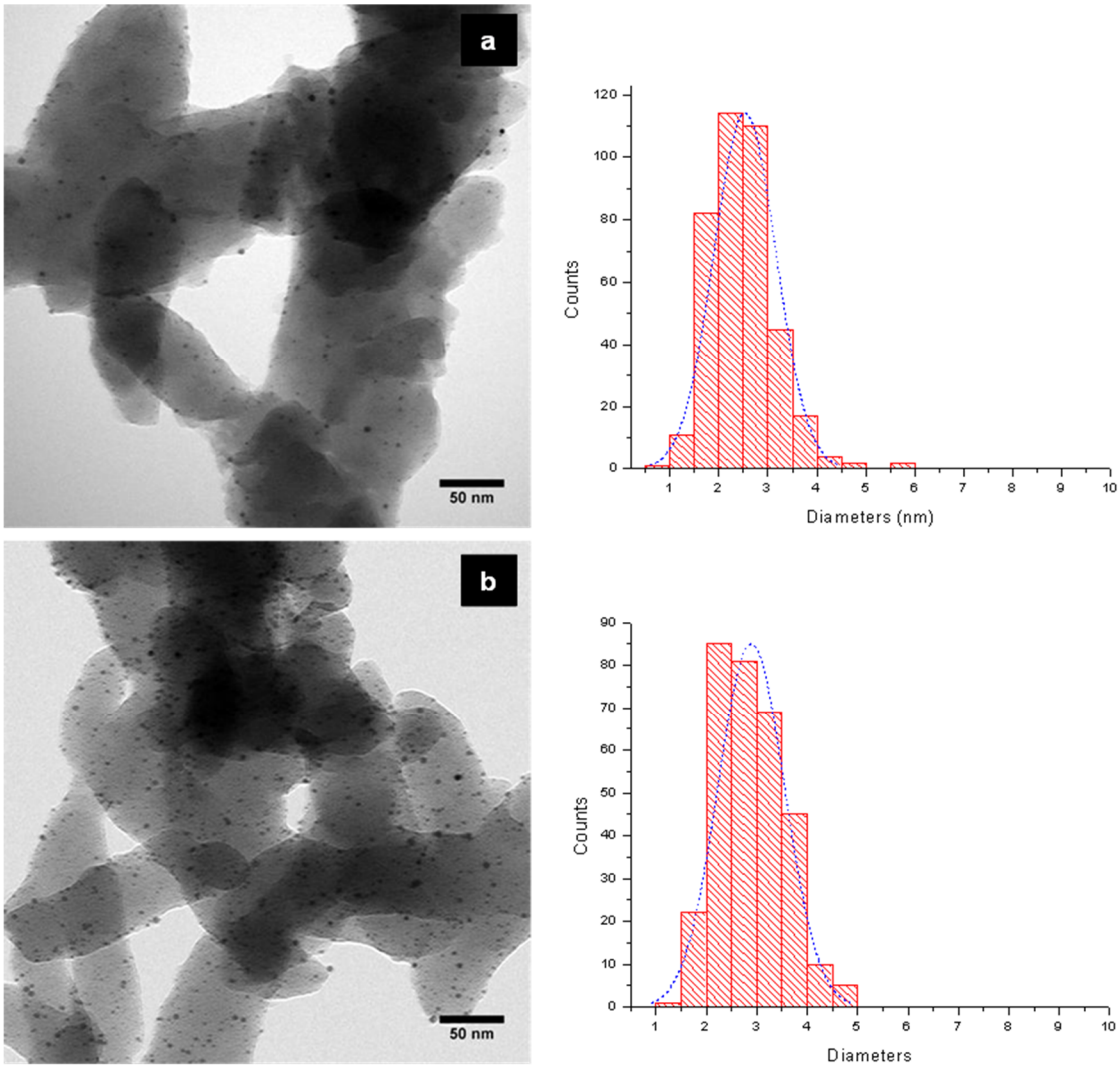

Figure 3.5. TEM images and particles size distribution of AuPANI-R (a) before and (b) after soaking in 1.0 M NaCl for 24 hours.

It does appear that, in general, electrostatically stabilized Au particles aggregate when their surface charge is reduced.[13] Our system, in which stabilization is achieved largely by charge transfer between PANI and Au particles, does not seem to follow this general observation. When AuPANI-R was soaked in a solution of 1 M NaCl overnight, the system remained fairly stable. Figure 3.5 shows TEM images and the particle size distribution of the AuPANI-R before and after soaking in NaCl. The average particle diameter increased very slightly from 2.5 ± 0.6 nm to 2.8 ± 0.7 nm indicating that the Na^+ ions, which are not know to *pseudo-protonate* PANI, and the Cl^- ions, had little or no effect on the stability of the Au nanoparticles. Similarly, addition of NaOH to AuPANI-R did not cause any particle aggregation. The observed increase in particles size with decrease in pH which mirrors the change in the degree on PANI protonation is therefore largely due the loss of the ability of PANI to transfer charge to metallic gold and the breakage of N–H···Cl bonds after conversion to a polysemiquinone radical cation.

3.3.3 Effect of $(NH_4)_2S_2O_8$ on the Size and the Stability of Gold Nanoparticles

Oxidizing agents like ammonium peroxydisulphate readily oxidize PANI from emeraldine to pernigraniline. When PANI exists as emeraldine, the number of amine nitrogen atoms is almost equal to the number of imine nitrogens. The oxidation of PANI involves the conversion of amine N to imine N. The oxidation state can be easily estimated from the relative intensities of the FTIR absorption peaks of the benzenoid and quinoid stretching vibrations.[27] However in our case we did not observe an increase in the intensity of the quinoid peak (~1580 cm^{-1}) relative to the benzenoid peak (~1500 cm^{-1}). Instead a decrease in the intensity of the FTIR peaks at 1578 cm^{-1} (stretching of N=Q=N) and 1280 cm^{-1} (C–N stretch in QBB or BBQ) was observed (Q denotes quinoid unit and B is the benzenoid unit). In addition, a small peak at 1671 cm^{-1} (stretching of C=O) and a sharp peak at 1043 cm^{-1} (stretching of C–O) were observed. These spectral changes, shown in Figure 3.6, indicate that treating AuPANI-R with 0.1 M of $(NH_4)_2S_2O_8$ leads to the degradation of PANI through the hydrolysis of imine. It has been shown that when the electrochemical potential of PANI rises above 0.7 V, on addition of oxidizing agents, the hydrolysis of C=N bonds occurs.[28, 29] This results in either chain breakage or the elimination of nitrogen atoms if end groups are involved[30] (Scheme 3.2).

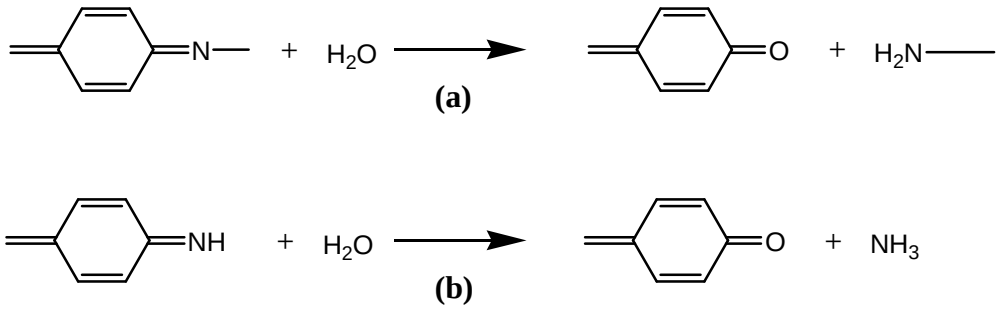

Scheme 3.2. Hydrolysis of PANI through (a) chain breakage and (b) elimination of terminal N and replacement with O.

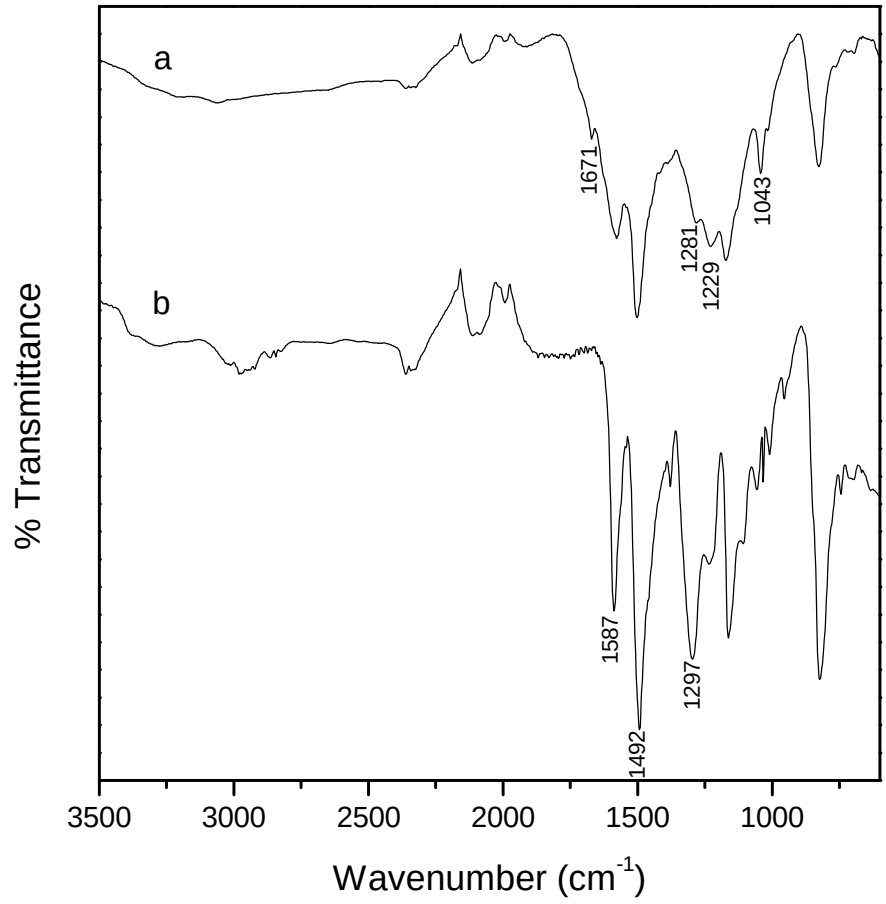

Figure 3.6. FTIR spectra of (a) AuPANI-R after treatment with $(NH_4)_2S_2O_8$ and (b) AuPANI-R without treatment with oxidizing agent.

The size of the Au NPs increased from about 2.6 nm to 8.2 nm after treating a sample of AuPANI with $(NH_4)_2S_2O_8$ as shown in Figure 3.7. The loss of C=N due to hydrolysis is likely to have caused a weakening in the interaction of Au NPs with PANI.

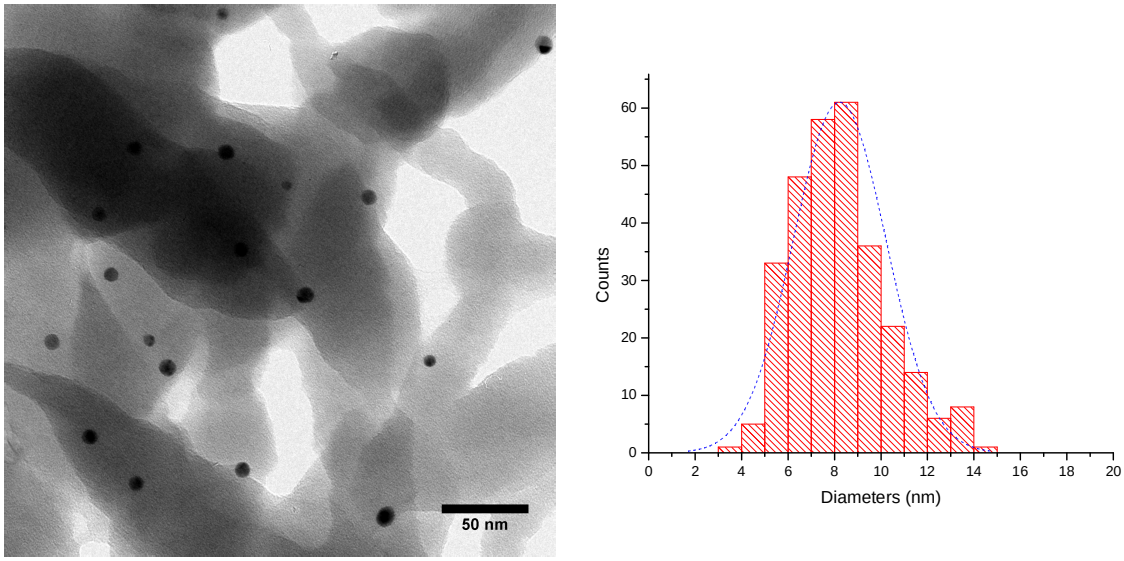

Figure 3.7. TEM image and particle size distribution for AuPANI-R after oxidizing with 0.1 M $(NH_4)_2S_2O_8$. The size of the gold nanoparticles increased from about 2.6 ±. 0.6 nm to 8.2 ±. 2.0 nm

3.3.4 Mechanism of Aggregation of AuNPs

The above experimental observations and existing literature makes it possible to postulate a mechanism for the aggregation of AuNPs dispersed on PANI. A number of reports have demonstrated that chain-like agglomerates of Au can be assembled by carefully manipulating the interparticle electrostatic repulsions.[14-16, 31, 32] In these studies the formation of Au networked structures was induced by either the addition of salts (NaCl and $NaBH_4$) or by substituting stabilizing ligands. These studies showed that the formation of nanoparticle chains is a result of the anisotropic character of the electrostatic repulsions. The mechanism can be summarized as follows. The isotropic electrostatic repulsions of Au NPs are lowered by increasing the ionic strength of the NP suspension (or changing the dielectric constant). Two Au NPs aggregate to form a dimer once the thickness of the double layer is small enough for the van der Waals attractive forces to predominate. After formation of a dimer the

electrostatic double layer re-arranges into a uniform layer surrounding the dimer. Wang and co-workers evaluated the electrostatic repulsion potentials of a gold nanoparticle interacting with a chain end (V_e^{end}) or the side of a chain (V_e^{side}).[15] Their calculations showed that V_e^{end} and V_e^{side} of a gold nanoparticle and a chain of *n* nanoparticles are given by Equations 3.5 and 3.6 where ρ is the charge density and *A* is the surface area.

$$V_e^{end} = \rho A \ln 2na \tag{3.5}$$

$$V_e^{side} = 2\rho A \ln na \tag{3.6}$$

Equations 3.5 and 3.6 indicate that V_e^{side} is always larger than V_e^{end}. The implication is that once a dimer has formed, other nanoparticles will preferentially attach to the ends of the dimer. This results in the formation of one-dimensional chains (Scheme 3.3).

The addition of NaCl and NaOH to the AuPANI suspension prepared in this study did not result in any aggregation of the gold nanoparticles. Aggregation occurred only when HCl, $NaBH_4$, or $(NH_4)_2S_2O_8$ were added to the suspension. This shows that the stabilization of AuNPs in AuPANI is achieved largely by the interaction of AuNPs with PANI rather than electric double layer interactions. However, once this charge-transfer interaction is interrupted by the addition of HCl (which protonates the polymer), $NaBH_4$ (which reduces PANI), or $(NH_4)_2S_2O_8$ (which oxidizes PANI), aggregation of Au NPs occurs. The formation of nano-chains over close-packed aggregates is probably determined by the rate of the aggregation, which could in turn be determined by the rate of the structural changes of PANI (oxidation, reduction, and

protonation). At a slower rate, the aggregation of Au NPs is likely to occur in a stepwise manner where dimers, trimers, tetramers, etc form in a sequential manner due to the anisotropic distribution of electric charge around the Au NPs. A fast rate of aggregation would then lead to the formation of close-packed aggregates.

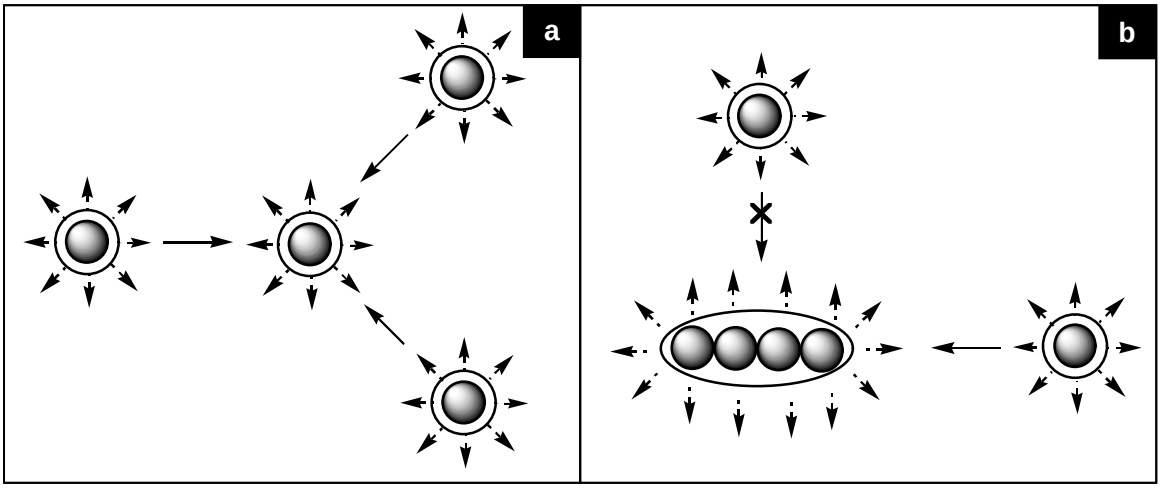

Scheme 3.3. The distribution of electric field around (a) monomeric Au NPs and (b) linearly aggregated AuNPs. The scheme shows the preferential attachment of AuNPs at the end of a chain. Adapted from Yang and co-workers.[32]

3.4 CONCLUSIONS

Results from this study showed that Au NPs are stabilized by PANI through (1) a charge transfer from the imine nitrogens on PANI to the AuNPs and (2) by H-bonding between unreduced $AuCl_4^-$ ions adsorbed on Au NPs. The addition of electrolytes such as NaCl or NaOH which do not cause structural changes to PANI that could affect either the charge transfer or the H-bonding did not cause any particle aggregation. Aggregation of Au NPs stabilized by PANI was only observed when solutions of $NaBH_4$, HCl, and $(NH_4)_2S_2O_8$ were added to dispersions of AuPANI.

Sodium borohydride reduces PANI by transforming the imine groups on PANI to amine groups. In addition, $NaBH_4$ reduces further the "unreduced" $AuCl_4^-$ ions that are adsorbed on AuNPs. The combined result is a reduction in the attractive forces between Au NPs and PANI and a decrease in the electrostatic repulsions between Au NPs due to the increase in the ionic strength of the suspension. The addition of a solution of HCl to a suspension of PANI causes (1) the formation of polysemiquinone cation radicals through the protonation of PANI and (2) an increase in the ionic strength of the suspension. This leads to the reduction in the ability of PANI to form H-bonds and a decrease in the thickness of the electric double layer. Similarly, the addition of $(NH_4)_2S_2O_8$ to the AuPANI suspension oxidizes PANI by transforming amine groups to imine groups. However the polymer degrades through the hydrolysis of the imine group under high electrochemical potentials (E > 0.7 V). All these conditions lead to the aggregation of Au NPs. The shape of the aggregates is determined by the rate of aggregation. Chain-like aggregate (nanowires) form when aggregation is induced by the reduction of PANI while close-packed aggregates form when PANI is oxidized or protonated.

3.5 REFERENCES

(1) Masters, J. G.; Sun, Y.; MacDiarmid, A. G.; Epstein, A. J. *Synth. Met,* **1991**, *41*, 715-718.

(2) Mallick, K.; Witcomb, M. J.; Dinsmore, A.; Scurrell, M. S. *Macromol. Rapid Commun.* **2005**, *26*, 232-235.

(3) Kulszewicz-Bajer, I.; Pron, A.; Abramowicz, J.; Jeandey, C.; Oddou, J.; Sobczak, J. W. *Chem. Mater.* **1999**, *11*, 552-556.

(4) Genoud, F.; Kulszewicz-Bajer, I.; Bedel, A.; Oddou, J. L.; Jeandey, C.; Pron, A. *Chem. Mater.* **2000**, *12*, 744-749.

(5) Dimitriev, O. P. *Polym. Bull.* **2003**, *50*, 83-90.

(6) Pillalamarri, S. K.; Blum, F. D.; Tokuhiro, A. T.; Bertino, M. F. *Chem. Mater.* **2005**, *17*, 5941-5944.

(7) Tseng, R. J.; Baker, C. O.; Shedd, B.; Huang, J.; Kaner, R. B.; Ouyang, J.; Yang, Y. *Appl. Phys. Lett.* **2007**, *90*, 053101-3.

(8) Tseng, R. J.; Huang, J.; Ouyang, J.; Kaner, R. B.; Yang, Y. *Nano Lett.* **2005**, *5*, 1077-1080.

(9) Ishida, T.; Kuroda, K.; Kinoshita, N.; Minagawa, W.; Haruta, M. *J. Colloid Interface Sci.* **2008**, *323*, 105-111.

(10) Biggs, S.; Mulvaney, P.; Zukoski, C. F.; Grieser, F. *J. Am. Chem. Soc.* **1994**, *116*, 9150-9157.

(11) Wall, J. F.; Franz Grieser, F.; Zukoski, H. F. *J. Chem. Soc., Faraday Trans.* **1997**, *93*, 4017-4020.

(12) Shaw, D. J. In *Colloid Stability;* Introduction to Colloid & Surface Chemistry; Butterworth-Heinemann: Oxford, 1992; pp 210-243.

(13) Chow, M. K.; Zukoski, C. F. *J. Colloid Interface Sci.* **1994**, *165*, 97-109.

(14) Kim, T.; Lee, K.; Gong, M.; Joo, S. *Langmuir* **2005**, *21*, 9524-9528.

(15) Zhang, H.; Wang, D. *Angew. Chem. Int. Ed.* **2008**, *47*, 3984-3987.

(16) Zhang, Z.; Wu, Y. *Langmuir* **2010**, *26*, 9214-9223.

(17) Bialek, B. *Surf. Sci.* **2006**, *600*, 1679-1683.

(18) Pong, B.; Elim, H. I.; Chong, J.; Ji, W.; Trout, B. L.; Lee, J. *J. Phys. Chem. C* **2007**, *111*, 6281-6287.

(19) Xie, J.; Zhang, Q.; Lee, J. Y.; Wang, D. I. C. *J. Phys. Chem. C* **2007**, *111*, 17158-17162.

(20) Yao, T.; Sun, Z.; Li, Y.; Pan, Z.; Wei, H.; Xie, Y.; Nomura, M.; Niwa, Y.; Yan, W.; Wu, Z.; Jiang, Y.; Liu, Q.; Wei, S. *J. Am. Chem. Soc.* **2010**, *132*, 7696-7701.

(21) Huang, W.; Humphrey, B. D.; MacDiarmid, A. G. *J. Chem. Soc., Faraday Trans. 1* **1986**, *82*, 2385-2400.

(22) Huang, W.; MacDiarmid, A. G.; Epstein, A. J. *J. Chem. Soc., Chem. Commun.* **1987**, *23*, 1784-1786.

(23) MacDiarmid, A. G.; Epstein, A. J. *Synth. Met.* **1995**, *69*, 85-92.

(24) Ponzio, E. A.; Echevarria, R.; Morales, G. M.; Barbero, C. *Polym. Int.* **2001**, *50*, 1180-1185.

(25) Chiang, J.; MacDiarmid, A. G. *Synth. Met.* **1986**, *13*, 193-205.

(26) Muangnapoh, T.; Sano, N.; Yusa, S.; Viriya-empikul, N.; Charinpanitkul, T. *Curr. Appl. Phys.* **2010**, *10*, 708-714.

(27) Hatchett, D. W.; Josowicz, M.; Janata, J.; Baer, D. R. *Chem. Mater.* **1999**, *11*, 2989-2994.

(28) Cui, C. Q.; Ong, L. H.; Tan, T. C.; Lee, J. Y. *Electrochim. Acta* **1993**, *38*, 1395-1404.

(29) Gospodinova, N.; Mokreva, P.; Terlemezyan, L. *Polym. Int.* **1996**, *41*, 79-84.

(30) Gospodinova, N.; Mokreva, P.; Terlemezyan, L. *Polymer*, **1994**, *35*, 3102-3106.

(31) Zhang, H.; Fung, K.; Hartmann, J.; Chan, C. T.; Wang, D. *J. Phys. Chem. C* **2008**, *112*, 16830-16839.

(32) Yang, M.; Chen, G.; Zhao, Y.; Silber, G.; Wang, Y.; Xing, S.; Han, Y.; Chen, H. *Phys. Chem. Chem. Phys.* **2010**, *12*, 11850-11860.

4 THE EFFECT OF SUBSTITUENTS ON THE REACTIVITY OF PANI WITH $HAuCl_4$ AND THE DISPERSION OF GOLD NANOPARTICLES

4.1 INTRODUCTION

The synthesis of polyaniline (PANI) and the study of its properties are well documented in literature. Several methods have been employed to direct the structure[1, 2] of PANI and to improve its solubility. Huang and Kaner[3] synthesized PANI nanofibers by rapidly mixing aniline and ammonium peroxydisulphate in an aqueous solution of 1 M hydrochloric acd. High quality PANI nanofibers were obtained and the average diameter of the nanofibers could be tuned from 30 nm using hydrochloric acid to 120 nm using perchloric acid. PANI is only soluble in special solvents like 1-methyl-2-pyrrolidinone. Solution processability of PANI is often improved by using ring substituted aniline monomers or by copolymerization using mixtures of substituted and unsubstituted anilines. Alkyl, alkoxy, and halogen substituted anilines have been successfully polymerized giving materials with improved solubility in common solvents like alcohols.[4]

Theoretical[5, 6] and experimental studies have shown that ring-substituted polyanilines have different geometrical and electronic properties when compared with PANI.[7, 8] For instance, methoxy- and nitro-substituted tetraanilines show an interaction between the oxygen of the substituent and nitrogen of the oligomer through H-bonding. This interaction reportedly modifies the torsion angle between adjacent rings of the polymer and has been shown to affect the ionization potential and bandgap (HOMO – LUMO energy difference) of the polymer. Wei and coworkers[8] reported that the π – π^* transition shifts from 330 nm for PANI to 311 nm for poly(*o*-ethylaniline)

indicating an increase in the bandgap (and a decrease in conductivity) due to a decrease in the extent of conjugation in the polymer. Theoretical calculations indicate that electron-withdrawing groups on the ring decreases the bandgap and the energy of the first optical transition. Both steric and electronic effects of the substituents have been offered as explanations for these variations.[5, 6]

PANI is known to form complexes with transition metals ions with high electrode potentials via a redox process.[9, 10] Reduction of the complexed metal ions results in the formation of metal nanoparticles stabilized by the polymer.[11] The stabilization of metal nanoparticles by PANI is thought to proceed through coordination of the metal with nitrogen atoms on PANI chains.[12] However, substituents on the aniline monomer have been shown to change the oxidation potential of the monomers and the corresponding polymer. For instance, the oxidation potential of poly(2-methoxyaniline) was found to be lower than that of PANI as measured by cyclic voltammetry.[13] In addition methoxy- and nitro-substituted polyanilines reportedly show an interaction between the oxygen of the substituent and nitrogen of the polymer through intra-chain H-bonding.[14]

In this Chapter, we explore how these substitution-induced variations in PANI would affect the reactivity of the polymer with $HAuCl_4$. In addition we explore how these would affect the stabilization of metal nanoparticles. We show by open-circuit measurements that the steric effects of the methyl and chlorine groups on poly(methylaniline) and poly(chloroaniline), respectively, causes a decrease in the reactivity of these polymers with $HAuCl_4$ compared to PANI. This affects the amount of gold incorporated onto the polymer matrix. However, the size of the gold

nanoparticles differed very little between these polymers. We show for the first time that due to the decrease in the basicity of the substituted PANIs caused by the bulky groups, the gold nanoparticles were more stable in these polymers in acidic media than those in PANI.

4.2 EXPERIMENTAL

Aniline, 2-methylaniline, 2-chloroaniline, and ammonium peroxydisulphate ($(NH_4)_2S_2O_8$) were all purchased from Sigma-Aldrich and were used as received. Tetrachloroauric acid ($HAuCl_4 \cdot 3H_2O$) was obtained from SA Precious Metals (Pty) Ltd. A stock solution of 10^{-2} M $HAuCl_4$ was prepared by dissolving 0.394 g of $HAuCl_4.3H_2O$ in enough distilled water to make a 100 mL solution.

Synthesis of PANI and derivatives. All the polymers were synthesized as described in the Chapter 2. However, 0.1 g of *p*-phenylenediamine was added to each reaction solution to initiate the polymerization for all the substituted monomers as described by Tran and Kaner.[15] The following acronyms were used: PANI, PANIMe, and PANICl to designate polyaniline, poly(2-methylaniline), and poly(2-chloroaniline), respectively.

Synthesis of gold-polymer nanocomposites. A typical protocol for the synthesis is as follows. PANI was first deprotonated by mixing 1 g of PANI (emeraldine) with 50 mL of 0.1 M NaOH solution. This mixture was stirred for 30 minutes and washed with distilled water until the pH of the filtrate dropped to 7. The filtrate was then suspended in 100 mL of distilled water to which 25 mL of 10^{-2} M $HAuCl_4$ solution was added while stirring. This should yield a maximum of 5% Au loading by weight.

The actual loading was measured by thermogravimetric analysis using a Perkin Elmer Thermogravimetric Analyser. After 2 hours the mixture was filtered, washed with distilled water, and divided in two equal parts. One part was labelled AuPANI-C (complex) and dried while the other was suspended in 50 mL of water to which 15 mg of $NaBH_4$ in 10 mL of distilled water was slowly added. After stirring for 1 hour the final product was filtered, washed with distilled water, and dried. This was labelled AuPANI-R.

Open circuit potential measurements. The polymerization of aniline and its derivatives was monitored as a function of time using a two electrode cell: Pt|reaction solution||saturated calomel electrode (SCE). For this purpose, 1 g of monomer was dissolved in 50 mL of 1 M HCl. A Pt electrode and SCE were dipped in the solution and left for 30 minutes to get an equilibrium reading. A solution of 1.6 g of $(NH_4)_2S_2O_8$ in 20 mL of 1 M HCl was rapidly added and the potential of the mixture recorded every 1 minute. *p*-Phenylenediamine (0.015 g) was added to all the reaction solutions except for the ca se of aniline.

Uv-vis spectroscopy. Absorbance UV-VIS spectra were recorded on a Varian Cary 50 spectrometer. All measurements were performed in a single quartz cuvette with a 1 cm path length. For in-situ measurements, 1 mL of 10^{-3} M $HAuCl_4$ was diluted to 10 mL in ethanol. This solution was added to a 1mg/10mL suspension of deprotonated PANI in ethanol (10 mL). A sample of 3 mL of this mixture was rapidly transferred to a UV-vis cuvette. Measurements were taken in the range of 200 nm – 450 nm every 1 minute at room temperature, about 22 ºC. The first measurement was recorded after about 20 seconds of mixing the reactants.

Transmission electron microscopy. A small amount of powdered sample was dispersed in methanol by sonication and a drop of the suspension placed on a lacey copper grid. A Technai Spirit G2 microscope was used to record images at 200 kV. The same instrument was used for energy dispersive spectroscopy (EDS).

FTIR ppectroscopy. All FTIR spectra in the mid-infrared range were collected using a Bruker Tensor 27 spectrometer equipped with MIRacle™ ATR accessory (Pike Technologies). A total of 64 scans were recorded for each sample with a resolution of 4 cm^{-1}.

4.3 RESULTS AND DISCUSSION

4.3.1 Synthesis of PANI and its derivatives

Open Circuit Potential Measurements. The synthesis of PANI and its derivatives, namely PANIMe and PANICl, were synthesised by rapidly adding a solution of oxidizing agent to an acidic solution of the monomer. Figure 4.1 shows potential-time profiles of the polymerization reactions. The profiles can be divided into three sections: (1) t_1, a rapid increase in the potential upon addition of oxidizing agent, (2) t_2, a somewhat flat region associated with the polymerization of monomer to the corresponding polymer in the pernigraniline state, and (3) t_3, a rapid decrease in the potential as the polymer is being converted from pernigraniline to emeraldine.[16, 17] In the latter stage pernigraniline takes over the role of oxidising agent and oxidizes any monomer left after complete consumption of ammonium peroxydisulphate.[18] The time (t_1 + t_2) is thus inversely proportional to the rate of polymerization.[17] According to Figure 4.1, aniline shows the highest rate of polymerization followed by

methylaniline. The polymerization of chloroaniline was not even close to completion within the time of the experiment, 20 minutes. This trend is somewhat consistent with theoretical calculations which predict electron withdrawing groups substituted on aniline retard the rate of polymerization. The electron donating/withdrawing effect of the substituent groups used in this study, as indicated by Hammett inductive substituent constants (σ_I) and their van der Waals radii are listed in Table 4.1.[19, 20] Steric effects are likely to explain why the rate of polymerization of methylaniline with an electron-donating group is slightly lower than that of aniline.

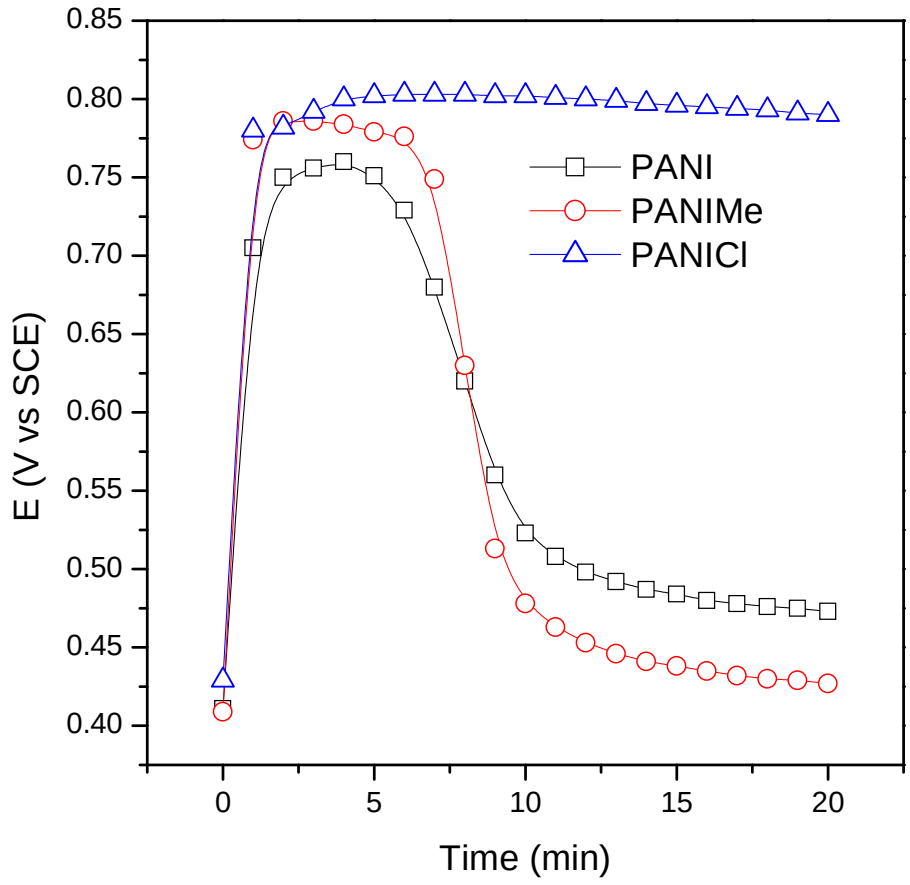

Figure 4.1. Potential-time profiles of the polymerization of aniline, methylaniline, and chloroaniline with ammonium peroxydisulphate in 1 M HCl**.**

Table 4.1. An indication of the electronic and steric effects of the various substituent groups studied.

Monomer	σ_I	van der Waals radius, Å
Chloro	0.46	1.75
Methyl	-0.04	1.70
H (aniline)	0	1.20

Uv-vis Spectroscopy. The uv-vis spectra of the polymers in 1-methyl-2-pyrrolidinone are show in Figure 4.2. The uv-vis spectrum of PANI after treatment with NaOH shows two peaks, one around 330 nm and the other at 639 nm. These correspond to a $\pi - \pi^*$ transition associated with the electrons of the benzene ring delocalized on N atoms (*B* peak) and to an excitation of an electron from the HOMO of the benzeniod to the LUMO of quinoid moiety (*Q* peak).[21-23] The spectra of PANIMe and PANICl show peaks due to the $\pi - \pi^*$ transition shifted from 330 nm to 315 nm. This shift indicates a decrease in the extent of π conjugation along the polymer chains caused by a decrease in the degree of orbital overlap between the phenyl π electrons and the lone pairs on nitrogen atom.[8] The decrease in the extent of conjugation can also lead to a decrease in the apparent oxidation state of the polymer. The oxidation state of polyaniline is determined by the relative amount of amine N to imine N (relative amount of benzenoid units to quinoid units). A decrease in π conjugation leads to a decrease in the number of imine N sites and consequently a lower oxidation state.

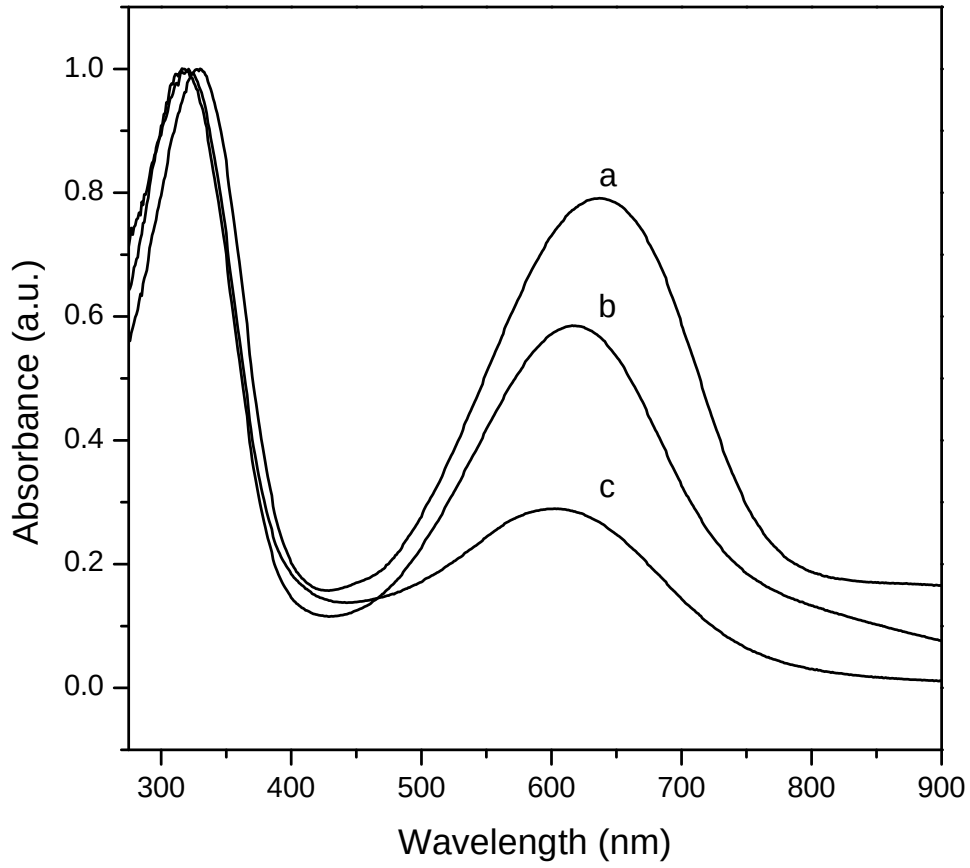

Figure 4.2. Uv-vis spectra of (a) PANI, (b) PANIMe, and (c) PANICl in 1-methyl-2-pyrrolidinone.

Table 4.2. Absorptions and *Q*/*B* ratios in the UV-vis spectra of PANI and its derivatives in NMP.

Polymer	Wavelength (nm)		*Q*/*B* Intensity ratio
	Q	*B*	
PANI	632	324	0.76
PANIMe	617	315	0.56
PANICl	589	315	0.28

The ratio of the intensities of the *Q* peak and the *B* peak (*Q*/*B*) gives an indication of the amount of quinoid units and benzenoid units along the polymer chain and the degree of oxidation of PANI and its derivatives.[22, 24] Zheng and Levon[25] showed that the maxima of the B and Q peaks shifted to lower wavelength with an increase in the amount of alkyl groups substituted on N atoms along the backbone of PANI. In addition, the ratio of *Q*/*B* decreased from about 0.90 for emeraldine PANI (deprotonated) to as low as 0.32 for *N*-dodecylated PANI. These changes were said to be caused by an increase in the torsional angle between adjacent benzene rings because of steric hindrance.[25] Similar observations were made by Yang and Mattes[22] when amines were introduced on PANI rings by substitution. The values in Table 4.2 show that even though the methyl group and chlorine atom have similar van der Waals radii, the effect of chlorine on the optical properties of the polymer is more pronounced. Clearly the electron-withdrawing effect of chlorine also plays a role. Low values of the *Q*/*B* ratio have been observed from the uv-vis spectra of halogen substituted polyanilines reported previously.[14, 26]

FTIR Spectroscopy. The FTIR spectra of PANIMe and PANICl show the characteristic peaks around 1600 cm^{-1} for the quinoid ring (stretching of N=Q=N) and around 1500 cm^{-1} for the benzoniod rings (stretching of N–B–N),[27, 28] where Q denotes the quinoid unit and B is the benzenoid unit (Figure 4.3). The peaks at 812 cm^{-1} (C–H out of plane bending) which are characteristic of a p-substituted benzene ring indicates that the polymers formed by 1,4-addition in the same manner as PANI. A major difference between the spectra of the PANI and substituted PANIs is the decreased intensity of the peaks around 1600 cm^{-1} in the latter. The decrease in the intensity of this peak relative to the peak around 1500 cm^{-1} is an indication of the

lower oxidation state of PANIMe and PANICl in agreement with uv-vis results. The decrease in the number of quinoid units in PANIMe and PANICl is further demonstrated by FTIR spectra of the two smples in the region 2800 cm^{-1} to 3500 cm^{-1}.

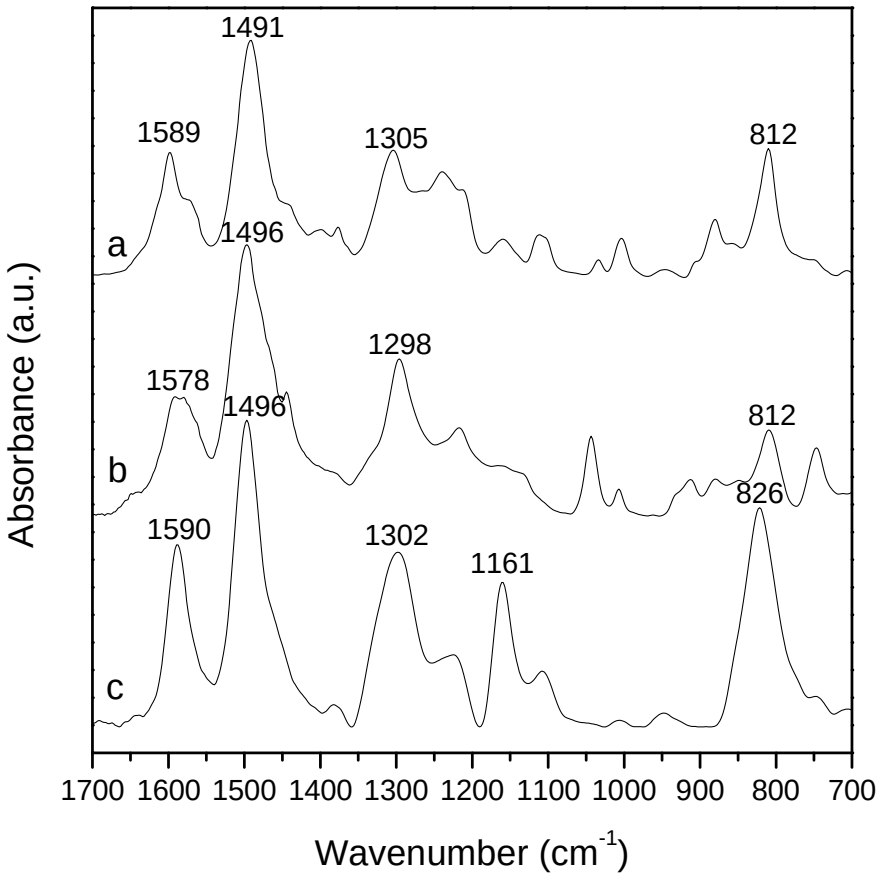

Figure 4.3. FTIR spectra of (a) PANIMe, (b) PANICl, and (c) PANI.

The spectrum of PANI (Figure 4.4c), shows two distinct absorbance peaks at 3384 cm^{-1} and 3313 cm^{-1} due to non-hydrogen bonded N–H and hydrogen bonded N–H stretching vibrations, respectively.[14, 22, 29, 30] A third peak at 3032 cm^{-1} is assigned to the stretching vibration of the benzene ring C–H bonds.[31] The spectrum of PANICl

shows a sharp peak at 3395 cm^{-1} (non-hydrogen bonded N–H stretch), a shoulder around 3300 cm^{-1} (hydrogen bonded N–H stretch), and a peak at 3056 cm^{-1} (aromatic C–H stretch). The spectrum of PANIMe show similar peaks with an addition peak at 2918 cm^{-1} due to the ring-substituted methyl group.

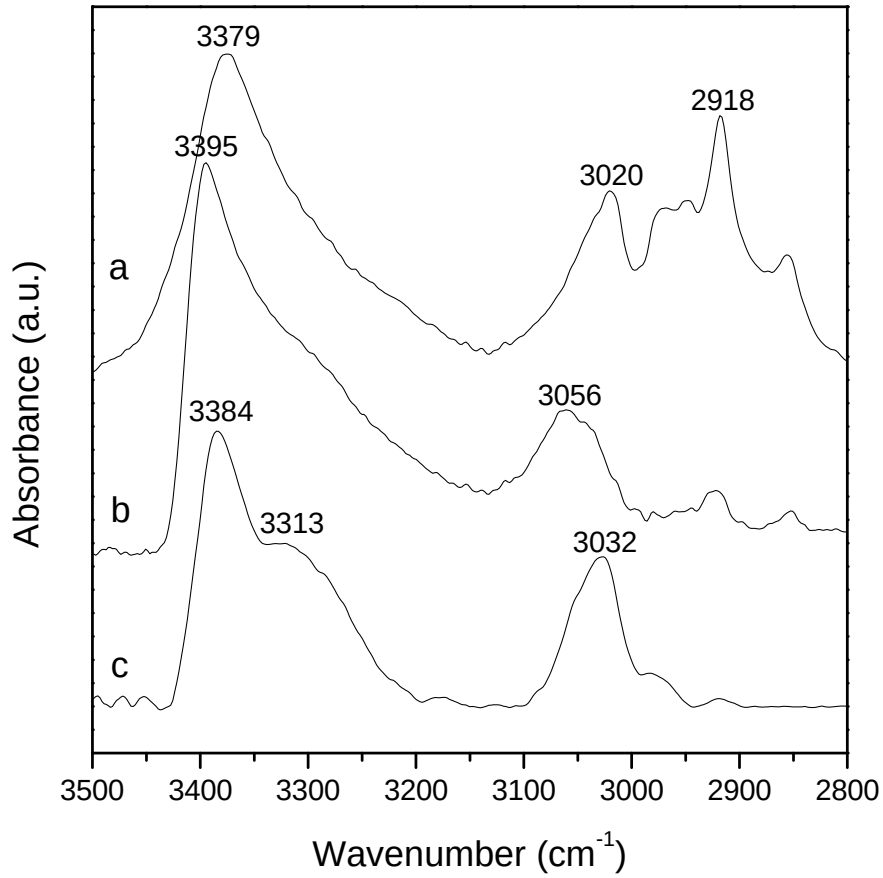

Figure 4.4. FTIR spectra of (a) PANIMe, (b) PANICl, and (c) PANI in the IR region of 2800 cm^{-1} to 3500 cm^{-1}.

The decreased intensity of the peak due to hydrogen bonded N–H interactions indicates a decrease in the degree of hydrogen bonding for the substituted polymers.

This is consistent with a decrease in the number of imine N groups on the polymer chain. In addition, the bulky methyl and chlorine groups substituted on the ring could sterically hinder the polymer chains from getting close enough for H-bonding to be displayed.

4.3.2 The Reactions of PANI, PANIMe, and PANICl with $HAuCl_4$

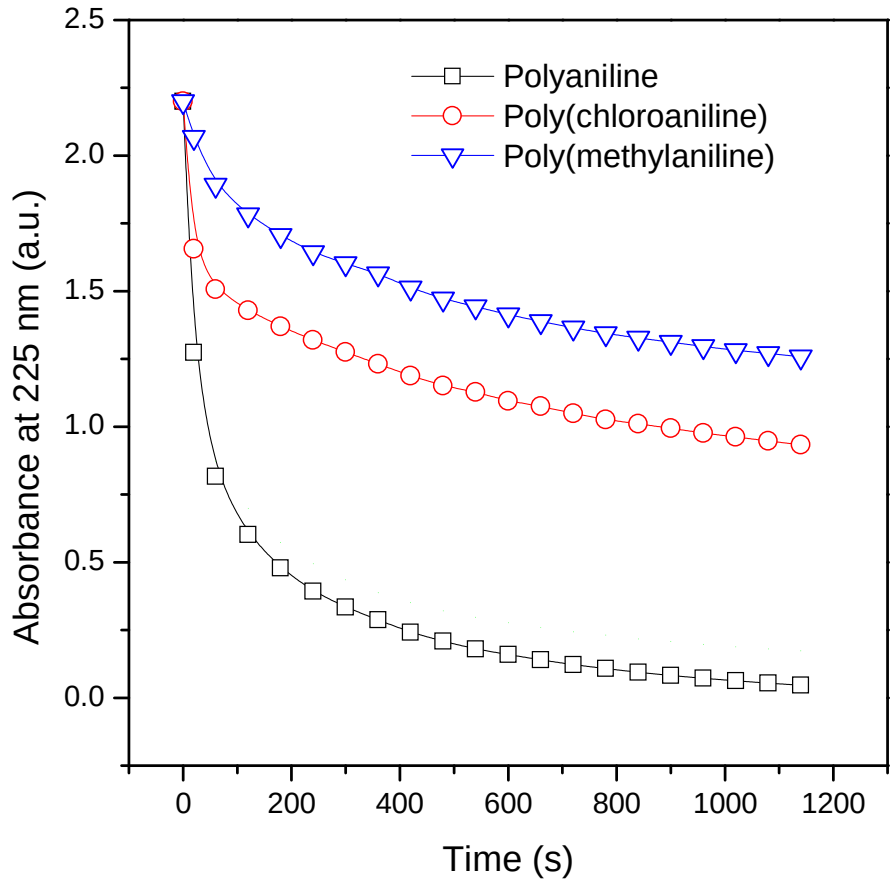

Figure 4.5. The reactivity of polyaniline and its derivatives towards $HAuCl_4$.]

Figure 4.5 shows that PANI readily reacts with $HAuCl_4$ as shown by the fast decrease in the UV absorbance of $AuCl_4^-$ at 225 nm. PANIMe exhibited the lowest reactivity

with $AuCl_4^-$. Substituents on the aniline monomer change the oxidation potential of the monomers. The rate of polymerization of chloroaniline was shown in the last section to be much slower than that of methylaniline. The two monomers have substituent groups with similar van der Waals radii but differed in that the chloro group is electron withdrawing while the methyl group is electron donating. While the electron withdrawing effect was the determining for the rate of polymerization of chloroaniline and methylaniline, the reactivity of the polymers with $AuCl_4^-$ seem to be determined largely by steric effects. Cyclic voltammetry measurements by D'Aprano and co-workers[4] have shown that the increase in the torsion angle due to the large groups on the benzene ring causes an increase in the redox potential of the substituted polymer compared to unsubstituted PANI. In addition, the incorporation of a large anion like $AuCl_4^-$ into the polymer matrix should be inhibited by large groups on the polymer backbone. This may explain the lower reactivity of PANIMe and PANICl towards $AuCl_4^-$.

The size of the gold nanoparticles does not seem to depend on the reactivity of $AuCl_4^-$ with the various polymers. While PANI showed the highest reactivity towards $AuCl_4^-$, the size of the gold nanoparticles were quite similar for PANI and PANICl at an average of 2.6 ± 0.7 nm and 2.4 ± 0.5 nm, respectively. The particle size of gold nanoparticles on PANIMe was slightly higher at 3.3 ± 1.0 nm. This is shown in Figure 4.6. It was shown in the last Chapter that the interaction of Au NP's and PANI occurs by charge transfer from N to Au and formation of H-bonds between PANI and partially reduced gold-chloride complexes. These results might seem puzzling since electron–withdrawing groups such as chlorine decreases the basicity of the nitrogen atom on the polymer backbone.[13]

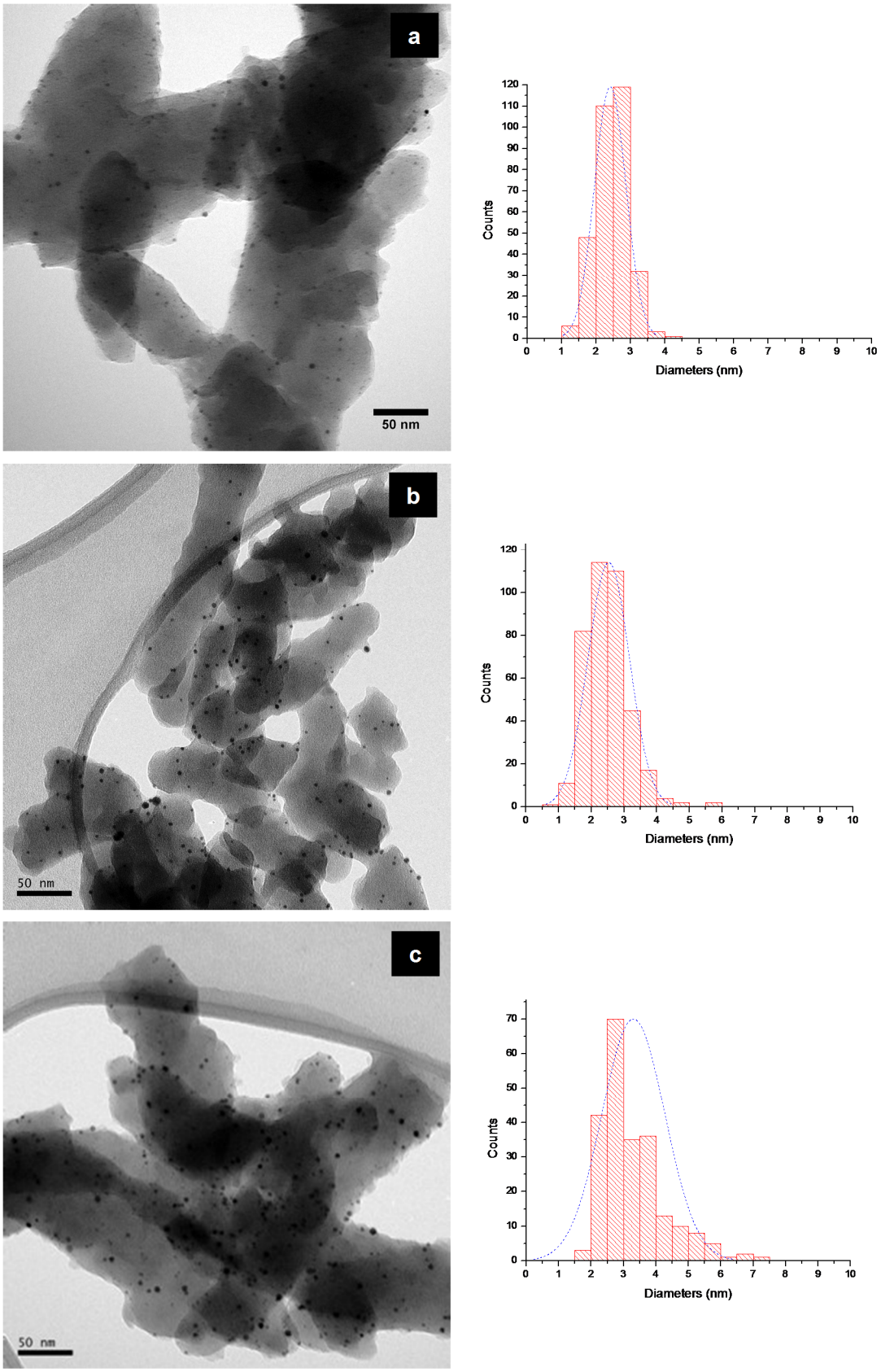

Figure 4.6. TEM images and particle size distributions of gold nanoparticles on (a) PANI, (b) PANICl, and (c) PANIMe

However, steric effects seem to always predominate for both methyl and chorine groups.[8] The smaller size of gold nanoparticles on PANICl compared with PANIMe could be a result of stronger interactions between AuNPs and PANICl. It has been shown that indeed the nature and strength of the interaction of metal particles and functional groups on a polymer has a significant effect on the size of the nanoparticles.[32, 33]

The amount of gold incorporated onto the polymer matrix varied with the reactivity of the polymer with $AuCl_4^-$. Metal loading as determined by thermogravimetric analysis shows that PANI, the most reactive of the three, had the highest loading of 5% by weight. This weight loading for AuPANICl and AuPANIMe were found to be 4% and 2%, respectively.

4.3.3 Stability of the Nanocomposites in Acidic Media

It was shown in the last Chapter that the gold nanoparticles on PANI sintered with a decrease in pH. Significant agglomeration of AuNPs occurred at pH ≈ 2 and lower. Addition of hydrochloric acid to PANI leads to the protonation of the polymer on the imine N and subsequently the formation of a polysemiquinone radical cation. This protonation increases rapidly below pH ≈ 2. The degree of the agglomeration of AuNPs (and the particle sizes) on PANI was observed to increase with an increase in the degree of protonation. Table 4.3 shows the average particle size for AuPANI, AuPANIMe, and AuPANICl composites after being soaked in HCl at various pH values for 24 hours. The effect of protonation of the various polymers on the stability of Au NPs is more pronounced for AuPANI that it is for AuPANIMe and AuPANICl.

The size of the particles increases, due to aggregation and coalescence, to about 5 nm for AuPANIMe and AuPANICl at pH = 1 compared to about 9 nm for AuPANI at pH = 1.

Table 4.3. The variation of the size of gold nanoparticles on PANI, PANIMe, and PANICl with pH

Sample	Particle Size (nm)		
	pH 5[a]	pH 2	pH 1
AuPANI	2.6 ± 0.7	5.9 ± 1.2	8.8 ± 4.0
AuPANIMe	3.3 ± 1.0	3.6 ± 1.0	4.8 ± 1.8
AuPANICl	2.4 ± 0.5	3.3 ± 0.6	4.9 ± 1.7

[a]Initial pH measured after formation of Au nanoparticles on the polymers.

The relative stability of Au NPs on the substituted polymers can be ascribed to the decreased basicity of the polymers due the bulky substituent groups. This decrease in the basicity of the nitrogen atoms shifts the point at which protonation occurs to lower values of pH. This point occurs around pH = 2 for PANI. Table 3 shows there is only a small increase in the size of Au NPs on PANIMe and PANICl at pH = 2 suggesting that there is little or no protonation taking place at this pH for the two polymers.

The FTIR spectra of the PANI and derivatives provide further insight into the protonation of these polymers. While FTIR cannot be used to quantify the degree of protonation, it does provide an indication of whether the polymer is protonated or not. This is seen by the appearance of an intense and broad IR absorption around 1100 cm^{-1}. This band has been interpreted as a stretching vibration of N–H due to an interchain $NH^{+}\cdots H$ bond.[29] Figure 4.7 shows that this band is only seen for AuPANI at pH = 1

but not for AuPANIMe and AuPANICl. Kang and co-workers[34] have shown that the presence of bulky substituents on PANI lowers the protonation level of the polymer and also hinders the charge transfer interactions with organic acceptors. By measuring the relative ratios of N^+/N and Cl/N using X-ray photoelectron spectroscopy, they observed lower values for poly(methylaniline) than PANI.

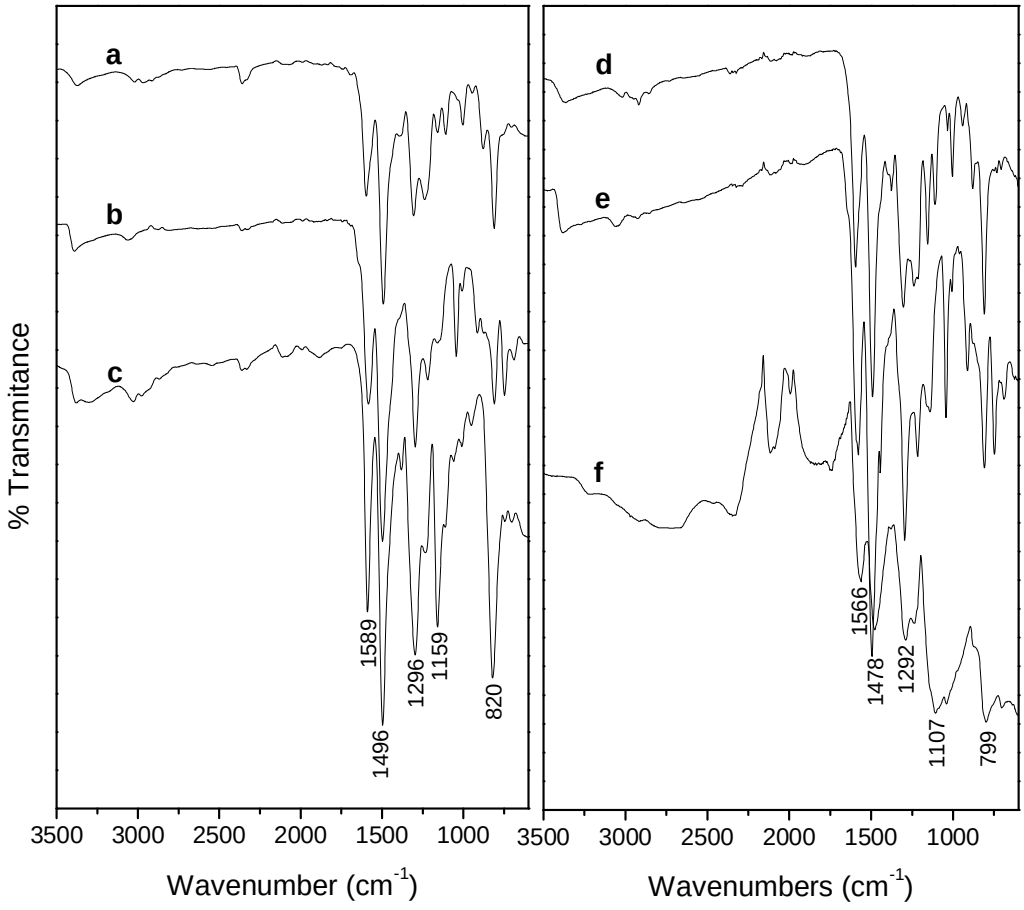

Figure 4.7. FTIR spectra indicating the protonation of (a) AuPANICl, (b) AuPANIMe, and (c)AuPANI. Spectra (a) to (c) are the unprotonated composites and spectra (d) to (f) are the spectra of the corresponding composites after HCl treatment at pH 1.

4.4 CONCLUSIONS

As expected from theoretical predictions the polymerization of aniline was affected the substituent group on the benzene ring. The rate of the polymerization varied as PANICl << PANIMe < PANI. While the rate of polymerization was determined largely by electronic effects of the substituent groups, the reactivity of the polymers was determined by the steric effects. The order of the rate of reaction of the polymers with AuCl-4 was PANIMe < PANICl << PANI. The amount of Au incorporated into the polymer matrix followed a similar trend. However the size of the gold nanoparticles did not differ greatly. Gold nanoparticles dispersed on PANICl and PANIMe were more stable in acidic media than those on PANI.

4.5 REFERENCES

(1) Michaelson, J. C.; McEvoy, A. J. *J. Chem. Soc., Chem. Commun.* **1994**, 79-80.

(2) Qiu, H. J.; Wan, M. X. *J. Polym. Sci. , Part A: Polym. Chem.* **2001**, *39*, 3485-3497.

(3) Huang, J.; Kaner, R. B. *Angew. Chem. Int. Ed.* **2004**, *43*, 5817-5821.

(4) D'Aprano, G.; Leclerc, M.; Zotti, G. *J Electroanal Chem* **1993**, *351*, 145-158.

(5) Vaschetto, M. E.; Retamal, B. A. *J. Phys. Chem. A* **1997**, *101*, 6945-6950.

(6) Vaschetto, M. E.; Retamal, B. A.; Monkman, A. P. *J.Mol. Struct. THEOCHEM* **1999**, *468*, 209-221.

(7) Focke, W. W.; Wnek, G. E.; Wei, Y. *J. Phys. Chem.* **1987**, *91*, 5813-5818.

(8) Wei, Y.; Focke, W. W.; Wnek, G. E.; Ray, A.; MacDiarmid, A. G. *J. Phys. Chem.* **1989**, *93*, 495-499.

(9) Kulszewicz-Bajer, I.; Pron, A.; Abramowicz, J.; Jeandey, C.; Oddou, J.; Sobczak, J. W. *Chem. Mater.* **1999**, *11*, 552-556.

(10) Genoud, F.; Kulszewicz-Bajer, I.; Bedel, A.; Oddou, J. L.; Jeandey, C.; Pron, A. *Chem. Mater.* **2000**, *12*, 744-749.

(11) Dimitriev, O. P. *Polym. Bull.* **2003**, *50*, 83-90.

(12) Tseng, R. J.; Baker, C. O.; Shedd, B.; Huang, J.; Kaner, R. B.; Ouyang, J.; Yang, Y. *Appl. Phys. Lett.* **2007**, *90*, 053101-3.

(13) Fabrizio, M.; Mengoli, G.; Musiani, M. M.; Paolucci, F. *Synth. Met.* **1991**, *44*, 271-280.

(14) Gruger, A.; Novak, A.; Régis, A.; Colomban, P. *J. Mol. Struct.* **1994**, *328*, 153-167.

(15) Tran, H. D.; Norris, I.; D'Arcy, J. M.; Tsang, H.; Wang, Y.; Mattes, B. R.; Kaner, R. B. *Macromolecules* **2008**, *41*, 7405-7410.

(16) Manohar, S. K.; Macdiarmid, A. G.; Epstein, A. J. *Synth. Met.* **1991**, *41*, 711-714.

(17) Wei, Y.; Hsueh, K. F.; Jang, G. *Polymer* **1994**, *35*, 3572-3575.

(18) Stejskal, J.; Kratochvíl, P.; Jenkins, A. D. *Polymer* **1996**, *37*, 367-369.

(19) Hine, J. In *Structural Effects on Equilibria in Organic Chemistry;* John Wiley & Sons: New York, 1975; .

(20) Bondi, A. *J. Phys. Chem.* **1964**, *68*, 441-451.

(21) de Albuquerque, J. E.; Mattoso, L. H. C.; Faria, R. M.; Masters, J. G.; MacDiarmid, A. G. *Synth. Met.* **2004**, *146*, 1-10.

(22) Yang, D.; Mattes, B. R. *Synth. Met.* **2002**, *129*, 249-260.

(23) Huang, W. S.; MacDiarmid, A. G. *Polymer* **1993**, *34*, 1833-1845.

(24) Albuquerque, J. E.; Mattoso, L. H. C.; Balogh, D. T.; Faria, R. M.; Masters, J. G.; MacDiarmid, A. G. *Synth. Met.* **2000**, *113*, 19-22.

(25) Zheng, W.; Levon, K.; Laakso, J.; Oesterholm, J. *Macromolecules* **1994**, *27*, 7754-7768.

(26) Gök, A.; Sarı, B.; Talu, M. *Synth. Met.* **2004**, *142*, 41-48.

(27) Tang, J.; Jing, X.; Wang, B.; Wang, F. *Synth. Met.* **1988**, *24*, 231-238.

(28) Ohira, M.; Sakai, T.; Takeuchi, M.; Kobayashi, Y.; Tsuji, M. *Synth. Met.* **1987**, *18*, 347-352.

(29) Colomban, P.; Gruger, A.; Novak, A.; Régis, A. *J. Mol. Struct.* **1994**, *317*, 261-271.

(30) Zheng, W.; Angelopoulos, M.; Epstein, A. J.; MacDiarmid, A. G. *Macromolecules* **1997**, *30*, 2953-2955.

(31) Socrates, G. In *Infrared and Raman Characteristic Group Frequencies;* John Wiley & Sons: Chichester, 2001; pp 157-167.

(32) Ishida, T.; Kuroda, K.; Kinoshita, N.; Minagawa, W.; Haruta, M. *J. Colloid Interface Sci.* **2008**, *323*, 105-111.

(33) Liu, W.; Yang, X.; Xie, L. *J. Colloid Interface Sci.* **2007**, *313*, 494-502.

(34) Kang, E. T.; Neoh, K. G.; Tan, K. L. *Synth. Met.* **1994**, *64*, 77-81.

5 THE CATALYTIC ACTIVITY OF GOLD NANOPARTICLES DISPERSED ON PANI AND ITS DERIVATIVES

5.1 INTRODUCTION

Gold was thought to be catalytically inactive until Haruta and coworkers showed that gold nanoparticles deposited on metal supports exhibit extraordinary catalytic activity towards a number of reactions.[1] There has been an interest lately on the use of gold nanoparticles dispersed on polymers for use as catalysts in liquid phase reactions.[2-7]

The incorporation of metallic nanoparticles in conducting polymers like polyaniline has attracted significant attention over the years because of the strong electronic interaction between the nanoparticles and the polymer.[8] It has been shown that a suitable combination of metal nanoparticles and conducting polymer could permit the generation of electrodes with enhanced electrocatalytic activities towards a number of reactions.[9] For instance, Tian and co-workers[10] reported on a multilayer film of polyaniline and mecrcaptosuccinic-acid-capped gold nanoparticles capable of catalyzing the oxidation of β-nicotinamide adenine dinucleotide (NADH).

The reduction of 4-nitrophenol (4-NP) to 4-aminophenol (4-AM) in excess sodium borohydride has been used extensively as a test reaction for a number of polymer-based catalysts.[7, 11-15] This reaction is used a model reaction because only one product can be produced and the degree of conversion can be easily monitored using uv-vis spectroscopy. The rate of decrease in the strong absorption at 400 nm due to 4-nitrophenolate is used to calculate the rate constants for the reaction. Two mechanisms for the catalyzed conversion of 4-NP to 4-AM have been offered. One

mechanism assumes that only hydrogen adsorbs on the surface of the catalyst (Eley-Rideal mechamism)[16] while the other states that both hydrogen and 4-nitrophenolate need to be adsorbed on the surface of the catalyst prior to the reaction (Langmuir-Hinshelwood mechanism).[17, 18]

In this Chapter, the catalytic activity of gold nanoparticles dispersed on PANI is tested using the hydrogenation of 4-NP as a model reaction. Further the effect of substituent groups on the polymer backbone will be tested by probing the catalytic activity of AuPANIMe and AuPANICl. The activity of the catalysts was influence largely the nature of the interactions of the Au NPs and the functional groups on the polymers.

5.2 EXPERIMENTAL

4-Nitrophenol and sodium borohydride ($NaBH_4$) were purchased from Sigma-Aldrich. These chemicals were used as received.

Synthesis of AuPANI, AuPANIMe, and AuPANICl. The synthesis of these catalysts has been described in the last Chapter. In brief, the synthesis was carried out by rapidly adding 25 mL of 10^{-2} M $HAuCl_4$ to a suspension of 1 g of the deprotonated polymer in 100 mL of distilled water. The mixture was stirred for 2 hours, centrifuged and washed with distilled water. The moist cake was then dispersed in 50 mL of distilled water to which 15 mg of sodium borohydride in 10 mL of distilled water was rapidly added to reduce gold ions to metallic gold. After one hour of stirring the catalyst was collected by centrifugation, washed with water and dried.

Tests on the catalytic activity of AuPANI, AuPANIMe, and AuPANICl. The catalytic conversion of 4-NP to 4-AP was conducted as follows. A 30 mL aqueous solution of 1.0×10^{-4} M 4-NP was added to a 50 mL beaker. Then 0.250 g of NaBH4 in 10 mL of water was added to the beaker with mild stirring. The catalyst (3.5 mg in 5 mL of water) was finally added. The reaction was monitored by transferring 3 mL aliquots from the reaction mixture to a uv-vis quartz cuvette for measurements. The absorption spectra of the reaction mixture were recorded on a Varian Cary 50 spectrometer in the range of 250 – 500 nm every 60 seconds. The catalytic tests were performed under ambient room temperature at around 22 ^{o}C. The concentration of 4-NP was varied from 0.1 mM to 0.4 mM and that of $NaBH_4$ from 0.042 M to 0.67 M. In addition the effect of the amount of catalyst on the rate of the reaction was tested.

5.3 RESULTS AND DISCUSSIONS

The catalytic activity of Au-PANI nanocomposites were investigated with the reduction of 4-nitrophenol in the presence of excess sodium borohydride as a reducing agent. The reduction of 4-NP using borohydride is a thermodynamically feasible reaction (E^o for 4-NP/4-AP = –0.76 V and H_3BO_3/BH_4^- = –1.33 V vs NHE) but is extremely slow in the absence of a catalyst.[19] The colour of the solution changed from light yellow to dark yellow due the formation of 4-nitrophenolate ion upon addition of $NaBH_4$ to a solution of 4-NP. The reduction of 4-NP can easily be monitored by the decrease in the intensity of the 4-nitrophenolate absorption peak at 400 nm (Figure 5.1). At the same time, a new peak at ~300 nm appears due to the formation of 4-AP. The isosbestic points at 280 nm and 310 nm indicate that the reduction occurs without the formation of by products.[20]

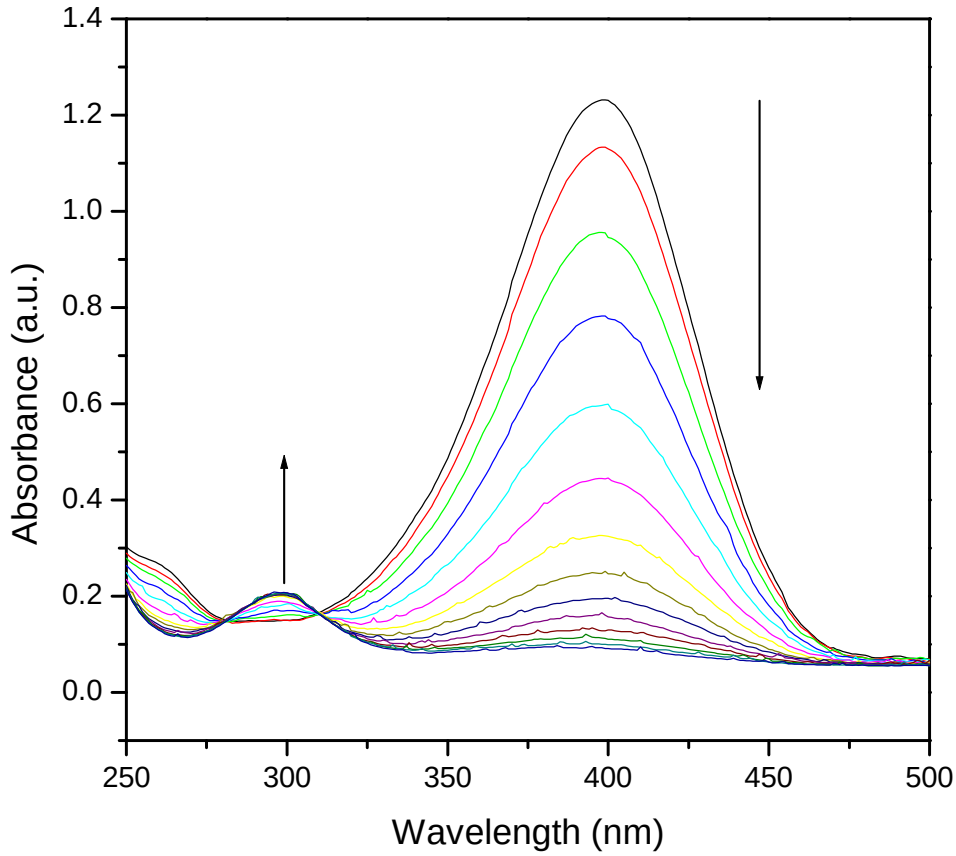

Figure 5.1. Time dependent absorption spectra for the reduction of 4-NP in the presence of Au-PANI. Conditions: [4-AP] = 1 mM; [$NaBH_4$] = 0.67 M; [Catalyst] = 0.7 g/L.

The amount of $NaBH_4$ was in excess and the reaction follows first order kinetics. The apparent rate constant, k_{app}, was obtained from the linear slope (Figure 5.2). The reduction of 4-nitrophenol by borohydride ion occurs as

$$4HOC_6H_4NO_2 + 3BH_4^- + H_2O \longrightarrow 4HOC_6H_4NH_2 + 3H_2BO_3^- \qquad (5.1)$$

In addition, BH_4^- spontaneously hydrolyses to generate borate ions and hydrogen (Equation 2).[21, 22] This reaction which competes with the catalytic reaction also causes

bubbling which affects the Uv-vis measurements at high concentrations of borohydride.

$$BH_4^- + 2H_2O \longrightarrow 4H_2 + BO_2^- \qquad (5.2)$$

The hydrolysis of BH_4^- is suppressed at high values of pH.[23] We did not adjust the pH of solutions and our results were nonetheless highly reproducible.

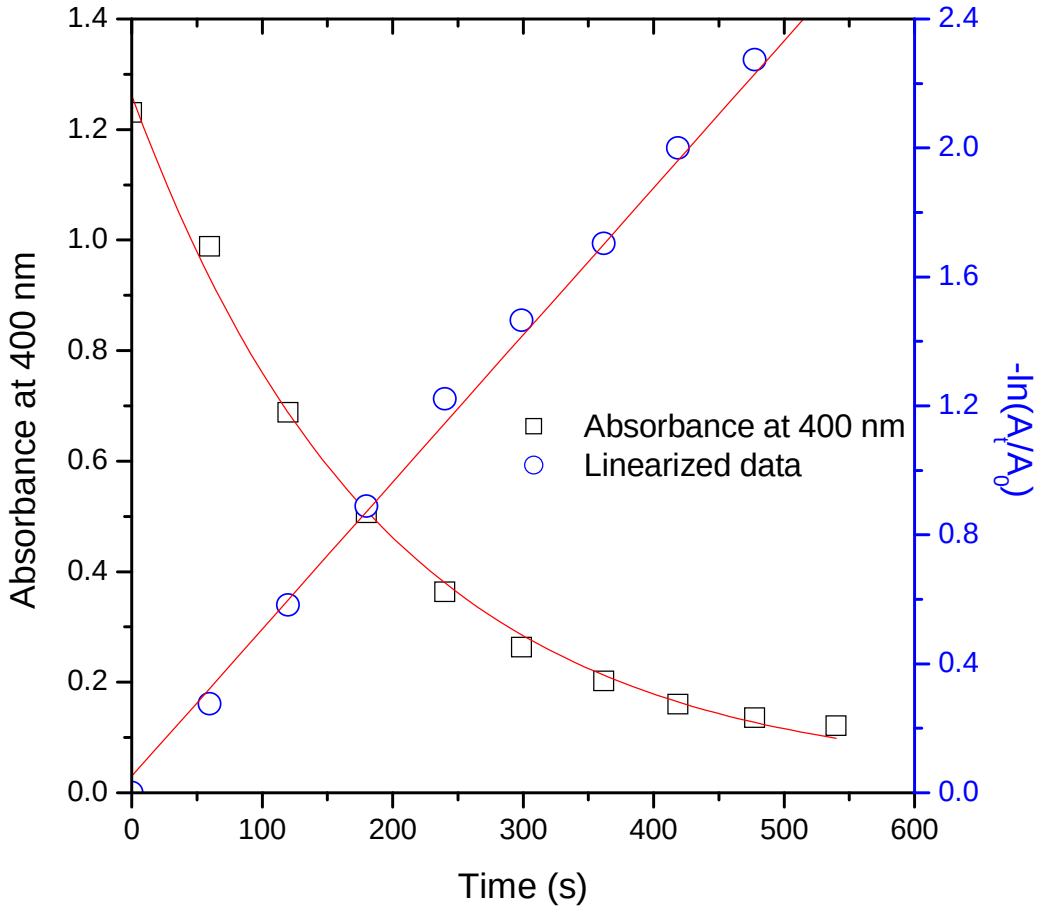

Figure 5.2. First order decay of the absorbance at 400 nm and the linearized data for the reduction of 4-NP.

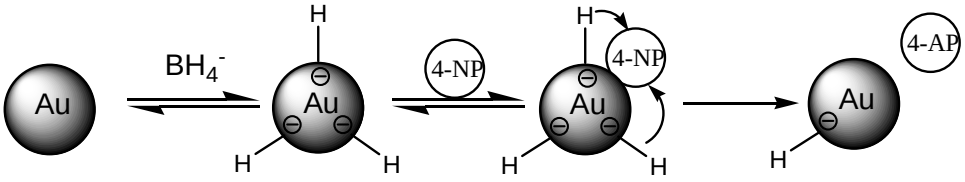

Figure.5.3. Schematic representation of the catalytic reduction of 4-NP in the presence of Au nanoparticles (Langmuir-Hinshelwood mechanism). Adapted from Ref 18.

5.3.1 Influence of the Concentration of 4-NP and Borohydride

The effect of the concentration of 4-NP on the apparent rate constant was studied by varying the concentration of 4-NP from 0.1 mM to 0.4 mM while keeping the concentration of $NaBH_4$ constant. Two different concentrations of $NaBH_4$ were used, viz. 0.17 M and 0.68 M. The results are summarized in Figure 5.4 showing an increase in k_{app} with increasing [4-NP] to some maximum value and drops. Several mechanisms have been proposed for the catalysed reduction of 4-NP using $NaBH_4$. One of these mechanisms involves the formation of metal hydride through the interaction of borohydride and metal nanoparticles. This step is then followed by the reaction of 4-NP with the surface hydride to yield the product 4-AM.[17] Wunder and co-workers[18] recently modelled this reaction in terms of a Langmuir-Hinshelwood mechanism in which both BH_4^- and 4-NP need to be adsorbed on the catalyst surface prior to reaction.

The other mechanism involves the storage of electrons on metal nanoparticles. The first step involves the transfer of electrons from borohydride to metal nanoparticles and their storage on the metal nanoparticles.[24-26] The second step, which is the slowest and rate determining is the diffusion of 4-NP to the metal nanoparticles and reduction

by the electrons on the surface of the metal nanoparticles. This mechanism assumes that only hydrogen needs to be adsorbed on the surface of the nanoparticles.[16]

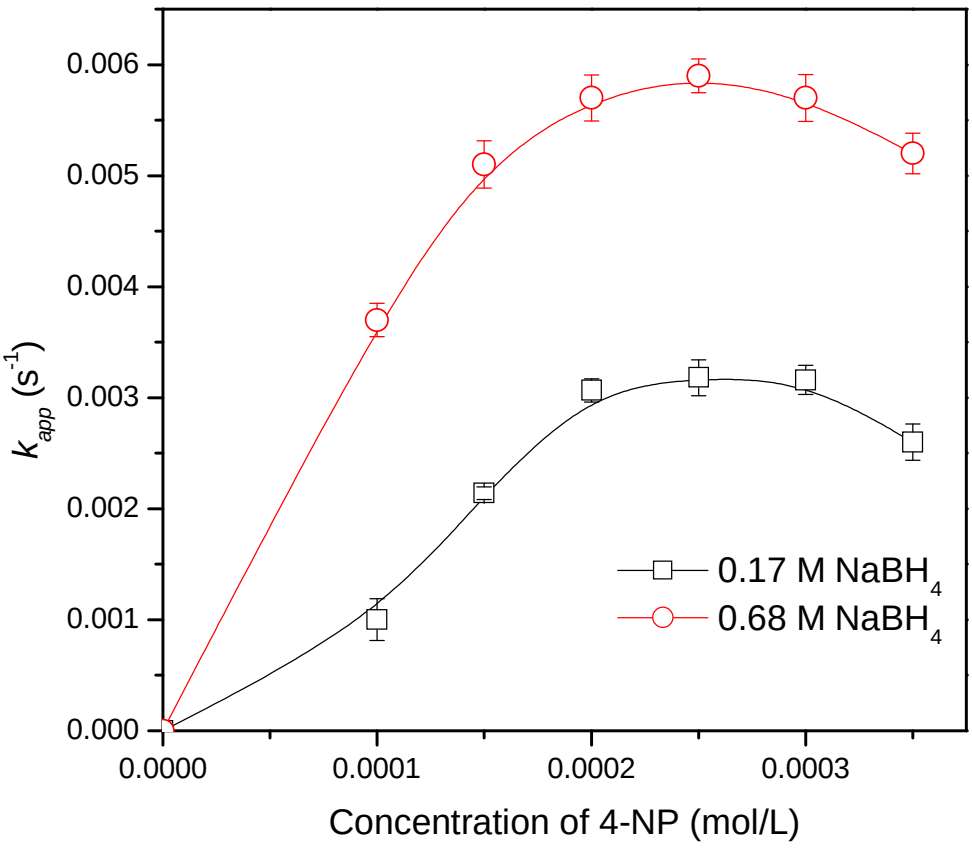

Figure 5.4. Variation of apparent rate constant k_{app} on the concentration of 4-AP. The concentration of the catalyst was 0.7 g/L.

The apparent rate constant, k_{app}, reaches a maximum value (which depends on the concentration of $NaBH_4$) and decreases at high concentration of 4-NP. This suggests that at high concentrations, 4-NP competes for surface sites with borohydride ions and impedes the injection of electrons on the metal surface by borohydride. This observation is in agreement with recent data on the catalytic reduction of 4-NP by Au and Pt nanoparticles.[18] Wunder and co-workers concluded that a high concentration of

4-NP leads to full coverage of the surface of the metal nanoparticles by 4-NP. The major difference between Wunder and coworkers[18] results and ours is that they did not observe any increase in k_{app} with the concentration of 4-NP. However the observed decrease in the k_{app} at high concentrations 4-NP in our case also suggest Langmuir-Hinshelwood kinetics.

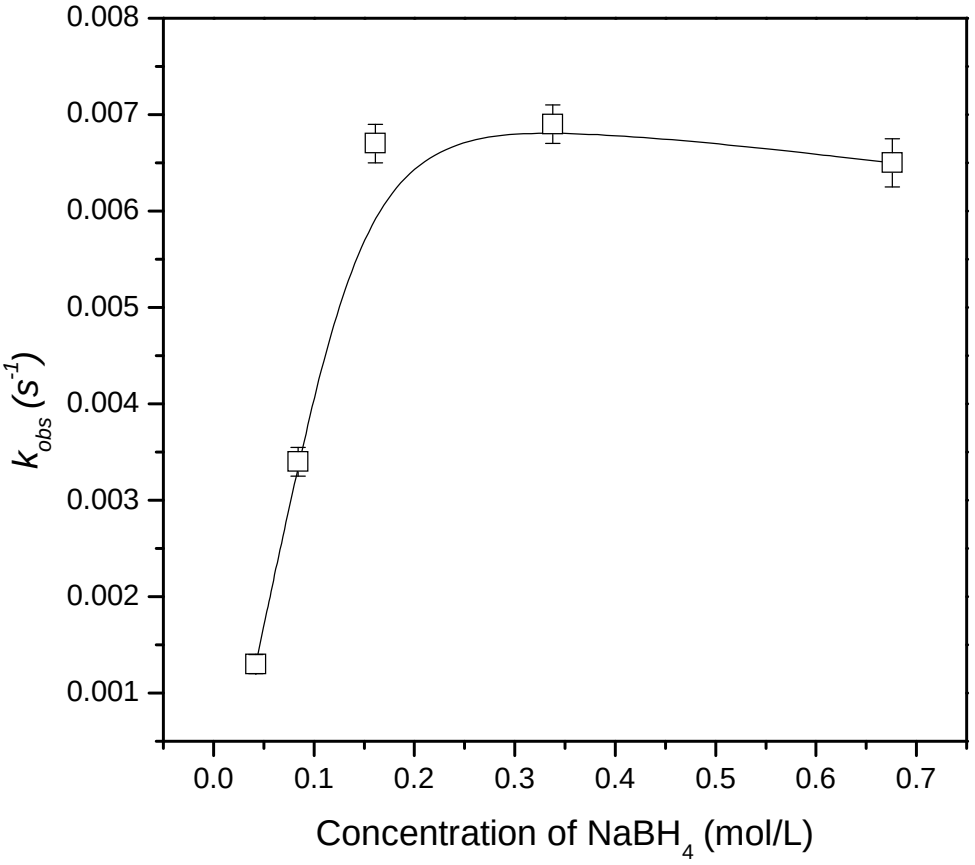

Figure 5.5. Variation of apparent rate constant k_{app} with the concentration of borohydride. The concentration of the catalyst was 0.7 g/L.

The influence of the concentration of borohydride on k_{app} is shown in Figures 5.4 and 5.5. In Figure 3, k_{app} increases with an increase in the concentration of 4-NP but was consistently lower when the concentration of borohydride was reduced for 0.68 M to

0.17 M. For a constant concentration of 4-NP the value of k_{app} increased in a somewhat linear manner for concentrations of borohydride below ~0.2 M. Thereafter, k_{app} asymptotes and decreases slightly with an increase in the concentration of borohydride (Figure 5.5). These observations further support the idea that there is competition for reactive sites by 4-NP and borohydride.

5.3.2 Influence of Catalyst Dose

The amount of catalyst was varied to test if indeed the reduction of 4-NP by borohydride takes place on the surface of our Au-PANI catalyst. Increasing the amount of the catalyst would result in an increase in the total surface area of Au. The rate of reactions in heterogeneous catalysis generally increases linearly with the amount of the catalyst. The apparent rate constant has been shown to be proportional to the total surface area of the metal nanoparticles in the reaction mixture[27, 28]

$$\frac{dC_t}{dt} = k_{app}C_t = k_1 S C_t \qquad (5.3)$$

where C_t is the concentration of 4-NP at time t and k_1 is the rate constant normalized to S, the total surface area of metal nanoparticles normalized to the unit volume of the reaction mixture. The total number of gold nanoparticles, N_{Au}, was estimated from

$$N_{Au} = \frac{3m_{Au}}{4\pi R^3 \rho_{Au}} \qquad (5.4)$$

where m_{Au} is the mass of gold nanoparticles in the catalyst, R is the radius of the Au nanoparticles, and ρ_{Au} is the density of Au. Values of 2.6 nm (from TEM) and 19.2 g/cm^3 for the nanoparticles radius and density of Au were used, respectively. The total surface are of Au was then calculated from

$$S_{tot} = \frac{3m_{Au}}{\rho_{Au}R} \tag{5.5}$$

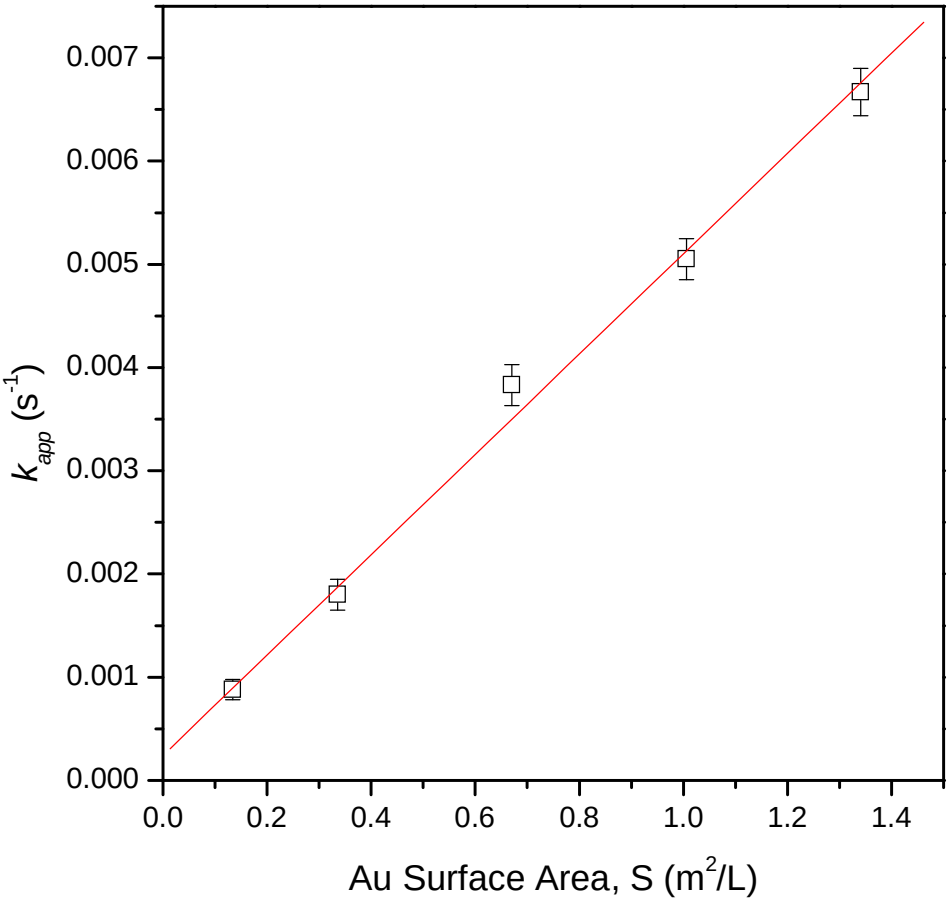

Figure 5.6. Variation of apparent rate constant k_{app} with the concentration of the catalyst. The concentration of the catalyst was 0.7 g/L.

Figure 5.6 shows that there is a linear relationship between the surface area of gold nanoparticles and the rate constant. This demonstrates that the reaction does indeed take place on the surface of the Au nanoparticles and that the nanoparticles are involved in the rate determining step of the reduction of 4-NP.

5.3.3 Influence of Substituents on the Polymer

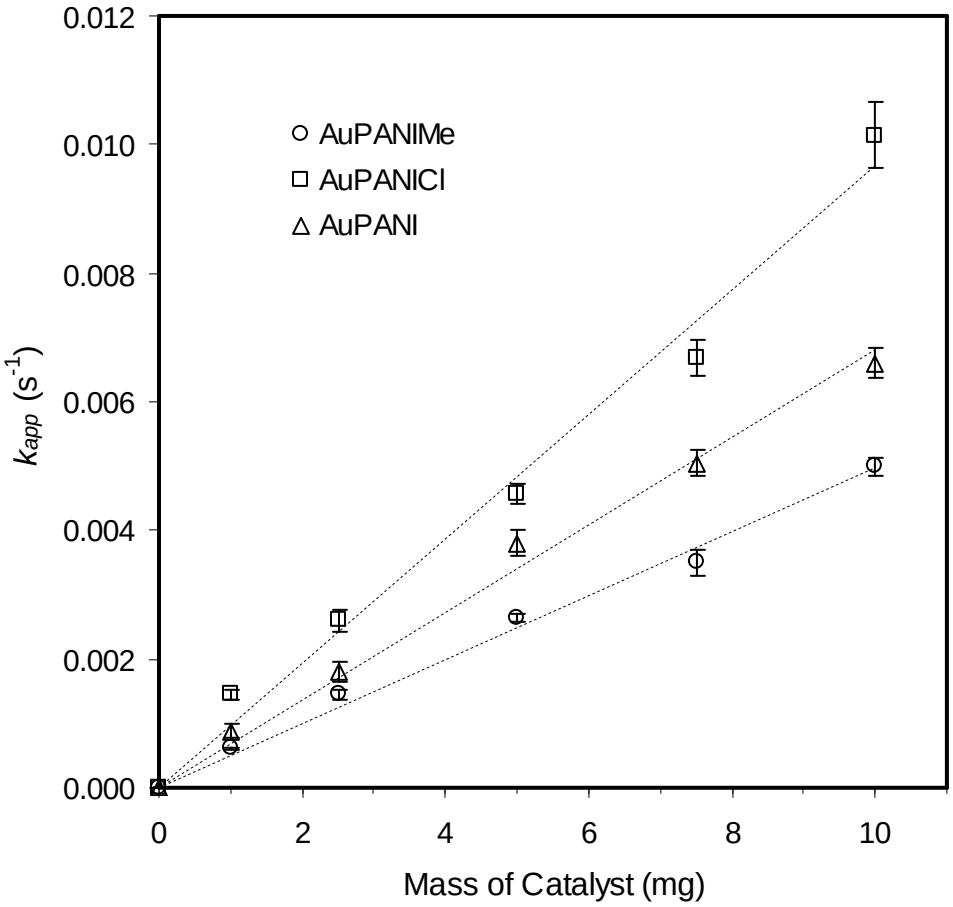

Figure 5.7. Rate constant k_{app} as a function of mass of catalyst for AuPANI, AuPANIMe, AuPANICl. The concentrations of the reactants were: [4-AP] = 1×10^{-4} M, [$NaBH_4$] = 0.68 M.

Figure 5.7 shows that the rate constant of the reduction of 4-NP varies linearly with the mass of catalyst as expected. A simple plot of the mass of catalyst vs. k_{app} gives the impression that AuPANICl is the most active catalyst of the three. The average rate constant normalized to the mass of catalyst for AuPANICl is higher that the other catalysts. Table 5.2 summaries the properties of the catalysts and their corresponding rate constants.

Table 5.1. Comparison of the catalytic activity of Au nanoparticles on PANI, PANIMe, and PANICl.

Catalyst	*d* (nm)	% Loading	k_1 (s^{-1} g^{-1})[a]	k_2 (s^{-1} m^{-2} L)[b]
AuPANI	2.6 ± 0.7	5.0	1.41×10^{1}	5.25×10^{-3}
AuPANIMe	3.3 ± 1.0	1.9	1.04×10^{1}	1.29×10^{-2}
AuPANICl	2.4 ± 0.5	4.0	1.93×10^{1}	8.31×10^{-3}

[a]Rate constant normalized to the mass of catalyst. [b]Rate constant normalized to the surface area of the particles in the system.

When the rate constant is however normalized to the total surface area of the Au NPs in the systems, AuPANIMe topped the trio. The high catalytic activity of Au is often explained by the high number of low-coordination surface atoms present when Au exists as small particles.[29] The observed increase in the catalytic activity of Au catalyst with is decrease in the particles size of Au NPs is attributed to the rapid increase in the relative number of edge and perimeter atoms with a decrease in particle diameter.[30] The differences in the size of Au NPs on AuPANI, AuPANICl, and AuPANIMe catalysts cannot explain the observed differences in the catalytic activities (per unit area) of these catalysts. The only plausible explanation for these results is the difference in the nature of the interaction of Au NPs with the polymers. PANI stabilizes Au NPs by coordination through the imine group and H-bonding.

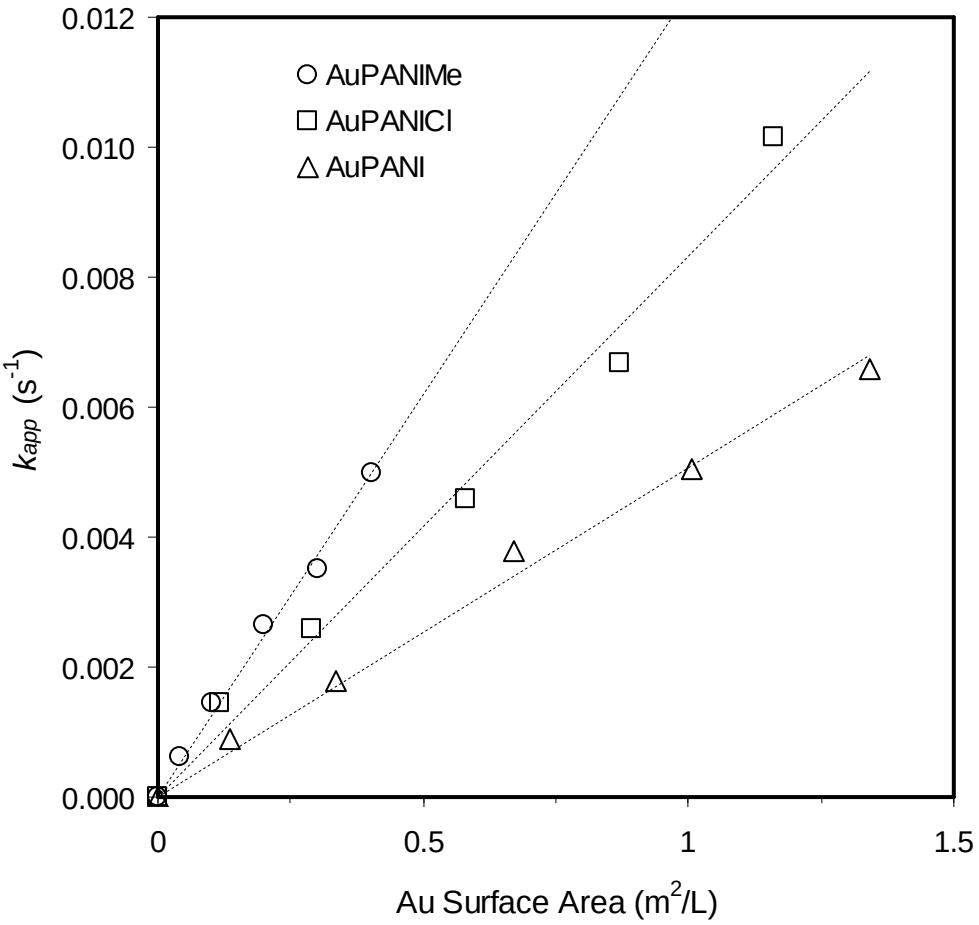

Figure 5.8. Rate constant k_{app} as a function of surface area Au nanoparticles normalized to the unit volume of the system for AuPANI, AuPANIMe, AuPANICl. The concentrations of the reactants were: [4-AP] = 1×10^{-4} M, [$NaBH_4$] = 0.68 M.

Bulky groups on the polymer chains like methyl groups or chlorine group are likely to weaken these interactions through steric hindrance. However a chlorine atom substituted on the benzene ring on PANI is likely to form H-bonds with $AuCl_4^-$ ions adsorbed on Au NPs. This then makes the interaction of Au NPs with PANICl stronger than those on PANIMe which cannot form H-bonds via the methyl group. Metal-support interactions have been shown to affect the catalytic activity of a number of polymer based catalysts.[3, 6] Functional groups that interacts strongly with Au NPs like mercapto group had lowered the activity of the catalyst despite the fact

that the small Au NPs.[3] The high catalytic activity of AuPANIMe is due the weak interactions between PANIMe and Au NPs because induced by the static hindrance due to the methyl group and its inability to form H-bonds.

5.4 CONCLUSIONS

The catalytic performance of AuPANI was evaluated using the reduction of 4-NP in the presence of $NaBH_4$ as a model catalyst. The reaction was observed to follow the Langmuir-Hinshelwood mechanism. The order of the catalytic activity for the reduction of 4-NP was AuPANIMe > AuPANICl > AuPANI. The activity of the catalyst was nature of the interaction of Au NPs with the polymer.

5.5 REFERENCES

(1) Haruta, M. *Catal. Today* **1997**, *36*, 153-166.

(2) Hayakawa, K.; Yoshimura, T.; Esumi, K. *Langmuir* **2003**, *19*, 5517-5521.

(3) Liu, W.; Yang, X.; Xie, L. *J. Colloid Interface Sci.* **2007**, *313*, 494-502.

(4) Kuroda, K.; Ishida, T.; Haruta, M. *J. Mol. Catal. A: Chem.* **2009**, *298*, 7-11

(5) Imawoto, M.; Kuroda, K.; Zaporojtchenko, V.; Hayashi, S.; Faupel, F. *Eur. Phys. J. D* **2003**, *24*, 365-367.

(6) Ishida, T.; Kuroda, K.; Kinoshita, N.; Minagawa, W.; Haruta, M. *J. Colloid Interface Sci.* **2008**, *323*, 105-111.

(7) Kuroda, K.; Ishida, T.; Haruta, M. *J. Mol. Catal. A: Chem.* **2009**, *298*, 7-11.

(8) Feng, X.; Mao, C.; Yang, G.; Hou, W.; Zhu, J. *Langmuir* **2006**, *22*, 4384-4389.

(9) Santhosh, P.; Gopalan, A.; Lee, K. *J. Catal.* **2006**, *238*, 177-185.

(10) Tian, S.; Liu, J.; Zhu, T.; Knoll, W. *Chem. Mater.* **2004**, *16*, 4103-4108.

(11) Kumar, S. S.; Kumar, C. S.; Mathiyarasu, J.; Phani, K. L. *Langmuir* **2007**, *23*, 3401-3408.

(12) Gao, Y.; Ding, X.; Zheng, Z.; Cheng, X.; Peng, Y. *Chem. Commun.* **2007**, 3720-3722.

(13) Harish, S.; Mathiyarasu, J.; Phani, K. L. N.; Yegnaraman, V. *Catal. Lett.* **2009**, *128*, 197-202.

(14) Esumi, K.; Isono, R.; Yoshimura, T. *Langmuir* **2004**, *20*, 237-243.

(15) Chang, Y.; Chen, D. *J. Hazard. Mater.* **2009**, *165*, 664-669.

(16) Khalavka, Y.; Becker, J.; Sönnichsen, C. *J. Am. Chem. Soc.* **2009**, *131*, 1871-1875.

(17) Zhang, H.; Li, X.; Chen, G. *J. Mat. Chem.* **2009**, *19*, 8223-8231.

(18) Wunder, S.; Polzer, F.; Lu, Y.; Mei, Y.; Ballauff, M. *J. Phys. Chem. C* **2010**, *114*, 8814-8820.

(19) Saha, S.; Pal, A.; Kundu, S.; Basu, S.; Pal, T. *Langmuir* **2010**, *26*, 2885-2893.

(20) Pradhan, N.; Pal, A.; Pal, T. *Colloids Surf. Physicochem. Eng. Aspects* **2002**, *196*, 247-257.

(21) Morris, J. H.; Gysling, H. J.; Reed, D. *Chem. Rev.* **1985**, *85*, 51-76.

(22) Ma, J.; Choudhury, N. A.; Sahai, Y. *Renewable Sustainable Energy Rev.* **2010**, *14*, 183-199.

(23) Chatenet, M.; Micoud, F.; Roche, I.; Chainet, E. *Electrochim. Acta* **2006**, *51*, 5459-5467.

(24) Henglein, A.; Lilie, J. *J. Am. Chem. Soc.* **1981**, *103*, 1059-1066.

(25) Henglein, A.; Lilie, J. *J. Phys. Chem.* **1981**, *85*, 1246-1251.

(26) Carregal-Romero, S.; Pèrez-Juste, J.; Hevès, P.; Liz-Marz'n, L.; Mulvaney, P. *Langmuir* **2010**, *26*, 1271-1277.

(27) Mei, Y.; Sharma, G.; Lu, Y.; Ballauff, M.; Drechsler, M.; Irrgang, T.; Kempe, R. *Langmuir* **2005**, *21*, 12229-12234.

(28) Panigrahi, S.; Basu, S.; Praharaj, S.; Pande, S.; Jana, S.; Pal, A.; Ghosh, S. K.; Pal, T. *J. Phys. Chem. C* **2007**, *111*, 4596-4605.

(29) Bond, G. C.; Thompson, D. T. *Catal. Rev. Sci. Eng.* **1999**, *41*, 319-388.

(30) Mavrikakis, M.; Stoltze, P.; Nørskov, J. K. *Catal. Lett.* **2000**, *64*, 101-106.